Iterative Techniques Based on Energy Spreading Transform for Wireless Communications

A Thesis
Presented to
The Academic Faculty

by

Taewon Hwang

In Partial Fulfillment
of the Requirements for the Degree
Doctor of Philosophy

School of Electrical and Computer Engineering
Georgia Institute of Technology
December 2005

Iterative Techniques Based on Energy Spreading Transform for Wireless Communications

Approved by:

Professor Ye (Geoffrey) Li, Advisor
School of Electrical and Computer Engineering
Georgia Institute of Technology

Professor Gregory D. Durgin
School of Electrical and Computer Engineering
Georgia Institute of Technology

Professor Gordon L. Stüber
School of Electrical and Computer Engineering
Georgia Institute of Technology

Professor Xingxing Yu
School of Mathematics
Georgia Institute of Technology

Professor John R. Barry
School of Electrical and Computer Engineering
Georgia Institute of Technology

Date Approved: October 24, 2005

To my parents,

for their endless support

ACKNOWLEDGEMENTS

I would like to express my sincere gratitude to my advisor, Prof. Ye (Geoffrey) Li. During my Ph.D. study, he has always been motivating, guiding, and encouraging me to be more fruitful in my research. This thesis has significantly benefited from his guidance and encouragement. I can never thank him enough for his time and efforts devoted on my papers.

I would like to thank my thesis committee members, Prof. Grodon L. Stüber, Prof. John R. Barry, Prof. Gregory D. Durgin, and Prof. Xingxing Yu. Their remarks and comments have made significant contributions to improving the quality of my thesis.

I am very thankful to the former and current members of the Information Transmission and Processing (ITP) Laboratory, Jingnong Yang, Goucong Song, Hua Zhang, Jianxuan Du, Zet Zhu, Uzoma Anaso Onunkwo, and Ghurumuruhan Ganesan for their help, encouragement, and numerous discussions. They were great companions in my long journey to this thesis.

Finally but not the least, I would like to thank my parents for their endless support. This thesis is dedicated to them.

TABLE OF CONTENTS

DEDICATION . . . . . **iii**

ACKNOWLEDGEMENTS . . . . . **iv**

LIST OF TABLES . . . . . **vii**

LIST OF FIGURES . . . . . **viii**

SUMMARY . . . . . **ix**

1 INTRODUCTION **1**

1.1 Channel Equalization 2

1.1.1 Conventional Methods 2

1.1.2 Turbo Equalization 2

1.2 MIMO signal detection 4

1.2.1 Conventional Methods 5

1.2.2 Turbo BLAST 5

2 ITERATIVE EQUALIZATION BASED ON EST **8**

2.1 System Description 8

2.2 Energy Spreading Transform 11

2.3 Complexity 13

2.4 Performance Analysis 13

2.4.1 MMSE Equalizer 16

2.4.2 Genie-Aided Equalizer 18

2.4.3 Iterative Equalizer with Hard Decision 19

2.4.4 Iterative Equalizer with Soft Decision 26

2.5 Simulation Results 28

2.5.1 Performance for Proakis-B channel 28

2.5.2 Performance for other challenging channels 31

3 IMPROVED SCHEME FOR ENERGY SPREADING TRANSFORM BASED EQUALIZATION **34**

3.1 Optimal Equalization Filter Design 34

3.1.1 Hard Decision 37

3.1.2 Soft Decision . . . 38
3.2 Simulation Results . . . 39
4 ITERATIVE MIMO SIGNAL DETECTION BASED ON EST: FLAT FADING CHANNELS . . . 44
4.1 System Description . . . 44
4.2 ST-EST and Its Impact . . . 46
4.3 Complexity . . . 48
4.4 Performance Analysis . . . 49
4.4.1 MMSE Receiver . . . 50
4.4.2 Genie-Aided Receiver . . . 52
4.4.3 Iterative Receiver with Hard Decision . . . 53
4.4.4 Iterative Receiver with Soft Decision . . . 55
4.5 Asymptotic Property of Rayleigh Fading Channels . . . 56
4.6 Simulation results . . . 60
5 ITERATIVE MIMO SIGNAL DETECTION BASED ON EST: FREQUENCY SELECTIVE FADING CHANNELS . . . 64
6 CONCLUSION . . . 69
APPENDIX A — DERIVATION OF (25) . . . 72
APPENDIX B — DERIVATION OF (52) . . . 73
APPENDIX C — DERIVATION OF (70) AND (100) . . . 74
APPENDIX D — PROOF OF (92) FOR SUFFICIENTLY HIGH SNR 75
APPENDIX E — PROOF OF ID-3 . . . 76
APPENDIX F — DERIVATION OF (193) . . . 77
APPENDIX G — DERIVATION OF (194) . . . 78
APPENDIX H — DERIVATION OF (195) . . . 80
REFERENCES . . . 81
VITA . . . 84

LIST OF TABLES

1 Spreading properties of some ESTs, $N = 2048$. 12

2 Computational Complexity. F-filter = frequency-domain filter, T-filter = time-domain filter, Y = required, N = not required. 13

3 Computational Complexity. Y = required, N = not required. 49

LIST OF FIGURES

1	Turbo equalization	3
2	Turbo BLAST	6
3	Low-complexity equalization	8
4	Principle of EST.	10
5	Equivalent system model	15
6	Performance of the EST-based equalizer for Proakis-B channel.	29
7	BER performance verses iteration with different block sizes N at 10 dB for Proakis-B channel and hard decision.	30
8	Performance of the EST-based equalizer for different types of channels.	32
9	Performance of the improved scheme with (a) hard decision and (b) soft decision for Proakis-B channel.	41
10	Performance of the improved scheme with (a) hard decision and (b) soft decision for Proakis-C channel.	42
11	(a) Iterative detection for MIMO flat fading channels and (b) its equivalent model.	44
12	Principle of ST-EST.	47
13	Distribution of (a) K_H and (b) Q_H for different numbers of $n_T = n_R$.	59
14	Performance of the proposed iterative signal-detection approach with (a) hard decision and (b) soft decision for MIMO flat fading channels when $n_T = n_R = 16$.	61
15	Performance of the proposed iterative signal-detection approach with (a) hard decision and (b) soft decision for MIMO flat fading channels when $n_T = n_R = 4$.	62
16	Required SNR to achieve BER $= 10^{-4}$ for different number of antennas.	63
17	Iterative detection for MIMO frequency-selective fading channels.	64
18	Performance of the proposed iterative signal-detection approach with (a) hard decision and (b) soft decision for MIMO frequency-selective fading channels when $n_T = n_R = L = 4$.	68

SUMMARY

The objective of the proposed research is to devise high-performance and low-complexity signal-detection algorithms for communication systems over fading channels. They include channel equalization to combat *intersymbol interference* (ISI) and *multiple input multiple output* (MIMO) signal detection to deal with *multiple access interference* (MAI) from other transmit antennas. As the demand for higher data-rate and more efficiency wireless communications increases, signal detection becomes more challenging.

We propose novel transmission and iterative signal-detection techniques based on *energy spreading transform* (EST). Different from the existing iterative methods based on the turbo principle, the proposed schemes are independent of channel coding. EST is an orthonormal that spreads a symbol energy over the symbol block in time and frequency for channel equalization; space and time for MIMO signal detection with flat fading channels; and space, time, and frequency for MIMO signal detection with frequency-selective fading channels. Due to the spreading, EST obtains diversity in the available domains for the specific application and increases the reliability of the feedback signal. Moreover, it enables iterative signal detection that has near interference-free performance only at the complexity of linear detectors.

Either a hard or soft decision can be fed back to the interference-cancellation stage at the subsequent iteration. The soft-decision scheme prevents error propagation of the hard-decision scheme for a low SNR and improves the performance. We analyze the performance of the proposed techniques. Analytical and simulation results show that these schemes perform very close to the interference-free systems.

CHAPTER 1

INTRODUCTION

Confronting severe interference is not unusual in modern wireless communication. Consider data transmission over terrestrial radio channels, which is characterized by multipaths resulting from natural and man-made objects between the transmitter and receiver. When symbol duration is shorter than multipath spread (or delay spread), channel equalization [1] is necessary to combat *intersymbol interference* (ISI). As another example, *multiple input multiple output* (MIMO) systems aimed at obtaining maximal efficiency [2, 3] should deal with *multiple access interference* (MAI) from other antennas. As the demand for higher data-rate and efficiency wireless services increases, those signal-detection problems in severe interference environments become more important.

To obtain optimal performance, *maximal likelihood* (ML) signal detection needs to be used; however, its complexity increases exponentially with channel memory for ISI channels and the number of transmit antennas for MIMO channels. Linear detectors and *decision feedback* (DF) detectors have favorable complexities, but their performance is limited because of noise enhancement or error propagation. Recently, iterative signal-detection schemes based on the turbo principle [4] have drawn much attention. Those turbo-like approaches have significantly better performance than linear and non-iterative schemes. However, these schemes rely on joint signal detection and soft-output channel decoding as in [5] or its variant [6], whose complexity is desired to be further reduced.

The objective of the proposed research is to devise high-performance and low-complexity signal-detection algorithms in severe interference environments. We propose novel transmission and iterative signal-detection techniques based on *energy spreading transform* (EST). EST is an orthogonal transform that spreads symbol energy over the symbol block and thereby increases the reliability of the feedback signal. Also, it enables iterative signal detection without channel coding; therefore, it saves the complexity of soft-output channel

decoding in turbo-like methods. Theoretical and simulation results show that these schemes perform very close to the interference-free systems only at the complexity of linear detectors.

In the rest of this introductory chapter, we present some relevant background material on channel equalization and MIMO signal detection.

1.1 Channel Equalization

Channel equalization is necessary to mitigate the effect of *intersymbol interference* (ISI). We review the existing techniques for channel equalization with emphasis on recently devised turbo equalization. For the ISI channel, we use the following received signal model.

$$r_n = \sum_{k=0}^{M-1} h_k x_{n-k} + n_n, \tag{1}$$

where r_n is the received signal, $\{h_k\}_{k=0}^{M-1}$ is the channel, x_n is the transmitted symbol with power σ_x^2, and n_n is the noise with power σ_n^2.

1.1.1 Conventional Methods

Traditional methods for channel equalization are *maximal likelihood sequence detection* (MLSD), *linear equalization* (LE), and *decision-feedback equalization* (DFE) [1]. The MLSD uses *Viterbi algorithm* (VA) to find the most likely transmitted sequence. It is optimal, but it suffers from high complexity for channels with large memory or large constellation sizes.

The LE and the DFE use linear filters to mitigate ISI. To calculate the filter coefficients, *zero forcing* (ZF) criterion tries to remove only ISI, but *minimum mean-square-error* (MMSE) criterion minimizes the total power of ISI and noise. They have favorable complexities, but their performances are far from the *matched filter bound* (MFB), especially for channels with high frequency selectivity. Noise enhancement and error propagation are the major causes of their performance loss.

1.1.2 Turbo Equalization

Figure 1 shows the block diagram of turbo equalization, where channel decoding is incorporated into a part of channel equalization. It is based on the iterative exchange of soft

information between the outer soft-output channel decoder and the inner soft-output symbol detector. Analogous to turbo codes [4], this scheme has been called turbo equalization.

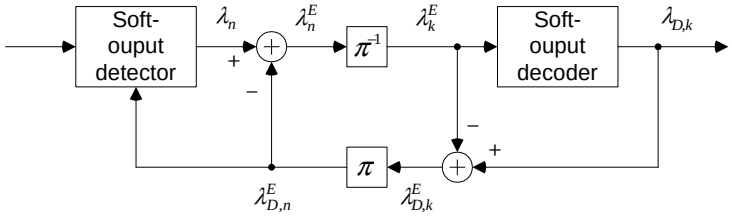

Figure 1. Turbo equalization

This technique was first proposed by Douillard [7] in 1995. It consists of a soft-output ML equalizer and a soft-output channel decoder. The Bahl-Cocke-Jelinek-Raviv (BCJR) algorithm [5] or its variants can be used in the soft-output ML equalizer and the soft-output decoder. The BCJR algorithm produces the sequence of the most likely bits along with their soft values in terms of *a posteriori log likelihood ratio* (LLR). However, only the extrinsic LLR (*a posteriori* LLR minus *a priori* LLR) is exchanged between the soft-output detector and decoder. The performance of the original turbo equalizer approaches the MFB. But its inner detector, which is soft-output MLSD, has prohibitive complexity for channels with large delay spread or large constellation sizes.

The filter-based turbo equalization [8,9] replaces the soft-output MLSD by a soft-output linear filter, which significantly reduces the complexity. The soft-output filter produces

$$y_n = \mathbf{c}_n^H(\mathbf{r}_n - \mathbf{H}\mathcal{E}\{\mathbf{x}_n\} + \mathcal{E}\{x_n\}\mathbf{s}), \tag{2}$$

where the superscript H is the Hermitian operator, $\mathbf{c}_n = [c_{n-N_2}, ..., c_{n+N_1}]^T$ is the filter with length $N = N_1 + N_2 + 1$, $\mathbf{r}_n = [r_{n-N_2}, ..., r_{n+N_1}]^T$ is the received signal vector, $\mathcal{E}\{\}$ denotes the expectation, $\mathbf{H}$ is the $N \times (N + M - 1)$ convolution matrix defined as

$$\mathbf{H} = \begin{pmatrix} h_{M-1} & h_{M-2} & ... & h_0 & 0 & ... & & 0 \\ 0 & h_{M-1} & h_{M-2} & ... & h_0 & 0 & ... & 0 \\ & & & \ddots & & & & \\ 0 & & & ... & 0 & h_{M-1} & h_{M-2} & ... & h_0 \end{pmatrix}, \tag{3}$$

and $\mathbf{s}$ is the $(M + N_2)$-th column of $\mathbf{H}$. The MMSE filter that minimizes the cost function

$\mathcal{E}\{|x_n - y_n|^2\}$ is

$$\mathbf{c}_n = \left(\frac{\sigma_n^2}{\sigma_x^2}\mathbf{I} + \mathbf{H}\mathbf{V}_n\mathbf{H}^H + (1 - v_n)\mathbf{s}\mathbf{s}^H\right)^{-1}\mathbf{s}, \tag{4}$$

where $v_n = \mathcal{E}\{|x_n - \mathcal{E}\{x_n\}|^2\}$ and $\mathbf{V}_n = \text{diag}\{v_{n-M-N_2}, ..., v_{n+N_1}\}$. The statistics $\mathcal{E}\{x_n\}$ and v_n can be calculated from the extrinsic LLR, $\lambda_{D,n}^E$, obtained from the soft-output decoder. For BSPK,

$$\mathcal{E}\{x_n\} = 1 \cdot p\{x_n = 1\} + (-1) \cdot p\{x_n = -1\} = tanh\left(\frac{\lambda_{D,n}^E}{2}\right) \tag{5}$$

$$v_n = 1 - |\mathcal{E}\{x_n\}|^2. \tag{6}$$

At the first iteration, since there is no LLR available from the soft-output decoder, we set $\lambda_{D,n}^E = 0$ and this yields $\mathcal{E}\{x_n\} = 0$ and $v_n = 1$. The complexity of the MMSE filter is rather high because it requires an $N \times N$ matrix inversion for each n.

Low-complexity approximation of the MMSE filter can be obtained by assuming 1) $\mathcal{E}\{x_n\} = 0$ or 2) $\mathcal{E}\{x_n\} = x_n$. Under the former assumption, (4) reduces to the MMSE LE solution:

$$\mathbf{c}_{NA} = (\frac{\sigma_n^2}{\sigma_x^2}\mathbf{I} + \mathbf{H}\mathbf{H}^H)^{-1}\mathbf{s} \tag{7}$$

and under the latter assumption, (4) reduces to the matched filter:

$$\mathbf{c}_{MF} = 1/(\sigma_n^2/\sigma_x^2 + \mathbf{s}^H\mathbf{s}) \cdot \mathbf{s}. \tag{8}$$

The output of the soft-output filter y_n, under the condition that $x_n = x \in \{+1, -1\}$ has been sent at the transmitter, is assumed to be Gaussian with mean $\mu_{x,n} = \mathcal{E}\{y_n|x_n = x\}$ and variance $\sigma_{x,n}^2 = \mathcal{E}\{|y_n - \mu_{x,n}|^2|x_n = x\}$. The soft-output detector passes the extrinsic LLR,

$$\lambda_n^E = log\frac{p\{y_n|x_n = +1\}}{p\{y_n|x_n = -1\}} = \frac{2y_n\mu_{+1,n}}{\sigma_{+1,n}^2} \tag{9}$$

to the soft-output decoder.

1.2 MIMO signal detection

Multiple input and multiple output (MIMO) technique can achieve high spectral efficiency [2, 3] and reliability [10]- [13] in wireless environments. We focus on the *Bell Labs layered*

space time (BLAST) architecture or the MIMO system aimed at achieving the maximal efficiency in a flat fading environment and review the existing signal-detection techniques. With n_T transmit antennas and n_R receive antennas, the MIMO channel is modeled as

$$\mathbf{r} = \mathbf{H}\mathbf{x} + \mathbf{n}, \tag{10}$$

where $\mathbf{r} = [r_1, ..., r_{n_R}]$ is the channel output, $\mathbf{H} \in \mathbb{C}^{n_R \times n_T}$ is the channel matrix, $\mathbf{x} = [x_1, ..., x_{n_T}]$ is the channel input, and $\mathbf{n} = [n_1, ..., n_{n_R}]$ is the noise.

1.2.1 Conventional Methods

Maximal likelihood (ML) detection chooses the decision vector $\hat{\mathbf{x}}$ that minimizes $\|\mathbf{r} - \mathbf{H}\hat{\mathbf{x}}\|^2$. With an exhaustive search, the complexity is $|\mathcal{X}|^{n_T}$, where $|\mathcal{X}|$ is the symbol alphabet size. Since it has an exponentially increasing complexity with the number of channel inputs, it is often prohibitively complex.

Linear detection and *decision-feedback* (DF) detection are suboptimal schemes with reduced complexity. For those detection methods, both ZF and MMSE criteria can be used. MMSE criterion minimizes total power of *multiple access interference* (MAI) and noise, while ZF criterion removes only MAI. The DF detection can be considered as a modification of the DFE for ISI channels. However, in the DF detection, symbol-detection ordering is possible [14]- [16]. It is shown in [14] that choosing the best SNR at each stage in the detection process leads to optimum ordering. The performance of the linear and DF detection is limited because of noise enhancement and error-propagation.

1.2.2 Turbo BLAST

Figure 2 shows the block diagram of turbo-BLAST [17]. Similar to turbo equalization, it has a concatenated structure of an inner soft-output detector and an outer soft-output decoder separated by an interleaver and a deinterleaver.

The soft-output detector calculates the decision variable for the k-th symbol ($1 \leq k \leq n_R$),

$$y_k = \mathbf{w}_k^H \mathbf{r} - u_k, \tag{11}$$

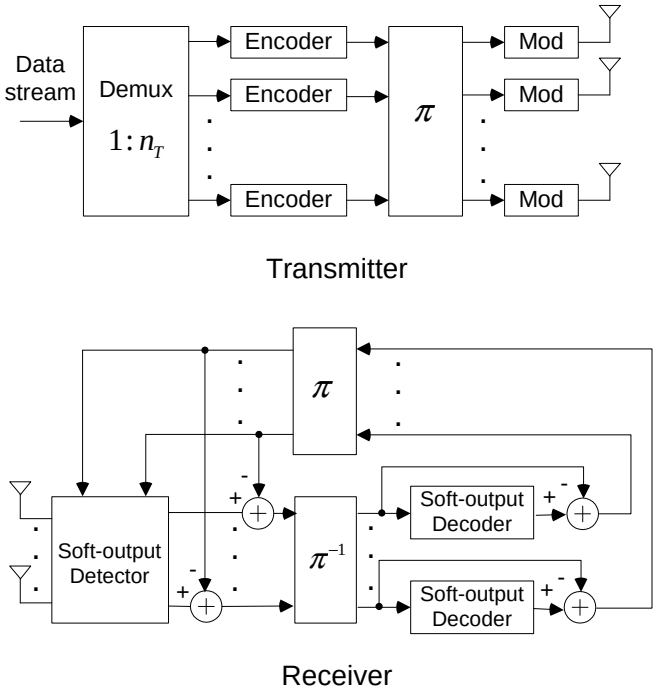

Figure 2. Turbo BLAST

where $\mathbf{w}_k \in \mathbb{C}^{n_R \times 1}$ and u_k are a linear filter and estimated interference, respectively. The optimum $\hat{\mathbf{w}}_k$ and $\hat{u}_k$ that minimize the cost function $\mathcal{E}\{|x_k - y_k|^2\}$ are

$$\hat{\mathbf{w}}_k = \left(\mathbf{h}_k\mathbf{h}_k^H + \mathbf{H}_k[\mathbf{I}_{(n_T-1)} - \mathrm{diag}\{\mathcal{E}\{\mathbf{x}_k\}\mathcal{E}\{\mathbf{x}_k\}^H\}]\mathbf{H}_k^H + \sigma_n^2/\sigma_x^2\mathbf{I}_{n_R}\right)^{-1}\mathbf{h}_k \quad (12)$$

$$\hat{u}_k = \mathbf{w}_k^H\mathbf{H}_k\mathcal{E}\{\mathbf{x}_k\}, \quad (13)$$

where $\mathbf{h}_k$ is the k-th column of $\mathbf{H}$, $\mathbf{H}_k \triangleq [\mathbf{h}_1, ..., \mathbf{h}_{k-1}, \mathbf{h}_{k+1}, ..., \mathbf{h}_{n_T}]$, $\mathbf{x}_k \triangleq [x_1, ..., x_{k-1}, x_{k+1}, ..., x_{n_T}]^T$, and diag$\{\}$ is the operator applied to a $L \times 1$ vector and outputs $L \times L$ diagonal matrix with the vector elements along the main diagonal. For the first iteration, $\mathcal{E}\{\mathbf{x}_k\} = \mathbf{0}$ and (12) reduces to a MMSE receiver

$$y_k = \mathbf{h}_k^H\left(\mathbf{H}\mathbf{H}^H + \frac{\sigma_n^2}{\sigma_x^2}\mathbf{I}_{n_R}\right)^{-1}\mathbf{r}. \quad (14)$$

As the iteration proceeds, we assume $\mathcal{E}\{\mathbf{x}_k\} \rightarrow \mathbf{x}_k$, and (12) simplifies to a perfect interference canceller:

$$y_k = (\mathbf{h}_k^H\mathbf{h}_h + \sigma_n^2/\sigma_x^2)^{-1}\mathbf{h}_k^H(\mathbf{r} - \mathbf{H}_k\mathbf{x}_k). \quad (15)$$

Similar to turbo equalization, $\mathcal{E}\{\mathbf{x}_k\}$ can be calculated from the extrinsic LLR of the

soft decoder. Also, y_k is assumed to be Gaussian and the extrinsic LLR of x_k calculated by the soft-output detector is input to the soft-output decoder.

CHAPTER 2

ITERATIVE EQUALIZATION BASED ON EST

2.1 System Description

The proposed iterative equalization is shown in Figure 3. A symbol block to be transmitted, $\{x_n\}_{n=0}^{N-1}$ with an average power σ_x^2 is mapped to $\{\tilde{x}_n\}_{n=0}^{N-1}$ by an EST, where N is the block size. A cyclic prefix with length ν is inserted between data blocks to prevent interblock interference.

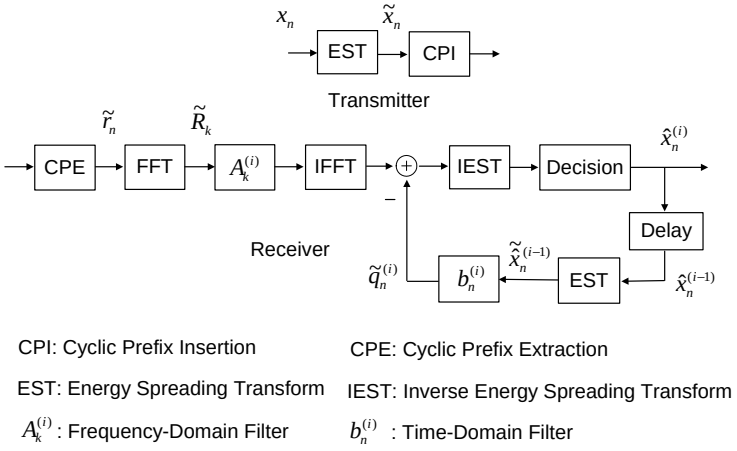

Figure 3. Low-complexity equalization

The channel is modeled as an $(L-1)$-th order FIR filter with coefficients, $\{h_k\}_{k=0}^{L-1}$, and *additive white Gaussian noise* (AWGN) with zero mean and variance σ_n^2. With enough length of cyclic prefix ($\nu \geq L-1$), the received samples can be expressed as the circular convolution [19] of the channel and the input symbols:

$$\tilde{r}_n = \sum_{k=0}^{L-1} h_k \tilde{x}_{(n-k)_N} + n_n, 0 \leq n \leq N-1, \tag{16}$$

where $(k)_N$ is the residue of k modulo N and n_n is the AWGN. It is assumed that the channel is static during a block and perfectly known at the receiver. After applying the *fast Fourier transform* (FFT), (16) can be represented by

$$\tilde{R}_k = H_k \tilde{X}_k + N_k, 0 \leq k \leq N-1, \tag{17}$$

where the uppercase letters represent the frequency-domain counterparts of their time-domain notations in lowercase letters.

Without the EST, the structure is just a *single-carrier system with frequency-domain equalization* (SC-FDE) [21]. With the EST, channel equalization can be iteratively performed to improve signal-detection performance. After forward frequency-domain equalization, the *inverse EST* (IEST) is performed for a hard or soft decision. The decided symbols are transformed by the EST and then fed back through the time-domain filter, which performs an N-point circular convolution.

At the first iteration, *minimum mean-square-error* (MMSE) criterion is used to determine the coefficients of the frequency-domain filter. Therefore, its frequency response will be

$$A_k^{(1)} = \frac{H_k^*}{|H_k|^2 + \sigma_n^2/\sigma_x^2}, k = 0, 1, ..., N-1, \tag{18}$$

where the superscript, $*$, denotes the complex conjugate. The impulse response of the time-domain filter is set to be zero:

$$b_n^{(1)} = 0.$$

From the second iteration ($i \geq 2$), the frequency-domain filter is chosen as the matched filter:

$$A_k^{(i)} = H_k^*.$$

The time-domain filter cancels the residual interference after the frequency-domain (matched) filter; therefore,

$$b_n^{(i)} = b_n \triangleq \begin{cases} g_n & (n \neq 0), \\ 0 & (n = 0), \end{cases} \tag{19}$$

where

$$g_n \triangleq \sum_l h_l h_{l-n}^*.$$

After the second iteration, we only iteratively process the same block of signal obtained from the *inverse FFT* (IFFT) at the second iteration.

As indicated in Section 2.2, the EST spreads the energy of each symbol to different frequencies and times. The purpose of frequency-domain spreading is to utilize the frequency

diversity; the symbol decision is based on the total energy transmitted over the whole bandwidth. By time-domain spreading, the energy of incorrectly decided symbols is spread to different times, which can be illustrated by Figure 4.

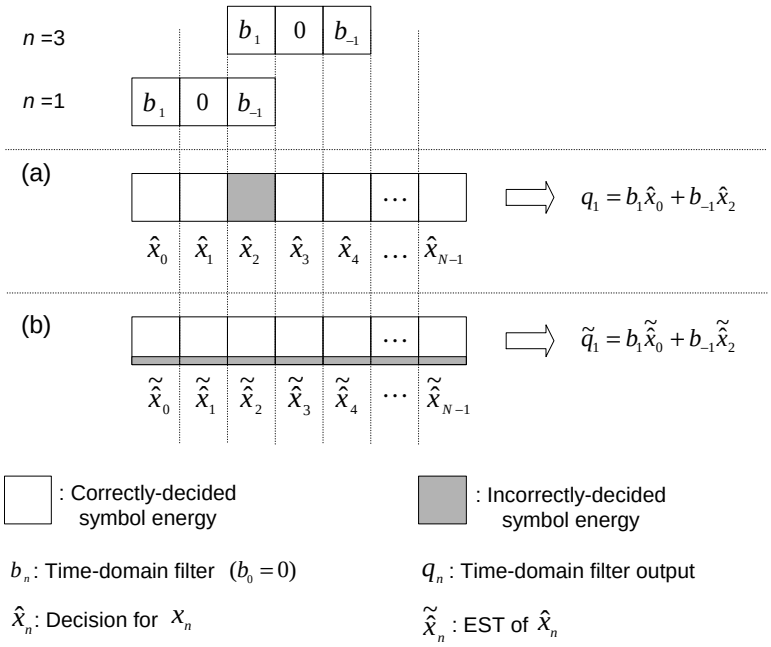

Figure 4. Principle of EST.

In Figure 4, we have assumed x_2 is incorrectly detected and the time-domain filter has three taps $\{b_{-1}, b_0, b_1\}$. Note that b_0 is always zero from (19). Without time-domain spreading, the incorrectly detected symbol will affect the detection of x_1 and x_3 through the time-domain filter as depicted in Figure 4 (a). If b_{-1} and b_1 are significant, the decision error of x_2 will cause large interference to the detection of x_1 and x_3. Consequently, the overall performance improvement will be limited. With time-domain spreading, on the other hand, the incorrectly detected symbol energy is spread over the whole block. Even though it affects detection of all the symbols in the block, as depicted in Figure 4 (b), the erroneous symbol energy captured by the time-domain filter for each symbol detection is reduced by a factor of the block size, N. Therefore, the probability of symbol decision error will be reduced compared with the equalizer without the EST if the initial number of incorrectly decided symbols is less than a certain threshold. Furthermore, the number of errors will keep on decreasing with iteration until it reaches the MFB.

2.2 Energy Spreading Transform

An EST is a normalized orthogonal transform whose role is to spread a symbol energy over the block in both the time and frequency domains. The "ideal EST" is an EST that has perfect spreading in both the time and frequency domain, that is,

$$|(\mathbf{E})_{l,n}| = |(\mathbf{FE})_{l,n}| = \frac{1}{\sqrt{N}} \tag{20}$$

and whose phase $\sphericalangle(\mathbf{E})_{l,n}$ is pseudo-randomly and even-symmetrically distributed in $[-\pi, \pi]$ for $0 \leq l, n \leq N-1$, where $\mathbf{E} \in \mathbb{C}^{N\times N}$ is the EST matrix, $(\mathbf{W})_{l,n}$ is the element of $\mathbf{W} \in \mathbb{C}^{N\times N}$ at the l-th row and n-th column, and $\mathbf{F} \in \mathbb{C}^{N\times N}$ is the normalized Fourier-transform matrix, i.e., $(\mathbf{F})_{l,n} = \frac{1}{\sqrt{N}} e^{-j2\pi ln/N}$.

An EST can be constructed by

$$\mathbf{E} = (\mathbf{P}_\mu)\mathbf{U}_\mu \mathbf{P}_{\mu-1}\mathbf{U}_{\mu-1}...\mathbf{P}_1\mathbf{U}_1, \tag{21}$$

where $\mathbf{U}_l \in \mathbb{C}^{N\times N}$ is a normalized unitary matrix, $\mathbf{P}_l \in \mathbb{C}^{N\times N}$ is a pseudo-random permutation matrix for $1 \leq l \leq \mu$, and μ is the number of unitary matrices.

To quantify the degree of spreading for an EST, we define the *time-* and *frequency-despreading factors* of $\mathbf{E}$, which will be shown to be closely related to the performance in Section 2.4. The n-th time-despreading factor of $\mathbf{E}$ is defined as

$$\mathbf{s}_T(\mathbf{E}^H; n) \triangleq \sum_{l=0}^{N-1} (|(\mathbf{E}^H)_{l,n}|^2 - \frac{1}{N})^2 \tag{22}$$

for $0 \leq n \leq N-1$, where the superscript H denotes the Hermitian transpose. Similarly, the n-th frequency-despreading factor of $\mathbf{E}$ is defined as

$$\mathbf{s}_F(\mathbf{E}; n) \triangleq \mathbf{s}_T(\mathbf{FE}; n) = \sum_{l=0}^{N-1} (|(\mathbf{FE})_{l,n}|^2 - \frac{1}{N})^2. \tag{23}$$

Because of the orthogonality and normality of $\mathbf{E}$, the n-th time- and frequency-despreading factors of $\mathbf{E}$ are bounded by

$$0 \leq s_T(\mathbf{E}^H; n), s_F(\mathbf{E}; n) \leq \frac{N-1}{N}. \tag{24}$$

It is obvious that an EST, $\mathbf{E}$ has perfect time spreading when $s_T(\mathbf{E}^H; n) = 0$ for all $0 \leq n \leq N-1$ and perfect frequency spreading when $s_F(\mathbf{E}; n) = 0$ for all $0 \leq n \leq N-1$.

In Table 1, we list six ESTs: $\mathbf{E}_1 \sim \mathbf{E}_3$ are based on Fourier transform and $\mathbf{E}_4 \sim \mathbf{E}_6$ are based on Hadamard transform. We use $\mathbf{T}$ to denote the normalized Hadamard matrix. When $\mathbf{E}_1$ is used, the system is equivalent to *orthogonal frequency-division multiplexing* (OFDM). Apparently, $\mathbf{E}_1$, $\mathbf{E}_2$, $\mathbf{E}_4$, and $\mathbf{E}_5$ have perfect time spreading, while $\mathbf{E}_3$ and $\mathbf{E}_6$ have perfect frequency spreading. It is shown in Appendix A that

$$s_F(\mathbf{E}_1; 0) = s_F(\mathbf{E}_2; 0) = s_T(\mathbf{E}_3^H; 0) = \frac{N-1}{N}, \tag{25}$$

independent of the permutation matrix $\mathbf{P}_1$. Similarly, it can also be shown that

$$s_F(\mathbf{E}_4; 0) = s_F(\mathbf{E}_5; 0) = s_T(\mathbf{E}_6^H; 0) = \frac{N-1}{N}. \tag{26}$$

Therefore, all the ESTs above have either the maximal time-despreading factor or the maximal frequency-despreading factor for $n = 0$. To compare the time- and frequency-despreading factors of different ESTs for $1 \le n \le N-1$, we have calculated $\mathcal{E}_d\{s_T(\mathbf{E}^H; n)\}$, $\mathcal{V}_d\{s_T(\mathbf{E}^H; n)\}$, $\mathcal{E}_d\{s_F(\mathbf{E}; n)\}$, and $\mathcal{V}_d\{s_F(\mathbf{E}; n)\}$, where $\mathcal{E}_d\{\}$ and $\mathcal{V}_d\{\}$ denote average and variance calculated over the index $1 \le n \le N-1$ (excluding $n = 0$), respectively. For the measurement of those parameters, we set $N = 2048$ and randomly generated the pseudo-random permutation matrix. From Table 1, $\mathbf{E}_1$ and $\mathbf{E}_4$ have a poor frequency spreading property, therefore, they are not good ESTs. We also see that the ESTs based on Fourier transform ($\mathbf{E}_2$ and $\mathbf{E}_3$) have better time- or frequency-spreading property than those based on Hadamard transform ($\mathbf{E}_5$ and $\mathbf{E}_6$).

Table 1. Spreading properties of some ESTs, $N = 2048$**.**

$\mathbf{E}_i$	$\mathcal{E}_d\{s_T(\mathbf{E}_i^H; n)\}$	$\mathcal{V}_d\{s_T(\mathbf{E}_i^H; n)\}$	$\mathcal{E}_d\{s_F(\mathbf{E}_i; n)\}$	$\mathcal{V}_d\{s_F(\mathbf{E}_i; n)\}$
$\mathbf{E}_1 = \mathbf{F}^H$	0	0	9.99×10^{-1}	0
$\mathbf{E}_2 = \mathbf{P}_1\mathbf{F}^H$	0	0	4.89×10^{-4}	4.73×10^{-10}
$\mathbf{E}_3 = \mathbf{F}^H\mathbf{P}_1\mathbf{F}^H$	4.89×10^{-4}	4.59×10^{-10}	0	0
$\mathbf{E}_4 = \mathbf{T}$	0	0	5.54×10^{-2}	3.43×10^{-3}
$\mathbf{E}_5 = \mathbf{P}_1\mathbf{T}$	0	0	4.89×10^{-4}	9.45×10^{-10}
$\mathbf{E}_6 = \mathbf{F}^H\mathbf{P}_1\mathbf{T}$	4.89×10^{-4}	5.81×10^{-10}	0	0

2.3 Complexity

Now, we discuss the complexity of the proposed scheme. In Table 2, listed are the required operations and the complexity (in number of multiplications) per block for the hard-decision receiver at each iteration. The block-wise complexity of (I)FFT, (I)EST, frequency-domain filter and time-domain filter are $Nlog_2N$, $\mu Nlog_2N$, N, and $(2L-2)N$, respectively, where μ is the number of the orthogonal matrices comprising the EST as defined in (21). Therefore, the block-wise complexity of the receiver for the first, the second, and the i-th ($i \geq 3$) iteration are $N((2+\mu)log_2N+1)$, $N(2(1+\mu)log_2N+2L-1)$, and $N(2\mu log_2N+2L-2)$, respectively. The block-wise complexity of the proposed scheme for each iteration is comparable to LE or DFE that is MN, where M is the total number of equalizer taps (feed forward and feedback) of LE or DFE.

Table 2. Computational Complexity. F-filter = frequency-domain filter, T-filter = time-domain filter, Y = required, N = not required.

Iteration (i)	FFT	F-filter	IFFT	IEST	EST	T-filter	Complexity
i = 1	Y	Y	Y	Y	N	N	$N((2+\mu)log_2N+1)$
i = 2	Y	Y	Y	Y	Y	Y	$N(2(1+\mu)log_2N+2L-1)$
i $\geq$ 3	N	N	N	Y	Y	Y	$N(2\mu log_2N+2L-2)$

2.4 Performance Analysis

We first summarize the notations and the matrix identities that will be used in our analysis. For any square matrix $\mathbf{W}=(x_{ij})_{i,j=0}^{N-1}$, define

$$tr\{\mathbf{W}\}=\sum_{n=0}^{N-1} w_{nn},$$

$$\mathcal{D}\{\mathbf{W}\}=\begin{pmatrix} w_{00} & 0 & \cdots & 0 \\ 0 & w_{11} & \ddots & 0 \\ \vdots & \ddots & \ddots & \vdots \\ 0 & 0 & \cdots & w_{N-1N-1} \end{pmatrix},$$

and

$$\bar{\mathcal{D}}\{\mathbf{W}\} = \mathbf{W} - \mathcal{D}\{\mathbf{W}\} = \begin{pmatrix} 0 & w_{01} & \cdots & w_{0N-1} \\ w_{10} & 0 & \ddots & w_{1N-1} \\ \vdots & \ddots & \ddots & \vdots \\ w_{N-1\ 0} & w_{N-1\ 1} & \cdots & 0 \end{pmatrix}.$$

From the above definitions, we have the following matrix identities,

- For $0 \leq n \leq N-1$,

$$(\mathcal{D}\{\mathbf{W}\}\mathcal{D}\{\mathbf{W}\}^H)_{n,n} = |(\mathbf{W})_{n,n}|^2, \tag{27}$$

and

$$\begin{aligned} (\bar{\mathcal{D}}\{\mathbf{W}\}\bar{\mathcal{D}}\{\mathbf{W}\}^H)_{n,n} &= (\mathbf{W}\mathbf{W}^H)_{n,n} - |(\mathbf{W})_{n,n}|^2 & (28) \\ &= \sum_{l \neq n} |(\mathbf{W})_{n,l}|^2. & (29) \end{aligned}$$

- For any orthogonal matrix $\mathbf{U}$,

$$tr\{\mathbf{U}^H \bar{\mathcal{D}}\{\mathbf{W}\}\mathbf{U}\} = 0. \tag{30}$$

- For any orthogonal matrix $\mathbf{U}$ and any diagonal matrix $\mathbf{W}_D$,

$$\mathcal{D}\{\mathbf{U}^H \mathbf{W}_D \mathbf{U}\} = m(\mathbf{W}_D)\mathbf{I} + \mathbf{\Delta}_D(\mathbf{W}_D; \mathbf{U}), \tag{31}$$

where

$$m(\mathbf{W}_D) \triangleq \frac{1}{N} \sum_{l=0}^{N-1} (\mathbf{W}_D)_{l,l} \tag{32}$$

is the average of the diagonal elements of $\mathbf{W}_D$ and $\mathbf{\Delta}_D(\mathbf{W}_D; \mathbf{U})$ is a diagonal matrix whose n-th diagonal element is

$$(\mathbf{\Delta}_D(\mathbf{W}_D; \mathbf{U}))_{n,n} \triangleq \sum_{l=0}^{N-1} (\mathbf{W}_D)_{l,l} (|(\mathbf{U})_{l,n}|^2 - \frac{1}{N}). \tag{33}$$

- Using the Cauchy-Schwarz inequality,

$$|\,(\mathbf{\Delta}_D(\mathbf{W}_D; \mathbf{U}))_{n,n}\,|^2 \leq \left(\sum_{l=0}^{N-1} |(\mathbf{W}_D)_{l,l}|^2 \right) s_T(\mathbf{U}; n), \tag{34}$$

where $s_T(\mathbf{U}; n)$ is the n-th time-despreading factor for $\mathbf{U}^H$ as defined in (22).

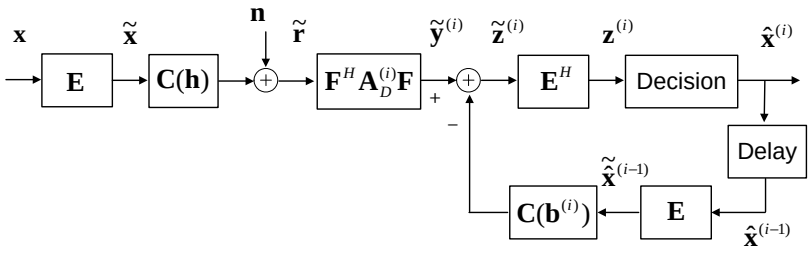

Figure 5. Equivalent system model

To facilitate our analysis, we use an equivalent model of the system in Figure 3. The equivalent model is shown in Figure 5. In the figure,

$$\mathbf{h} \triangleq [h_0, h_1, ..., h_{L-1}, \underbrace{0, ..., 0}_{N-L \ zeros}]^T \tag{35}$$

is an N-dimensional vector whose first L elements are $\{h_k\}_{k=0}^{L-1}$ and the rest are zero. $\mathbf{C}(\mathbf{h}) \in \mathbb{C}^{N\times N}$ is the circulant matrix [22] defined as

$$\mathbf{C}(\mathbf{h}) \triangleq \begin{pmatrix} h_0 & 0 & \cdots & 0 & h_{L-1} & \cdots & h_1 \\ h_1 & h_0 & \ddots & \ddots & 0 & \ddots & \vdots \\ \vdots & h_1 & \ddots & 0 & \vdots & \ddots & h_{L-1} \\ h_{L-1} & \vdots & \ddots & h_0 & 0 & \ddots & 0 \\ 0 & h_{L-1} & \ddots & h_1 & h_0 & \ddots & \vdots \\ \vdots & 0 & \ddots & \vdots & \vdots & \ddots & 0 \\ 0 & \vdots & \ddots & h_{L-1} & h_{L-2} & \ddots & h_0 \end{pmatrix}. \tag{36}$$

It is well-known that a circulant matrix can be diagonalized by the DFT matrix. For example,

$$\mathbf{C}(\mathbf{h}) = \mathbf{F}^H \mathbf{H}_D \mathbf{F}, \tag{37}$$

where

$$\mathbf{H}_D = \text{diag}(\mathbf{H}),$$

and $\mathbf{H}$ is the DFT of $\mathbf{h}$:

$$\mathbf{H} = \sqrt{N}\mathbf{F}\mathbf{h}.$$

Also, $\mathbf{b}$, $\mathbf{C}(\mathbf{b})$, $\mathbf{B}$, and $\mathbf{B}_D$ are similarly defined.

From Figure 5, the decision vector for the i-th iteration is

$$\begin{aligned}\mathbf{z}^{(i)} &= \mathbf{E}^H\mathbf{F}^H\mathbf{A}_D^{(i)}\mathbf{H}_D\mathbf{F}\mathbf{E}\mathbf{x} - \mathbf{E}^H\mathbf{C}(\mathbf{b}^{(i)})\mathbf{E}\hat{\mathbf{x}}^{(i-1)} \\ &\quad +\mathbf{E}^H\mathbf{F}^H\mathbf{A}_D^{(i)}\mathbf{F}\mathbf{n}, \end{aligned} \tag{38}$$

where $\mathbf{E}$ is the EST matrix defined in (21), $\hat{\mathbf{x}}^{(i-1)}$ is the hard- or soft-decision vector for $\mathbf{x}$ at the $(i-1)$-th iteration, and

$$\mathbf{A}_D^{(i)} = \mathrm{diag}(A_0^{(i)}, \cdots, A_{N-1}^{(i)}).$$

At each iteration, the n-th decision variable, $z_n^{(i)}$, consists of the desired signal, interference from other symbols, and noise components, whose powers are denoted as $\mathrm{P}_{si,n}^{(i)}$, $\mathrm{P}_{in,n}^{(i)}$, and $\mathrm{P}_{no,n}^{(i)}$, respectively. Then, the *symbol-error rate* (SER) at the i-th iteration, $p^{(i)}$, is the average of the SERs of each symbol, $p_n^{(i)}$:

$$p^{(i)} = \frac{1}{N}\sum_{n=0}^{N-1} p_n^{(i)} = \frac{1}{N}\sum_{n=0}^{N-1} \Psi(\mathrm{SINR}_n^{(i)}), \tag{39}$$

where

$$\mathrm{SINR}_n^{(i)} = \frac{\mathrm{P}_{si,n}^{(i)}}{\mathrm{P}_{in,n}^{(i)} + \mathrm{P}_{no,n}^{(i)}} \tag{40}$$

is the *signal-to-interference-noise ratio* (SINR) at the n-th symbol at the i-th iteration, and $\Psi(\cdot)$ is a function that maps SINR into SER for a given modulation scheme.

For the convenience of our analysis, we assume that the interference from other symbols be Gaussian. Consequently, for QPSK modulation [1],

$$\Psi(x) = 1 - [1 - Q(\sqrt{x})]^2. \tag{41}$$

2.4.1 MMSE Equalizer

At the first iteration, an MMSE equalizer is used. Therefore, the decision vector can be written as

$$\begin{aligned}\mathbf{z}^{(1)} &= \underbrace{\mathcal{D}\{\mathbf{E}^H\mathbf{F}^H\mathbf{M}_D\mathbf{F}\mathbf{E}\}\mathbf{x}}_{signal} + \underbrace{\bar{\mathcal{D}}\{\mathbf{E}^H\mathbf{F}^H\mathbf{M}_D\mathbf{F}\mathbf{E}\}\mathbf{x}}_{interference} \\ &\quad + \underbrace{\mathbf{E}^H\mathbf{F}^H\mathbf{A}_D^{(1)}\mathbf{F}\mathbf{n}}_{noise}, \end{aligned} \tag{42}$$

where

$$\mathbf{M}_D \triangleq \mathbf{A}_D^{(1)}\mathbf{H}_D.$$

From (28) and (42), the desired signal, interference, and noise powers for the n-th decision variable are

$$\mathrm{P}_{si,n}^{(1)} = \sigma_x^2\{(\mathbf{E}^H\mathbf{F}^H\mathbf{M}_D\mathbf{F}\mathbf{E})_{n,n}\}^2,$$

$$\mathrm{P}_{in,n}^{(1)} = \sigma_x^2[(\mathbf{E}^H\mathbf{F}^H\mathbf{M}_D^2\mathbf{F}\mathbf{E})_{n,n} - \{(\mathbf{E}^H\mathbf{F}^H\mathbf{M}_D\mathbf{F}\mathbf{E})_{n,n}\}^2],$$

and

$$\mathrm{P}_{no,n}^{(1)} = \sigma_n^2(\mathbf{E}^H\mathbf{F}^H|\mathbf{A}_D^{(1)}|^2\mathbf{F}\mathbf{E})_{n,n}.$$

As indicated before, $\mathbf{E} = \mathbf{F}^H$ corresponds to an OFDM system. In this case, interference from other symbols is zero and the SINR for the n-th decision variable is

$$\mathrm{SINR}_n^{ofdm} = \frac{\sigma_x^2|(\mathbf{H}_D)_{n,n}|^2}{\sigma_n^2}.$$

On the other hand, if $\mathbf{E} = \mathbf{I}$, the system will be SC-FDE with MMSE equalization. In this case, the SINR for the n-th decision variable is independent of n and can be expressed as

$$\mathrm{SINR}_n^{sc-mmse} = \frac{\sigma_x^2 m_{si}^2}{\sigma_x^2 m_{in} + \sigma_n^2 m_{no}}, \tag{43}$$

where m_{si}, m_{in}, and m_{no} are

$$m_{si} = \frac{1}{N}\sum_{l=0}^{N-1}(\mathbf{M}_D)_{l,l}, \tag{44}$$

$$m_{in} = \frac{1}{N}\sum_{l=0}^{N-1}\{(\mathbf{M}_D)_{l,l}\}^2 - \{\frac{1}{N}\sum_{l=0}^{N-1}(\mathbf{M}_D)_{l,l}\}^2, \tag{45}$$

and

$$m_{no} = \frac{1}{N}\sum_{l=0}^{N-1}|(\mathbf{A}_D^{(1)})_{l,l}|^2. \tag{46}$$

In general, the desired signal, interference, and noise powers for the n-th decision variable can be written as

$$\mathrm{P}_{si,n}^{(1)} = \sigma_x^2[m_{si} + \alpha_n]^2,$$

$$\mathrm{P}_{in,n}^{(1)} = \sigma_x^2[m_{in} + \beta_n - 2m_{si}\alpha_n - \alpha_n^2],$$

and

$$\mathrm{P}_{no,n}^{(1)} = \sigma_n^2[m_{no} + \gamma_n],$$

where

$$\alpha_n = (\mathbf{E}^H \bar{\mathcal{D}}\{\mathbf{F}^H \mathbf{M}_D \mathbf{F}\}\mathbf{E})_{n,n},$$

$$\beta_n = (\mathbf{E}^H \bar{\mathcal{D}}\{\mathbf{F}^H \mathbf{M}_D^2 \mathbf{F}\}\mathbf{E})_{n,n},$$

and

$$\gamma_n = (\mathbf{E}^H \bar{\mathcal{D}}\{\mathbf{F}^H |\mathbf{A}_D^{(1)}|^2 \mathbf{F}\}\mathbf{E})_{n,n}.$$

are perturbations. From (30), the averages of the perturbations are all zero:

$$\frac{1}{N}\sum_n \alpha_n = \frac{1}{N}\sum_n \beta_n = \frac{1}{N}\sum_n \gamma_n = 0.$$

Also, using matrix identity (31),

$$\alpha_n = \mathbf{\Delta}_D(\mathbf{M}_D; \mathbf{FE})_{n,n}, \tag{47}$$

$$\beta_n = \mathbf{\Delta}_D(\mathbf{M}_D^2; \mathbf{FE})_{n,n}, \tag{48}$$

and

$$\gamma_n = \mathbf{\Delta}_D(|\mathbf{A}_D^{(1)}|^2; \mathbf{FE})_{n,n}. \tag{49}$$

From (34) and (47)-(49), when $s_T(\mathbf{FE}; n)$ or $s_F(\mathbf{E}; n)$ is sufficiently small, α_n, β_n, and γ_n can be ignored and the SER can be approximated by

$$p^{(1)} = \frac{1}{N}\sum_{n=0}^{N-1} \Psi(\mathrm{SINR}_n^{(1)}) \simeq \Psi(\overline{\mathrm{SINR}}^{(1)}), \tag{50}$$

where $\overline{\mathrm{SINR}}^{(1)}$ is the mean SINR obtained by ignoring the perturbations in $\mathrm{SINR}_n^{(1)}$. For the EST with perfect frequency spreading, i.e., $s_F(\mathbf{E}; n) = 0$ for $0 \le n \le N-1$, α_n, β_n, and γ_n are all zero and (50) is an exact expression of the SER.

2.4.2 Genie-Aided Equalizer

For the genie-aided equalizer, the interference symbols are assumed to be known when detecting the desired symbol. Therefore, their effect on the desired symbol can be completely cancelled. It is derived in Appendix B that the decision vector will be

$$\mathbf{z}^{(g)} = g_0 \mathbf{x} + \mathbf{E}^H \mathbf{F}^H \mathbf{H}_D^H \mathbf{F}\mathbf{n}, \tag{51}$$

where

$$g_0 = (\mathbf{E}^H \mathcal{D}\{\mathbf{F}^H |\mathbf{H}_D|^2 \mathbf{F}\}\mathbf{E})_{n,n} = \frac{1}{N}\sum_l (|\mathbf{H}_D|^2)_{l,l}.$$

Consequently, the desired signal and noise power for the n-th decision variable are

$$\mathrm{P}_{si,n}^{(g)} = g_0^2 \sigma_x^2,$$

and

$$\mathrm{P}_{no,n}^{(g)} = \sigma_n^2 (g_0 + \xi_n),$$

respectively, where

$$\xi_n = (\mathbf{E}^H \bar{\mathcal{D}}\{\mathbf{F}^H |\mathbf{H}_D|^2 \mathbf{F}\}\mathbf{E})_{n,n}.$$

As discussed before, the average of ξ_n is zero, and for the EST with sufficiently small $s_F(\mathbf{E}; n)$, ξ_n can be neglected. Consequently, SER can be approximated as

$$p^{(g)} = \frac{1}{N}\sum_{n=0}^{N-1} \Psi(\mathrm{SINR}_n^{(g)}) \simeq \Psi(\overline{\mathrm{SINR}}^{(g)}), \tag{52}$$

where $\overline{\mathrm{SINR}}^{(g)}$ is the SINR obtained by ignoring the perturbation ξ_n in $\mathrm{SINR}_n^{(g)}$. Similar to Subsection 2.4.1, for the EST with perfect frequency spreading, i.e., $s_F(\mathbf{E}; n) = 0$ for $0 \le n \le N-1$, the perturbation $\xi_n = 0$ and (52) is an exact expression of the SER.

2.4.3 Iterative Equalizer with Hard Decision

We analyze the performance of the iterative equalizer with a hard decision. In this subsection, $\hat{\mathbf{x}}$ is used to denote the hard decision for $\mathbf{x}$. We first present a performance analysis for a finite block size and then describe a simplified analysis for an infinite block size.

It is shown in Appendix B that the decision vector for the iterative equalizer ($i \ge 2$) is

$$\mathbf{z}^{(i)} = \underbrace{g_0 \mathbf{x}}_{signal} + \underbrace{\mathbf{E}^H \mathbf{C}(\mathbf{b}) \mathbf{E} \mathbf{d}^{(i-1)}}_{interference} + \underbrace{\mathbf{E}^H \mathbf{F}^H \mathbf{H}_D^H \mathbf{F} \mathbf{n}}_{noise}, \tag{53}$$

where

$$\mathbf{d}^{(i)} = \mathbf{x} - \hat{\mathbf{x}}^{(i)} \tag{54}$$

is the hard-decision-error vector at the i-th iteration. Therefore, the desired signal and noise powers are same as those of the genie-aided receiver:

$$\mathrm{P}_{si,n}^{(i)} = \mathrm{P}_{si,n}^{(g)}, \tag{55}$$

and

$$\mathrm{P}_{no,n}^{(i)} = \mathrm{P}_{no,n}^{(g)}, \tag{56}$$

respectively.

The power of interference from other symbols depends on the number and location of errors at the previous iteration. Denote $D^{(i)}$ to be the set of the indices of incorrectly detected symbols in a block after the i-th iteration, whose cardinality is $N^{(i)}$. Then, the power of interference from other symbols in the n-th decision is

$$\mathrm{P}_{in,n}^{(i)}(D^{(i-1)}) = (\mathbf{E}^H\mathbf{C}(\mathbf{b})\mathbf{E}\mathbf{\Omega}(D^{(i-1)})\mathbf{E}^H\mathbf{C}(\mathbf{b})^H\mathbf{E})_{n,n}, \tag{57}$$

where

$$\mathbf{\Omega}(D^{(i-1)}) \triangleq \mathcal{E}\{\mathbf{d}^{(i-1)}{\mathbf{d}^{(i-1)}}^H | D^{(i-1)}\} \tag{58}$$

is the conditional error covariance matrix. $\mathbf{\Omega}(D^{(i)})$ is a diagonal matrix whose main diagonal consists of $N^{(i)}$ nonzero elements and $(N - N^{(i)})$ zero elements, and

$$\mathbf{\Omega}(D^{(i)})_{n,n} = \begin{cases} \kappa(N^{(i)}/N)\sigma_x^2 & \text{if } n \in D^{(i)} \\ 0 & \text{if } n \notin D^{(i)} \end{cases}, \tag{59}$$

where

$$\kappa(p) \triangleq \frac{\mathcal{E}\{|d_n|^2 | n \in D^{(i)}\}}{\sigma_x^2} \tag{60}$$

is a function of SER that depends on the modulation scheme. It can be shown that for QPSK,

$$\kappa(p) \simeq \frac{4}{2 - \frac{1}{2}p}. \tag{61}$$

By direct calculation, the power of interference in (57) can be decomposed into

$$\mathrm{P}_{in,n}^{(i)}(D^{(i-1)}) = \frac{N^{(i-1)}}{N}\kappa(\frac{N^{(i-1)}}{N})\sigma_x^2 g_0^2(K_n + \epsilon_n), \tag{62}$$

where

$$K_n = \frac{(\mathbf{E}^H\mathcal{D}\{\mathbf{C}(\mathbf{b})\mathcal{D}\{\mathbf{E}\mathbf{\Omega}(D^{(i-1)})\mathbf{E}^H\}\mathbf{C}(\mathbf{b})^H\}\mathbf{E})_{n,n}}{\frac{N^{(i-1)}}{N}\kappa(\frac{N^{(i-1)}}{N})\sigma_x^2 g_0^2} \tag{63}$$

and

$$\begin{aligned} \epsilon_n &= \frac{(\mathbf{E}^H\mathcal{D}\{\mathbf{C}(\mathbf{b})\bar{\mathcal{D}}\{\mathbf{E}\mathbf{\Omega}(D^{(i-1)})\mathbf{E}^H\}\mathbf{C}(\mathbf{b})^H\}\mathbf{E})_{n,n}}{\frac{N^{(i-1)}}{N}\kappa(\frac{N^{(i-1)}}{N})\sigma_x^2 g_0^2} \\ &+ \frac{(\mathbf{E}^H\bar{\mathcal{D}}\{\mathbf{C}(\mathbf{b})\mathbf{E}\mathbf{\Omega}(D^{(i-1)})\mathbf{E}^H\mathbf{C}(\mathbf{b})^H\}\mathbf{E})_{n,n}}{\frac{N^{(i-1)}}{N}\kappa(\frac{N^{(i-1)}}{N})\sigma_x^2 g_0^2}. \end{aligned} \tag{64}$$

By matrix identities (31) and (34), if $s_T(\mathbf{E}^H; n)$ is sufficiently small, K_n can be well approximated as a constant:

$$K_h \triangleq \frac{2}{g_0^2} \sum_{l=1}^{L-1} |g_l|^2, \tag{65}$$

which indicates the frequency selectivity of the channel. However, the perturbation term, ϵ_n, is comparable with K_h and it can not be ignored unless N is large enough. The conditional SINR for the n-th decision variable given $D^{(i-1)}$ is

$$\mathrm{SINR}_n^{(i)}(D^{(i-1)}) = \frac{1}{\frac{N^{(i-1)}}{N}\kappa(\frac{N^{(i-1)}}{N})(K_n + \epsilon_n) + \frac{g_0+\xi_n}{g_0^2 \mathrm{SNR}}}. \tag{66}$$

The probability that the symbol errors occur only at the indices in $D^{(i)}$ at the i-th iteration is

$$\mathcal{P}\{D^{(i)}\} = \prod_{n \in D^{(i)}} p_n^{(i)} \prod_{n \notin D^{(i)}} (1 - p_n^{(i)}). \tag{67}$$

Thus, the SER for the n-th symbol at the i-th iteration is

$$p_n^{(i)} = \sum_{D^{(i-1)}} \Psi(\mathrm{SINR}_n^{(i)}(D^{(i-1)})) \mathcal{P}\{D^{(i-1)}\},$$

where $\mathcal{P}\{\cdot\}$ stands for probability. From this, the the SER at each iteration can be calculated recursively.

Previously, we obtained a recursive formula to calculate the exact SER of the iterative equalizer for a finite block size. Here, we derive a simplified SER expression of the iterative equalizer for an infinite block size. For simplicity, we assume the EST is ideal. In this case, $s_F(\mathbf{E}; n) = 0$ for all $0 \leq n \leq N-1$; therefore, the perturbation terms disappear from the SINR_n expressions for MMSE and genie-aided equalizers:

$$\mathrm{SINR}_n^{(1)} = \overline{\mathrm{SINR}}^{(1)}, \tag{68}$$

$$\mathrm{SINR}_n^{(g)} = \overline{\mathrm{SINR}}^{(g)}, \tag{69}$$

which are independent of the symbol index n. Consequently, the SINR after MMSE equalization can be expressed as

$$\overline{\mathrm{SINR}}^{(1)} = \frac{1}{\frac{1}{N}\sum_{k=0}^{N-1} \frac{1}{\mathrm{SNR}|H_k|^2+1}} - 1. \tag{70}$$

The corresponding SER can be calculated by

$$p^{(1)} = \Psi(\overline{\mathrm{SINR}}^{(1)}). \tag{71}$$

Now, we show that the perturbation term that depends on n in the conditional interference power $\mathrm{P}_{in,n}^{(i)}(D^{(i-1)})$ in (62) can be ignored for a large N. From the definition of the ideal EST, we can write $(\mathbf{E})_{n,l} = \frac{1}{\sqrt{N}} e^{j\theta_{n,l}}$, where $\{\theta_{n,l}\}_{n,l=0}^{N-1}$ is pseudo-randomly and even-symmetrically distributed in $[-\pi, \pi]$. Define v_n as the interference component in the n-th decision variable of $\mathbf{z}^{(i)}$ in (53) given $D^{(i-1)}$:

$$v_n = \sum_{l \in D^{(i-1)}} c_{n,l} d_l^{(i-1)}, \tag{72}$$

where

$$\begin{aligned} c_{n,l} &\triangleq (\mathbf{E}^H \mathbf{C}(\mathbf{b}) \mathbf{E})_{n,l} \\ &= \frac{1}{N} \sum_{m_1=0}^{N-1} \sum_{m_2=0}^{N-1} (\mathbf{C}(\mathbf{b}))_{m_1,m_2} e^{j(\theta_{m_2,l} - \theta_{m_1,n})}. \end{aligned} \tag{73}$$

Considering $\theta_{m,l}$ as an independent random variable with zero mean, $c_{n,l}$ can be treated as a Gaussian random variable invoking the central limit theorem [23]. In this case, the mean and variance of $c_{n,l}$ are

$$\mathcal{E}\{c_{n,l}\} = 0,$$

and

$$\mathcal{V}\{c_{n,l}\} = \frac{1}{N^2} \sum_{m_1} \sum_{m_2} |(\mathbf{C}(\mathbf{b}))_{m_1,m_2}|^2 = \frac{g_0^2 K_h}{N},$$

respectively, where $\mathcal{E}\{\cdot\}$ and $\mathcal{V}\{\cdot\}$ denote statistical expectation and variance, respectively. Also, we see that c_{n,l_1} and c_{n,l_2} are independent for $l_1 \neq l_2$ since they are Gaussian and $\mathcal{E}\{c_{n,l_1} c_{n,l_2}\} = \mathcal{E}\{c_{n,l_1}\}\mathcal{E}\{c_{n,l_2}\} = 0$. Therefore, v_n in (72) is the sum of $N^{(i-1)}$ independent complex Gaussian random variables. Consequently, the conditional interference power for the n-th decision variable,

$$Y_n \triangleq P_{in,n}^{(i)}(D^{(i-1)}) = \mathcal{E}\{|v_n|^2 | D^{(i-1)}\} \tag{74}$$

is a χ^2-distributed random variable with $2N^{(i-1)}$ degrees of freedom, whose *probability density function* (PDF) is

$$\begin{aligned} f_{Y_n}(y|D^{(i-1)}) &= \frac{1}{\sigma_\chi^2 2^{N^{(i-1)}}\Gamma(N^{(i-1)})} y^{N^{(i-1)}-1} e^{-y/2\sigma_\chi^2} \\ &= f_{Y_n}(y|N^{(i-1)}), \end{aligned} \tag{75}$$

where

$$\sigma_\chi^2 = \frac{\kappa(\frac{N^{(i-1)}}{N})\sigma_x^2 g_0^2 K_h}{2N}.$$

In (75) we changed the condition of $f_{Y_n}(y|D^{(i-1)})$ to $N^{(i-1)}$ since it depends only on $N^{(i-1)}$ rather than $D^{(i-1)}$. Hereafter, for this reason, we change the condition from $D^{(i-1)}$ to $N^{(i-1)}$ in all the related conditional functions, i.e., the power of interference, SINR, and SER. The mean and variance of Y_n are

$$\mathcal{E}\{Y_n\} = 2N^{(i-1)}\sigma_\chi^2 = \frac{N^{(i-1)}}{N}\kappa(\frac{N^{(i-1)}}{N})\sigma_x^2 g_0^2 K_h, \tag{76}$$

and

$$\mathcal{V}\{Y_n\} = 4N^{(i-1)}\sigma_\chi^4 = \frac{N^{(i-1)}}{N^2}\kappa(\frac{N^{(i-1)}}{N})^2\sigma_x^4 g_0^4 K_h^2, \tag{77}$$

respectively. Therefore, for a large N, $\mathcal{V}\{Y_n\}$ is small and $P_{in,n}^{(i)}(N^{(i-1)})$ can be approximated to its mean in (76), which is independent of the symbol index n.

From the above discussion, for an iterative equalizer with the ideal EST and a large N, the SINR can be simplified to

$$\overline{\mathrm{SINR}}^{(i)}(N^{(i-1)}) = \frac{1}{\frac{N^{(i-1)}}{N}\kappa(\frac{N^{(i-1)}}{N})K_h + \frac{1}{g_0\mathrm{SNR}}}. \tag{78}$$

Consequently, the conditional SER is

$$p^{(i)}(N^{(i-1)}) = \Psi(\overline{\mathrm{SINR}}^{(i)}(N^{(i-1)})). \tag{79}$$

In this case, SER is independent of n and the probability of having k symbol-errors in an N-symbol block at the i-th iteration is

$$\mathcal{P}\{N^{(i)} = k\} = \binom{N}{k}(p^{(i)})^k(1-p^{(i)})^{N-k}, \tag{80}$$

for $k = 0,\ 1, \cdots, N$. Consequently, the SER at the i-th ($i \geq 2$) iteration is

$$p^{(i)} = \sum_{n=0}^{N} p^{(i)}(N^{(i-1)} = n)\mathcal{P}\{N^{(i-1)} = n\}. \tag{81}$$

From Equations (70), (71), and (78) - (81), the SER after the i iteration can be calculated.

To study the asymptotic property, we first define the relative frequency of symbol error in a block after the i-th iteration by

$$F^{(i)} \triangleq \frac{N^{(i)}}{N}. \tag{82}$$

Therefore, (81) can be expressed in terms of $F^{(i-1)}$ as

$$p^{(i)} = \sum_{n=0}^{N} p^{(i)}(F^{(i-1)} = \frac{n}{N})\mathcal{P}\{F^{(i-1)} = \frac{n}{N}\}. \tag{83}$$

When $N \longrightarrow \infty$, (83) can be written as

$$p^{(i)} = \int_0^1 \Psi(\overline{\mathrm{SINR}}^{(i)}(F^{(i-1)} = x)) f_{F^{(i-1)}}(x)dx, \tag{84}$$

where $f_{F^{(i-1)}}(x)$ is the PDF of $F^{(i-1)}$. From the DeMoivre-Laplace Theorem [23], $f_{F^{(i-1)}}(x)$ can be approximated as Gaussian PDF with mean $p^{(i-1)}$ and variance $\frac{p^{(i-1)}(1-p^{(i-1)})}{N}$. By the definition of the Dirac Delta function $\delta(x)$ [24],

$$\lim_{N\to\infty} f_{F^{(i-1)}}(x) = \delta(x - p^{(i-1)}).$$

Therefore, the effective SINR is

$$\begin{aligned} \overline{\mathrm{SINR}}^{(i)} &= \overline{\mathrm{SINR}}^{(i)}(F^{(i-1)} = p^{(i-1)}) & (85)\\ &= \frac{1}{K_h p^{(i-1)} \kappa(p^{(i-1)}) + \frac{1}{g_0 \mathrm{SNR}}}. & (86) \end{aligned}$$

and

$$p^{(i)} = \Psi(\overline{\mathrm{SINR}}^{(i)}). \tag{87}$$

The strong law of large numbers states that the relative frequency $F^{(i-1)}$ approaches $p^{(i-1)}$ *almost everywhere* (AE) [23]. Let

$$r(x) \triangleq \Psi(\frac{1}{K_h x \kappa(x) + \frac{1}{g_0 \mathrm{SNR}}}).$$

Then $r(x)$ is continuous in the interval $[0,1]$ and differentiable in $(0,1)$, and

$$|r(F^{(i-1)}) - r(p^{(i-1)})| \leq \mathrm{R}_{max}|F^{(i-1)} - p^{(i-1)}|$$

where $\mathrm{R}_{max} = \max_{x\in(0,1)} |\frac{dr}{dx}|$ is a finite number. Therefore, the convergence in (87) is also AE.

From (86) and (87), the SINR after the i-th iteration is inversely proportional to $p^{(i-1)}$, and $p^{(i)}$ monotonically decreases with $\mathrm{SINR}^{(i)}$. Therefore, if

$$\overline{\mathrm{SINR}}^{(1)} < \overline{\mathrm{SINR}}^{(2)}, \tag{88}$$

then $\check{p} = \lim_{i\to\infty} p^{(i)}$ and $\overline{\check{\mathrm{SINR}}} = \lim_{i\to\infty} \overline{\mathrm{SINR}}^{(i)}$ exist and satisfy the following equations

$$\check{p} = \Psi(\overline{\check{\mathrm{SINR}}}) \tag{89}$$

and

$$\overline{\check{\mathrm{SINR}}} = \frac{1}{K_h\check{p}\alpha(\check{p}) + \frac{1}{g_0\mathrm{SNR}}}. \tag{90}$$

In particular, from (41), (86) and (89), for QPSK symbols, $\check{p}$ is determined by

$$1 - \left[1 - Q\left(\sqrt{\left(\frac{4}{2-0.5\check{p}}K_h\check{p} + \frac{1}{g_0\mathrm{SNR}}\right)^{-1}}\right)\right]^2 = \check{p} \tag{91}$$

It can be seen from (91) that for a sufficiently small $\check{p}$, the interference term is negligible compared with $1/(g_0\mathrm{SNR})$; consequently, $\overline{\check{\mathrm{SINR}}}$ is very close to SNR, the MFB.

From the above discussion, the iterative equalization converges above a SNR threshold, SNR_T that satisfies $\overline{\mathrm{SINR}}^{(1)} = \overline{\mathrm{SINR}}^{(2)}$. Equivalently, if $\mathrm{SNR} > \mathrm{SNR}_T$, the following inequality holds:

$$\frac{1}{\frac{1}{N}\sum_{k=0}^{N-1}\frac{1}{\mathrm{SNR}|H_k|^2+1}} - 1 < \frac{1}{\alpha(p_s^{(1)})K_hp^{(1)} + \frac{1}{g_0\mathrm{SNR}}}. \tag{92}$$

Furthermore, we have proved in Appendix D that SNR_T exists for all channels. Therefore, the iterative approach always converges to the MFB as long as SNR is large enough.

2.4.4 Iterative Equalizer with Soft Decision

By feeding back the soft decision, we can prevent error propagation in the hard-decision equalizer and further enhance the performance, especially at low SNR. In this subsection, we denote $\hat{\mathbf{x}}$ as the soft decision for $\mathbf{x}$. Also, for simplicity, we assume that QPSK and the ideal EST are employed.

We consider the normalized decision vector at the i-th iteration

$$\mathbf{z}^{(i)} = \mathbf{x} + \mathbf{e}^{(i)}, \tag{93}$$

where $\mathbf{e}^{(i)}$ is the pre-decision-error vector that consists of noise and interference. As in the previous section, each element $e_n^{(i)}$ of $\mathbf{e}^{(i)}$ is assumed to be independent for different n's and complex Gaussian with power $(\sigma_{e,n}^{(i)})^2$. For QAM modulation, all the variables in (93) are complex, they can be decomposed into real (in-phase) and imaginary (quadrature) components, that is, $z_n^{(i)} \triangleq z_{I,n}^{(i)} + j z_{Q,n}^{(i)}$, $x_n \triangleq x_{I,n} + j x_{Q,n}$, and $e_n^{(i)} \triangleq e_{I,n}^{(i)} + j e_{Q,n}^{(i)}$. Hereafter, to avoid repetition, we will describe only the in-phase component of a complex variable. The quadrature component can be similarly defined.

Log-likelihood ratio (LLR), which is widely known in the turbo literature [4, 8, 9], is employed here for the soft decision. The *a posteriori* LLR of $x_{I,n}$ at the i-th iteration is

$$\lambda_{I,n}^{(i)} \triangleq \log \frac{\mathcal{P}[x_{I,n} = +1 | z_{I,n}^{(i)}]}{\mathcal{P}[x_{I,n} = -1 | z_{I,n}^{(i)}]}. \tag{94}$$

It can be decomposed into

$$\lambda_{I,n}^{(i)} = \lambda_{I,n}^{E,(i)} + \lambda_{I,n}^{P,(i)}, \tag{95}$$

where

$$\lambda_{I,n}^{E,(i)} \triangleq \log \frac{\mathcal{P}[z_{I,n}^{(i)} | x_{I,n} = +1]}{\mathcal{P}[z_{I,n}^{(i)} | x_{I,n} = -1]} = \frac{2 z_{I,n}^{(i)}}{(\sigma_{e,I,n}^{(i)})^2} \tag{96}$$

and

$$\lambda_{I,n}^{P,(i)} \triangleq \log \frac{\mathcal{P}[x_{I,n} = +1]}{\mathcal{P}[x_{I,n} = -1]} \tag{97}$$

are the *extrinsic* LLR and the *a priori* LLR, respectively. We use the *extrinsic* LLR from the previous iteration as the *a priori* LLR:

$$\lambda_{I,n}^{P,(i)} = \lambda_{I,n}^{E,(i-1)}. \tag{98}$$

For the first iteration, since there is no *a priori* LLR available, we set $\lambda_{I,n}^{P,(1)} = 0$. Also, as shown in Appendix C, pre-decision-error power after MMSE equalization is

$$(\sigma_{e,n}^{(1)})^2 = \left(\frac{1}{\frac{1}{N}\sum_k \frac{|H_k|^2}{|H_k|^2+1/\mathrm{SNR}}} - 1 \right) \sigma_x^2 \tag{99}$$

$$\triangleq (\sigma_e^{(1)})^2, \tag{100}$$

which is independent of n. Each component has the same pre-detection-error power after MMSE equalization, that is, $(\sigma_{e,I}^{(1)})^2 = (\sigma_{e,Q}^{(1)})^2 = (\sigma_e^{(1)})^2/2$.

The soft decision for $x_{I,n}$ is the conditional expectation of $x_{I,n}$ given the observation $z_{I,n}^{(i)}$:

$$\hat{x}_{I,n}^{(i)} \triangleq \mathcal{E}\{x_{I,n}|z_{I,n}^{(i)}\} = \mathcal{P}[x_{I,n} = 1|z_{I,n}^{(i)}] - \mathcal{P}[x_{I,n} = -1|z_{I,n}^{(i)}], \tag{101}$$

which, in terms of LLR, can be easily shown to be

$$\hat{x}_{I,n}^{(i)} = tanh(\frac{\lambda_{I,n}^{(i)}}{2}). \tag{102}$$

The soft-decision error for the n-th symbol at the i-th iteration is defined as

$$\bar{d}_n^{(i)} \triangleq x_n - \hat{x}_n^{(i)}. \tag{103}$$

The power of its in-phase component is

$$\mathcal{E}\{(\bar{d}_{I,n}^{(i)})^2|z_{I,n}^{(i)}\} = (1-\hat{x}_{I,n}^{(i)})^2\mathcal{P}\{x_{I,n} = 1|z_{I,n}^{(i)}\} + (1+\hat{x}_{I,n}^{(i)})^2\mathcal{P}\{x_{I,n} = -1|z_{I,n}^{(i)}\}$$

$$= 1 - (\hat{x}_{I,n}^{(i)})^2. \tag{104}$$

Similar to the hard-decision case in (B.5), the decision variable (after normalization) is

$$\mathbf{z}^{(i)} = \underbrace{\mathbf{x}}_{signal} + \underbrace{\frac{1}{g_0}\mathbf{E}^H\mathbf{C}(\mathbf{b}^{(i)})\mathbf{E}\bar{\mathbf{d}}^{(i-1)}}_{interference} + \underbrace{\frac{1}{g_0}\mathbf{E}^H\mathbf{F}^H\mathbf{H}_D^H\mathbf{F}\mathbf{n}}_{noise}, \tag{105}$$

where $\bar{\mathbf{d}}^{(i)}$ is the soft-decision error vector at the i-th iteration. The conditional interference power given $\mathbf{z}^{(i-1)}$ is

$$\mathrm{P}_{in,n}(\mathbf{z}^{(i-1)}) = \frac{1}{g_0^2}(\mathbf{E}^H\mathbf{C}(\mathbf{b})\mathbf{E}\bar{\mathbf{\Omega}}(k)_D\mathbf{E}^H\mathbf{C}(\mathbf{b})^H\mathbf{E})_{n,n}, \tag{106}$$

where

$$\bar{\mathbf{\Omega}}(k)_D \triangleq \mathcal{E}\{\bar{\mathbf{d}}^{(i-1)}\bar{\mathbf{d}}^{(i-1)H}|\mathbf{z}^{(i-1)}\} \tag{107}$$

is the conditional soft-decision-error covariance matrix. As in the previous section, for a finite block size, $\mathrm{P}_{in,n}(\mathbf{z}^{(i-1)})$ depends on the index n and the complexity of calculating its value for each n, $0 \leq n \leq N-1$, is high. However, for an infinite block size and employing the ideal EST, $\mathrm{P}_{in,n}(\mathbf{z}^{(i-1)})$ is equal to its average value,

$$P_{in}^{(i)} = \frac{K_h}{N} \sum_{n=0}^{N-1} \mathcal{E}\{|\bar{d}_n^{(i-1)}|^2 | z_n^{(i-1)}\},$$

which does not depend on n. In this case, the pre-decision error power at the i-th iteration ($i \geq 2$) is independent of n and given by

$$(\sigma_{e,I}^{(i)})^2 = P_{in,I}^{(i)} + \frac{\sigma_{n,I}^2}{g_0}, \tag{108}$$

where

$$P_{in,I}^{(i)} = \frac{K_h}{N} \sum_{n=0}^{N-1} \mathcal{E}\{(\bar{d}_{I,n}^{(i-1)})^2 | z_{I,n}^{(i-1)}\}.$$

Finally, for an infinite block length, the SER at the i-th iteration ($i \geq 1$) is

$$p^{(i)} = \Psi(\frac{\sigma_x^2}{(\sigma_e^{(i)})^2}), \tag{109}$$

where $(\sigma_e^{(i)})^2 = (\sigma_{e,I}^{(i)})^2 + (\sigma_{e,Q}^{(i)})^2$.

2.5 Simulation Results

In this section, we present simulation results using QPSK modulation. Since the performance of an equalizer usually depends on the characteristics of a channel, we present our results for different types of channels.

2.5.1 Performance for Proakis-B channel

In this subsection, we present the performance of the hard- and soft-decision equalizer with different ESTs and block sizes using the Proakis-B channel [1], whose impulse response and K_h are

$$h_n^{Proakis-B} = 0.407\delta_n + 0.815\delta_{n-1} + 0.407\delta_{n-2},$$

$$K_h = 0.94,$$

respectively. We consider $\mathbf{E}_1$, $\mathbf{E}_2$, $\mathbf{E}_5$ in Table 1 in our simulation. Since each EST in Table 1 has either the maximal time- or the maximal frequency-despreading factor for $n = 0$, we send a dummy symbol for x_0 and transmit information through the rest of the $N - 1$ symbols.

Figure 6 (a) compares the analytical and simulation results for the hard-decision equalizer. To calculate analytical performance, we used the ideal EST and an infinite block size. For the simulation results, we used $\mathbf{E}_1$, $\mathbf{E}_2$, and $\mathbf{E}_5$ for the EST and set the block size at $N = 2048$. Note that the hard-decision equalizer with $\mathbf{E}_1$ corresponds to OFDM. From the

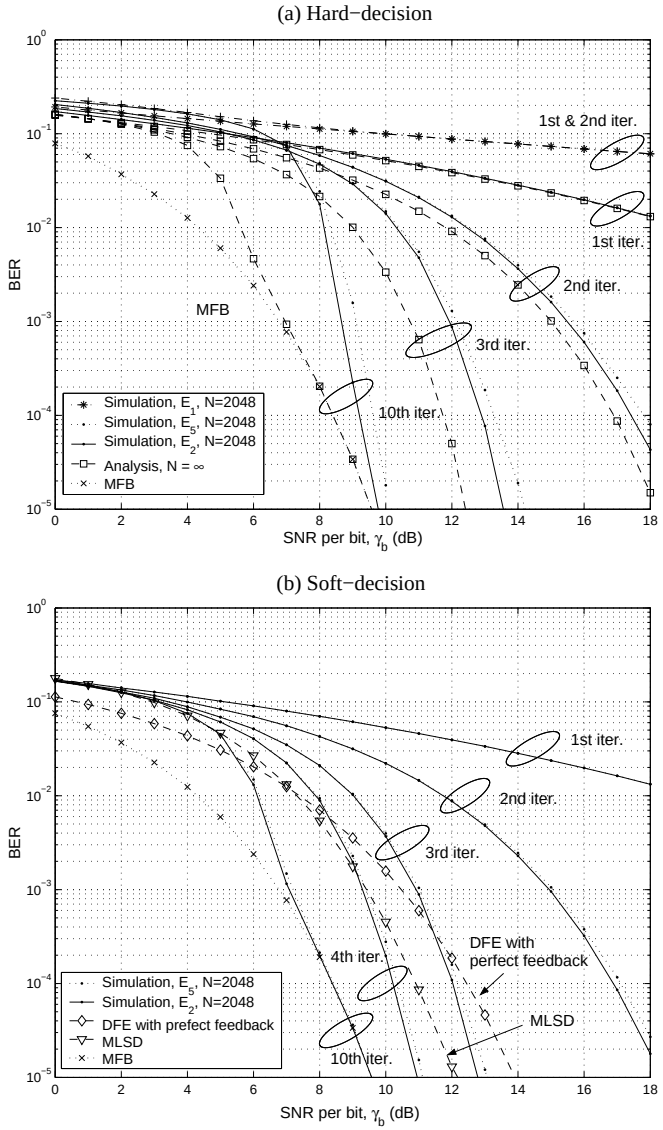

Figure 6. Performance of the EST-based equalizer for Proakis-B channel.

figure, the iterative equalizer with $\mathbf{E}_1$ as an EST has no performance improvement with iteration since $\mathbf{E}_1$ has poor frequency spreading. The BER of the equalizer based on $\mathbf{E}_2$ improves with the number of iterations when SNR is above 7 dB. After the tenth iteration, the required SNR for a 10^{-5} BER is about 9.8 dB, which is only 0.2 dB from the MFB. The equalizer based on $\mathbf{E}_5$ shows slightly worse performance than that based on $\mathbf{E}_2$. The analysis for the MMSE equalizer (1st iteration) is very close to the simulation result. There is a performance gap between the analytical and simulation results for the other iterations, which is due to finite block length and imperfect energy spreading.

Figure 6 (b) shows the performance of the soft-decision equalizer compared with that of the MLSD [1] and the DFE assuming perfect feedback [1], which are two conventional schemes that do not employ the EST. By feeding back the soft decision, the performance is significantly improved over the hard-decision case, especially at a low SNR. After the tenth iteration, there is almost a 2 dB gain for the soft decision at BER = 10^{-2} over the hard decision. The soft-decision equalizer based on $\mathbf{E}_2$, after the third iteration, outperforms the DFE with perfect feedback by 0.4 dB at BER = 10^{-4}. After the tenth iteration and at BER = 10^{-4}, its performance is 2.5 dB better than the MLSD and is very close to the MFB.

Figure 7 shows the relationship between the performance of the hard-decision equalizer at 10 dB and its block size. The performance degrades as block size decreases, which can

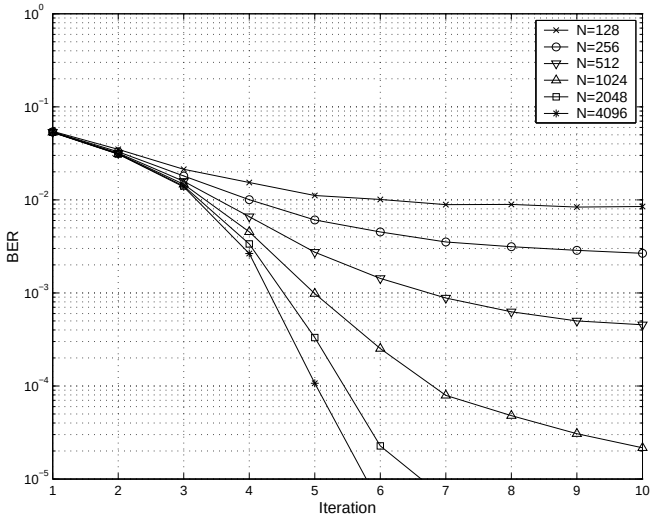

Figure 7. BER performance verses iteration with different block sizes N at 10 dB for Proakis-B channel and hard decision.

be anticipated from the variance of $Y_n \triangleq P_{in,n}^{(i)}(D^{(i-1)})$ in (77); the block performance, conditioned on $D^{(i-1)}$, is dominated by the symbol detection with the largest $P_{in,n}^{(i)}(D^{(i-1)})$, but decreasing block size increases the variance of $P_{in,n}^{(i)}(D^{(i-1)})$.

2.5.2 Performance for other challenging channels

In this subsection, we present the performance of the equalizer for other challenging channels. In the simulation, we use $\mathbf{E}_2$ for the EST and the block size N is assumed to be 2048 if not explicitly stated.

Figure 8 (a) shows the performance of the equalizer for the channel proposed by Porat and Friedlander [26], whose normalized impulse response and K_h are

$$\begin{aligned} h_n^{Porat\,et\,al} &= (0.485 - 0.097j)\delta_n + (0.364 + 0.437j)\delta_{n-1} + 0.243\delta_{n-2} \\ &\quad + (0.291 - 0.315j)\delta_{n-3} + (0.194 + 0.388j)\delta_{n-4}, \\ K_h &= 0.73, \end{aligned}$$

respectively. The SNR threshold for the hard-decision equalizer occurs near 3.1 dB. Also, its performance after the tenth iteration and above 6 dB is similar to that of the soft-decision equalizer and very close to the MFB.

Figure 8 (b) shows the performance of the equalizer for the Proakis-C channel, whose impulse response and K_h are

$$\begin{aligned} h_n^{Proakis-C} &= 0.227\delta_n + 0.460\delta_{n-1} + 0.688\delta_{n-2} + 0.460\delta_{n-3} + 0.227\delta_{n-4}, \\ K_h &= 2.13, \end{aligned}$$

respectively. This channel has the severest frequency selectivity among the deterministic channels used for the simulation. With this channel, because of the high K_h, $N = 2048$ is not sufficiently large for the hard-decision equalizer to be approximated as the ideal hard-decision equalizer with an infinite block size. Therefore, we use $N = 4096$ for the simulation with this channel. The SNR threshold occurs near 22.6 dB, which is much higher than that of the previous channels. However, the performance of the equalizer with the soft decision, after the tenth iteration and at BER $= 10^{-5}$, has 8.5 dB gain over the hard decision and

(a) Porat and Friedlander channel

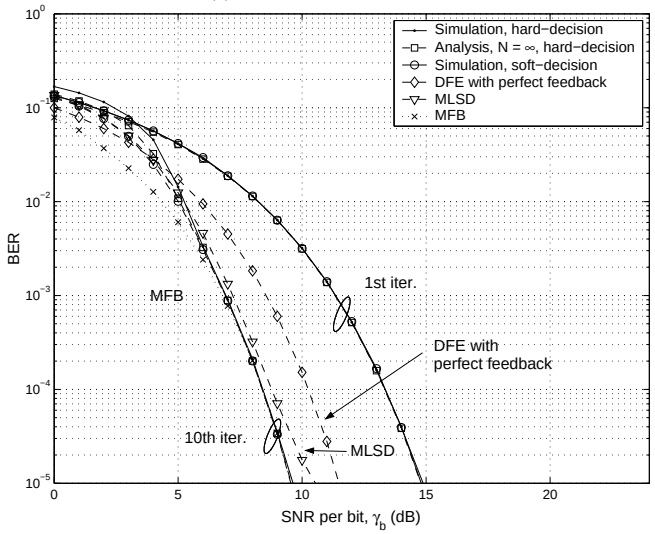

(b) Proakis−C channel

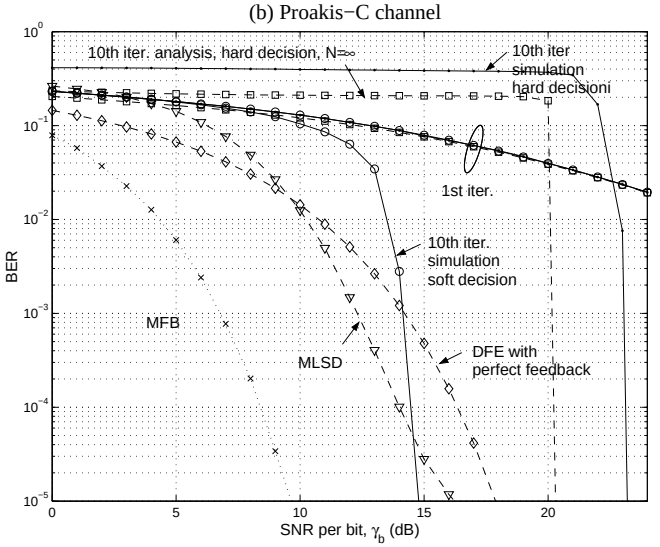

(c) BU channel

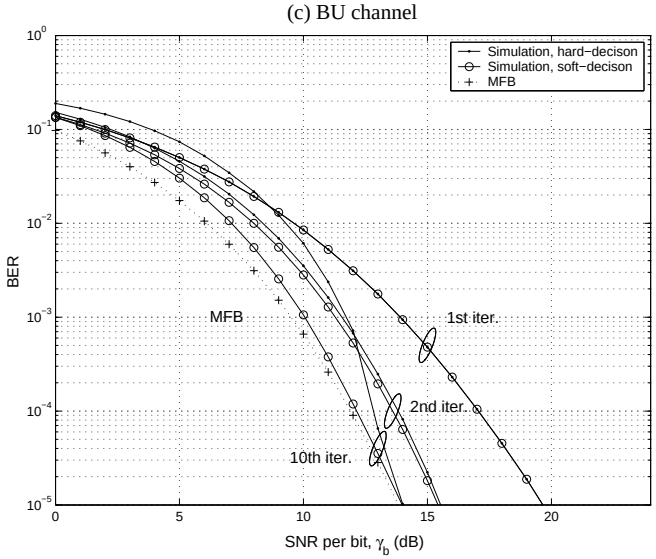

Figure 8. Performance of the EST-based equalizer for different types of channels.

outperforms the MLSD and the DEF with perfect feedback by 1.5 dB and 3 dB, respectively. From the slope of the BER curves of the equalizer and the MFB, we can estimate that the proposed equalizer, after the tenth iteration, will reach the MFB at a very low BER (far below 10^{-5}) near 15 dB and 23.3 dB for a soft decision and a hard decision, respectively.

Figure 8 (c) shows the average performance of the equalizer for reduced *bad-urban* (BU) [29] channel. We use reduced BU power delay profile to generate 1000 *finite impulse response* (FIR) channel realizations that have, assuming 0.95 μs symbol duration, 11 symbol-spaced taps. For those channel realizations, the mean and variance of K_h are 0.63 and 0.045, respectively. Also, the mean and variance of g_0 are 1.0 and 0.261, respectively. For the channel realizations with low g_0 and/or high K_h, the SNR threshold will be high. Below 13 dB, as shown in the figure, the performance of the hard-decision equalizer, after the tenth iteration, is dominated by error propagation of those channels with a high SNR threshold. However, the soft-decision equalizer prevents error propagation and shows good performance, which is close to the MFB after the tenth iteration.

CHAPTER 3

IMPROVED SCHEME FOR ENERGY SPREADING TRANSFORM BASED EQUALIZATION

3.1 Optimal Equalization Filter Design

In Chapter 2, conventional MMSE equalization [1] is used at the first iteration, and matched filter (in frequency-domain) and the corresponding interference canceller (in time-domain) are employed at the remaining iterations. For the improved equalization, however, we employ optimal frequency- and time-domain filters that maximize SINR at each iteration.

Denote the coefficients of the frequency-domain filter at the ith iteration to be $\{A_k^{(i)}\}_{k=0}^{N-1}$. The time-domain filter, $\{b_n\}$, is to cancel the residual interference after the frequency-domain filtering; therefore, it is dependant on the frequency-domain filter and channel by

$$b_n^{(i)} \triangleq g_n^{(i)} - g_0^{(i)}\delta_n, \tag{110}$$

where

$$g_n^{(i)} \triangleq \frac{1}{N}\sum_{k=0}^{N-1} A_k^{(i)} H_k e^{\frac{2\pi kn}{N}} \tag{111}$$

is an *inverse fast Fourier transform* (IFFT) of $A_k^{(i)}H_k$, and δ_n is the Kronecker delta. Assuming most of the energy of $g_n^{(i)}$ is concentrated near g_0 (in the circular sense with period N), we truncate g_n for $L' \leq n \leq N - L'$, where $L' \geq L$ is chosen to be sufficiently larger than the channel length L. At the first iteration, the conventional linear MMSE equalization [1] is used since there is no feedback signal available. In Chapter 2, we used matched filter and the corresponding interference canceller for the frequency- and time-domain filter, respectively, after the first iteration.

For the improved equalization, however, we employ optimal frequency- and time-domain filters that maximize SINR at each iteration. The idea of using the optimal filters maximizing SINR for block iterative equalization was proposed in [27] and [28]. Here, we rederive

the optimal filters that fit into our equalization based on EST. Denote

$$d_n^{(i)} \triangleq x_n - \hat{x}_n^{(i)} \tag{112}$$

to be the post-detection error at the ith iteration, where $\hat{x}_n^{(i)}$ is either a hard or soft decision of x_n at the ith iteration. The symbol decisions are based on the vector after the IEST, which can be obtained from the equivalent model in Figure 5:

$$\mathbf{z}^{(i)} = \underbrace{g_0\mathbf{x}}_{signal} + \underbrace{\mathbf{E}^H\mathbf{C}(\mathbf{b}^{(i)})\mathbf{E}\mathbf{d}^{(i-1)}}_{interference} + \underbrace{\mathbf{E}^H\mathbf{F}^H\mathbf{A}_D^{(i)}\mathbf{F}\mathbf{n}}_{noise}, \tag{113}$$

where $\mathbf{z}^{(i)} \in \mathbb{C}^{N\times 1}$, $\mathbf{d}^{(i)} \in \mathbb{C}^{N\times 1}$, $\mathbf{b}^{(i)} \in \mathbb{C}^{N\times 1}$ are vectors whose elements are $\{z_n^{(i)}\}$, $\{d_n^{(i)}\}$, and $\{b_n^{(i)}\}$, respectively; $\mathbf{A}_D^{(i)} \in \mathbb{C}^{N\times N} \triangleq \text{diag}(A_0^{(i)}, A_1^{(i)}, ..., A_{N-1}^{(i)})$ is a diagonal matrix; and $\mathbf{C}(\mathbf{b})$ is a circulant matrix similarly defined as in (36). We assume the symbols $\{x_n\}_{n=0}^{N-1}$, the decisions $\{\hat{x}_n^{(i)}\}_{n=0}^{N-1}$, and the post-detection errors $\{d_n^{(i)}\}_{n=0}^{N-1}$ are statistically independent sequences, respectively.

The processed signal at the ith iteration after subtracting the feedback signal is

$$\tilde{z}_n^{(i)} = \underbrace{g_0^{(i)}\tilde{x}_n}_{\text{signal}} + \underbrace{b_n^{(i)} \circledast \tilde{d}_n^{(i-1)}}_{\text{interference}} + \underbrace{a_n^{(i)} \circledast n_n}_{\text{noise}}, \tag{114}$$

where $\tilde{d}_n^{(i-1)}$ and $a_n^{(i)}$ are the EST of $d_n^{(i-1)}$ and the IFFT of $A_k^{(i)}$, respectively. Since an EST is an orthogonal transform and $\{d_n^{(i)}\}_{n=0}^{N-1}$ are independent, $\{\tilde{d}_n^{(i)}\}_{n=0}^{N-1}$ are also independent. The power of the post-detection error in the EST domain can be expressed as

$$(\sigma_{d,n}^{(i)})^2 \triangleq \mathcal{E}\{|\tilde{d}_n^{(i)}|^2|\mathbf{z}^{(i)}\} = (\mathbf{E}\mathcal{E}\{\mathbf{d}^{(i)}\mathbf{d}^{(i)^H}|\mathbf{z}^{(i)}\}\mathbf{E}^H)_{n,n}, \tag{115}$$

where $\mathcal{E}\{\cdot|\mathbf{z}^{(i)}\}$ denotes conditional expectation when $\mathbf{z}^{(i)}$ is given. Using the ideal EST, (115) can be written as

$$\begin{aligned}(\sigma_{d,n}^{(i)})^2 &= \frac{1}{N}\sum_{n=0}^{N-1}\mathcal{E}\{|d_n^{(i)}|^2|\mathbf{z}^{(i)}\} \\ &\triangleq (\sigma_d^{(i)})^2,\end{aligned} \tag{116}$$

where we omitted the symbol index n in the post-detection error power since it does not depend on n. Since $\tilde{d}_n^{(i)}$ is an independent sequence with power $(\sigma_d^{(i)})^2$, as shown above, the

interference power (conditioned on $\mathbf{z}^{(i-1)}$) in (114) can be shown to be

$$\tilde{P}_{in}^{(i)}(\mathbf{z}^{(i-1)}) = (g_0^{(i)})^2 K_h^{(i)} (\sigma_d^{(i-1)})^2, \tag{117}$$

where

$$K_h^{(i)} \triangleq \frac{1}{(g_0^{(i)})^2} \sum_{n \neq 0} |g_n^{(i)}|^2. \tag{118}$$

Also, using (110) and (111), (117) can be written in terms of the frequency-domain filter $A_k^{(i)}$, that is,

$$\begin{aligned} \tilde{P}_{in}^{(i)}(\mathbf{z}^{(i-1)}) &= (\sigma_d^{(i-1)})^2 \sum_n |\frac{1}{N} \sum_{k=0}^{N-1} A_k^{(i)} H_k e^{j\frac{2\pi kn}{N}} \\ &- (\frac{1}{N} \sum_{k=0}^{N-1} A_k^{(i)} H_k) \delta_n|^2. \end{aligned} \tag{119}$$

Similarly, the signal and noise power in (114) can be easily found to be

$$\tilde{P}_{si}^{(i)} = \sigma_x^2 |\frac{1}{N} \sum_{k=0}^{N-1} A_k^{(i)} H_k|^2 \tag{120}$$

and

$$\tilde{P}_{no}^{(i)} = \frac{\sigma_n^2}{N} \sum_{k=0}^{N-1} |A_k^{(i)}|^2, \tag{121}$$

respectively. Following the standard maximization procedure, SINR at the ith iteration,

$$\tilde{\text{SINR}}^{(i)}(\mathbf{z}^{(i-1)}) \triangleq \frac{\tilde{P}_{si}^{(i)}}{\tilde{P}_{in}^{(i)}(\mathbf{z}^{(i-1)}) + \tilde{P}_{no}^{(i)}} \tag{122}$$

can be maximized by the frequency-domain filter,

$$A_k^{(i)} = \frac{\alpha H_k^*}{(\sigma_d^{(i-1)})^2 |H_k|^2 + \sigma_n^2}, \tag{123}$$

where the superscript * denotes complex conjugate and α is a scaling factor. Since α can be arbitrary, we choose

$$\alpha = \left(\frac{1}{N} \sum_k \frac{|H|_k^2}{(\sigma_d^{(i-1)})^2 |H_k|^2 + \sigma_n^2} \right)^{-1} \tag{124}$$

to normalize the signal power in (114), or to make $g_0^{(i)} = 1$, for convenience. As previously indicated, the time-domain filter can be obtained by taking IFFT of $A_k^{(i)} H_k$. Note that the frequency-domain filter in (123) is equal (within a scaling factor) to the conventional

linear MMSE filter [1] at the first iteration ($i = 1$), when there is no available feedback and therefore, $(\sigma_d^{(0)})^2 = \sigma_x^2$. On the other hand, when $(\sigma_d^{(i-1)})^2 = 0$, (123) is equal to the matched filter.

We consider the decision vector in (113) after the normalization in (124). Since $g_0 = 1$, signal power is

$$\mathrm{P}_{si}^{(i)} = \sigma_x^2. \tag{125}$$

Following the procedure in Section 2.4, assuming the ideal EST and a large N, we can obtain interference and noise power to be

$$\mathrm{P}_{in}^{(i)}(\mathbf{z}^{(i-1)}) = K_h^{(i)}(\sigma_d^{(i-1)})^2 \tag{126}$$

and

$$\mathrm{P}_{no}^{(i)} = \frac{\sigma_n^2}{N}\sum_{k=0}^{N-1}|A_k^{(i)}|^2, \tag{127}$$

respectively. Note that since $\mathbf{E}$ is unitary, (125), (126), and (127) can be also obtained directly from (120), (119), and (121), respectively using the Parseval's theorem and the fact that $g_0 = 1$ after normalization.

Now, we describe how to calculate the post-detection error power in (116) to use in the frequency-domain filter in (123) for the hard- and soft-decision equalization, respectively.

3.1.1 Hard Decision

Denote $D^{(i)}$ and $N^{(i)}$ to be the set of indexes of incorrectly decided symbols after hard decision at the ith iteration and its cardinality, respectively. Given $N^{(i)}$, (116) becomes

$$(\sigma_d^{(i)})^2 = \kappa(\frac{N^{(i)}}{N})\sigma_x^2\frac{N^{(i)}}{N}, \tag{128}$$

where

$$\kappa(\frac{N^{(i)}}{N}) \triangleq \frac{\mathcal{E}\{|d_n|^2 | n \in D^{(i)}\}}{\sigma_x^2}. \tag{129}$$

From (125), (126), and (127), the SINR at the ith iteration conditioned on $N^{(i-1)}$ is

$$\mathrm{SINR}^{(i)}(N^{(i-1)}) = \frac{P_{si}^{(i)}}{P_{in}^{(i)}(N^{(i-1)}) + P_{no}^{(i)}} \tag{130}$$

and the corresponding *symbol-error-rate* (SER) (conditioned on $N^{(i-1)}$) can be calculated from the SINR using

$$p^{(i)}(N^{(i-1)}) = \Psi(\text{SINR}^{(i)}(N^{(i-1)})), \tag{131}$$

where Ψ is a modulation-dependent function that maps SINR to SER.

Then, we invoke the law of large numbers [23]: For an infinite N, each block has the same number of symbol errors $Np^{(i)}$, or $N^{(i)} = Np^{(i)}$, where $p^{(i)}$ is SER. In this case, as shown in Subsection 2.4.3, the SER is

$$p^{(i)} = \Psi(\text{SINR}^{(i)}(N^{(i-1)} = Np^{(i-1)})) \tag{132}$$

and (128) becomes,

$$(\sigma_d^{(i)})^2 = \kappa(p^{(i)})\sigma_x^2 p^{(i)}. \tag{133}$$

3.1.2 Soft Decision

In this subsection, $\hat{x}_n$ is used for the soft-decision. Also, for simplicity, we assume that QPSK and the ideal EST are employed. Each element of (113) can be decomposed into its in-phase and quadrature components, that is, $z_n^{(i)} = z_{I,n}^{(i)} + jz_{Q,n}^{(i)}$, $x_n = x_{I,n} + jx_{Q,n}$, $d_n^{(i)} = d_{I,n} + jd_{Q,n}$, and $n_n = n_{I,n} + jn_{Q,n}$. To avoid repetition, we describe only the in-phase component of a complex variable. The quadrature component can be similarly defined.

Employing *log-likelihood ratio* (LLR) [5], the *a posteriori* LLR of $x_{I,n}$ at the ith iteration is

$$\begin{aligned} \lambda_{I,n}^{(i)} &\triangleq \log\frac{\mathcal{P}[x_{I,n} = +1|z_{I,n}^{(i)}]}{\mathcal{P}[x_{I,n} = -1|z_{I,n}^{(i)}]} \\ &= \lambda_{I,n}^{E,(i)} + \lambda_{I,n}^{P,(i)}, \end{aligned} \tag{134}$$

where

$$\lambda_{I,n}^{E,(i)} \triangleq \log\frac{\mathcal{P}[z_{I,n}^{(i)}|x_{I,n} = +1]}{\mathcal{P}[z_{I,n}^{(i)}|x_{I,n} = -1]} = \frac{2z_{I,n}^{(i)}}{P_{in,I}^{(i)} + P_{no,I}^{(i)}} \tag{135}$$

and

$$\lambda_{I,n}^{P,(i)} \triangleq \log\frac{\mathcal{P}[x_{I,n} = +1]}{\mathcal{P}[x_{I,n} = -1]} \tag{136}$$

are the *extrinsic* LLR and the *a priori* LLR, respectively. As the *a priori* LLR, the *extrinsic* LLR from the previous iteration is used, that is,

$$\lambda_{I,n}^{P,(i)} = \lambda_{I,n}^{E,(i-1)}. \tag{137}$$

The soft-decision $\hat{x}_{I,n}^{(i)}$ to feed the EST and the time-domain filter is the conditional expectation of $x_{I,n}$ given the observation $z_{I,n}^{(i)}$, that is,

$$\hat{x}_{I,n}^{(i)} = \mathcal{E}\{x_{I,n}|z_{I,n}^{(i)}\}. \tag{138}$$

The soft-decision (138) can be written in terms of LLR as

$$\hat{x}_{I,n}^{(i)} = \tanh(\frac{\lambda_{I,n}^{E,(i)}}{2}), \tag{139}$$

where we used the *extrinsic* LLR in the improved equalization while the *a posteriori* LLR is used in Subsection 2.4.4. Also, the (in-phase) post-detection error power is

$$\begin{aligned}(\sigma_{d,I}^{(i)})^2 &= \frac{1}{N}\sum_{n=0}^{N-1}\mathcal{E}\{(d_{I,n}^{(i)})^2|z_{I,n}^{(i)}\} &(140)\\ &= \frac{1}{N}\sum_{n=0}^{N-1}[1-(\hat{x}_{I,n}^{(i)})^2]. &(141)\end{aligned}$$

Clearly, $(\sigma_d^{(i)})^2 = (\sigma_{d,I}^{(i)})^2 + (\sigma_{d,Q}^{(i)})^2$, and the decision of the transmitted bit after the final iteration should be based on the *a posteriori* LLR in (134).

3.2 Simulation Results

In this section, we present simulation results of the improved equalization using QPSK modulation. The block size is $N = 4096$, and the EST is chosen as $\mathbf{E} = \mathbf{P}\mathbf{F}^H$, where $\mathbf{P}$ is a random permutation matrix. As indicated in Section 2.2, the first symbol has poor spreading property; therefore, a dummy symbol is used for the first symbol x_0 in the block. The *bit error rate* (BER) performance is compared with the original equalization in Chapter 2 and *maximum likelihood sequence detection* (MLSD) [1]. The performance of equalization depends on the frequency selectivity of the channel, defined as

$$K_h \triangleq \frac{1}{g_0^2}\sum_{n\neq 0}|g_n|^2, \tag{142}$$

where

$$g_n \triangleq h^*_{-n} \circledast h_n.$$

Note that K_h is equal to $K_h^{(i)}$ in (118) when the frequency-domain filter is chosen as the matched filter, that is, $A_k^{(i)} = H_k^*$.

Figure 9(a) shows the performance of the hard-decision equalizer using Proakis-B channel [1], whose impulse response and frequency selectivity are

$$\begin{aligned} h_n^B &= 0.407\delta_n + 0.815\delta_{n-1} + 0.407\delta_{n-2}, \\ K_h &= 0.94, \end{aligned}$$

respectively. The performance of the improved hard-decision equalizer is compared with that of the original hard-decision equalizer and the asymptotic analysis assuming an infinite block size. For each iteration from the second, the improved equalization shows better BER performance than the original equalization. At BER = 10^{-4} and the second iteration, the improved equalizer performs about 2 dB better than the original scheme. The difference between the analysis and the simulation can be accounted for the non-ideal property of the employed EST and the finite block size. Figure 9(b) shows the simulation results for the soft-decision equalizer using Proakis-B channel. Similar to the hard-decision case, the improved soft-decision equalizer performs better than the original soft-decision equalizer. At BER = 10^{-4}, the improved equalization outperforms the original one by 0.8 dB at the second and by 0.7 dB at the third iteration.

Figure 10(a) shows the results for the hard-decision equalizer using Proakis-C channel [1], whose impulse response and K_h are

$$\begin{aligned} h_n^C &= 0.227\delta_n + 0.460\delta_{n-1} + 0.688\delta_{n-2} + 0.460\delta_{n-3} \\ &+ 0.227\delta_{n-4}, \\ K_h &= 2.13, \end{aligned}$$

respectively. The performance of the hard-decision equalizer converges to the MFB above the SNR threshold near 15 dB while significant error propagation occurs below the SNR threshold. For Proakis-C channel, the performance enhancement is more significant than

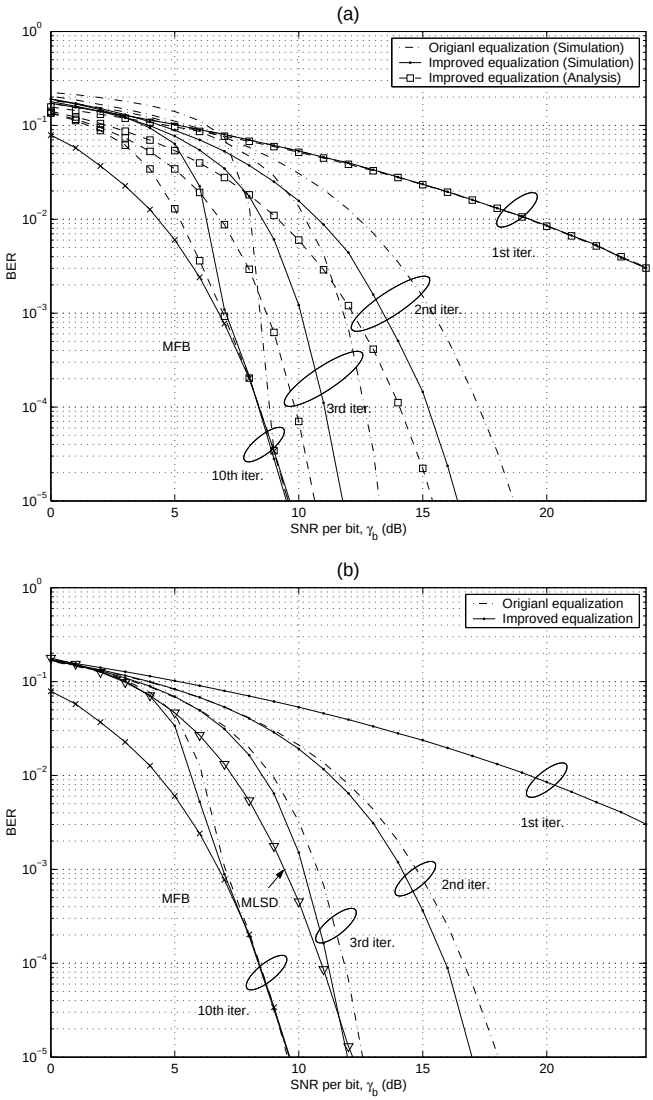

Figure 9. Performance of the improved scheme with (a) hard decision and (b) soft decision for Proakis-B channel.

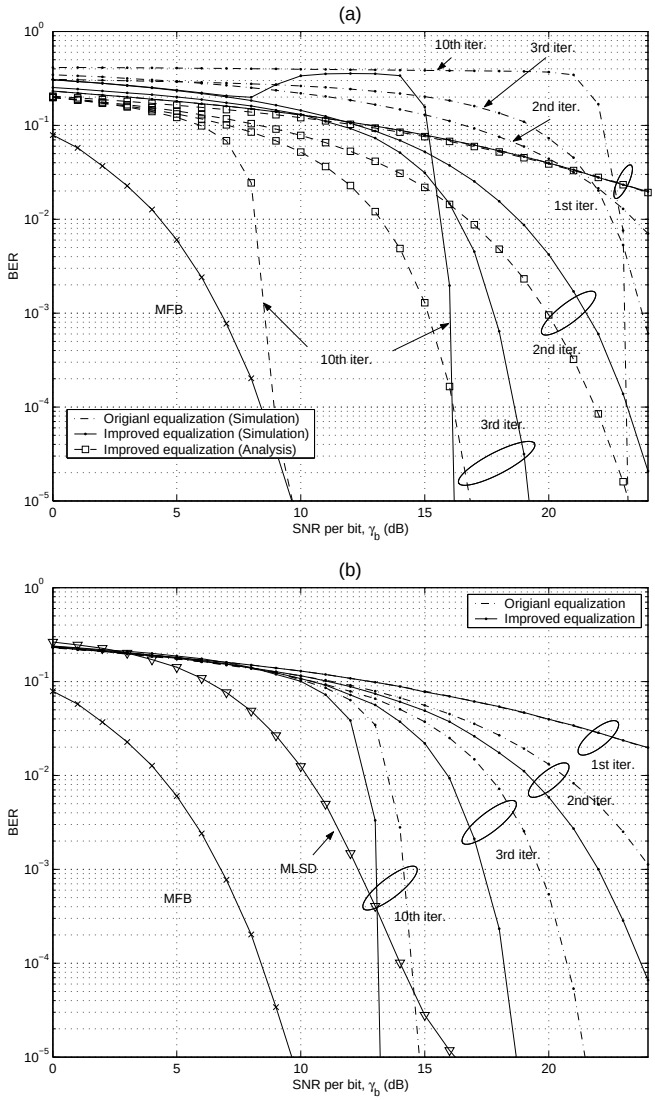

Figure 10. Performance of the improved scheme with (a) hard decision and (b) soft decision for Proakis-C channel.

that for Proakis-B channel. At the 10th iteration and BER = 10^{-4}, the improved hard-decision equalizer outperforms the original scheme by 7 dB. The gap between the simulation and the asymptotic analysis assuming an infinite block size and the ideal EST increases with each iteration. At the 10th iteration and BER = 10^{-4}, there is a 7 dB gap between the analysis and the simulation. This can be explained by the significant accumulation of the error in the estimation of SER, the post-detection error power in (133), and the interference power in (126) for the channels with a large K_h. Finally, Figure 10(b) shows the simulation results for the soft-decision equalizer using Proakis-C channel. The soft-decision equalizer can prevent sever error propagation below the SNR threshold of the hard-decision equalizer and shows significantly better performance in the low SNR region. Also, the performance enhancement over the original equalization is observed. At the third iteration and BER = 10^{-4}, the improved equalization outperforms the original scheme by 2.5 dB. And, at the 10th iteration and BER = 10^{-4}, the improved equalization outperforms the MLSD by 0.9 dB while the original one performs 0.43 dB worse than the MLSD.

CHAPTER 4

ITERATIVE MIMO SIGNAL DETECTION BASED ON EST: FLAT FADING CHANNELS

4.1 System Description

Figure 11 (a) demonstrates an EST-based iterative signal-detection scheme for a flat fading channel with n_T transmit antennas and n_R receive antennas. Denote $\mathbb{C}$ to be a complex field. In the figure, $\underline{\mathbf{x}}$ is the transmitted symbol block, defined as $[x_0, x_1, ..., x_{N-1}]^T$. The

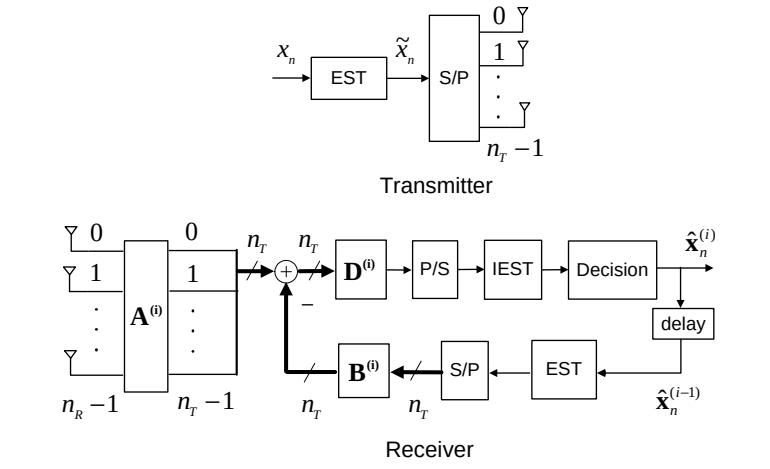

(a)

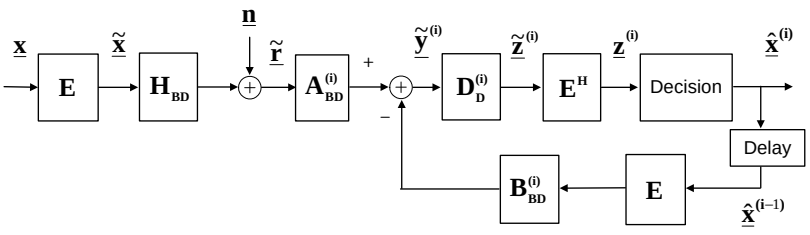

(b)

Figure 11. (a) Iterative detection for MIMO flat fading channels and (b) its equivalent model.

N complex symbols in $\underline{\mathbf{x}}$ are assumed to be independent, with zero-mean and variance σ_x^2. The symbol block is first transformed to $\underline{\tilde{\mathbf{x}}} = [\tilde{x}_0, \tilde{x}_1, ..., \tilde{x}_{N-1}]^T$ by an ST-EST, which will be discussed in Section 4.2.

The transformed symbol block, $\underline{\tilde{\mathbf{x}}}$, is then divided into $N_b \triangleq N/n_T$ transmit vectors with n_T-elements by

$$\tilde{\mathbf{x}}_n = [\tilde{x}_{n_T n}, \tilde{x}_{n_T n+1}, ..., \tilde{x}_{n_T n+n_T-1}]^T,$$

for $n = 0,\ 1, \cdots, N_b - 1$. The q-th element of $\tilde{\mathbf{x}}_n$ is transmitted by the q-th transmit antenna.

The MIMO channel is assumed to be with flat fading and can be described by a channel matrix $\mathbf{H} \in \mathbb{C}^{n_R \times n_T}$. Furthermore, the elements of $\mathbf{H}$, $(\mathbf{H})_{m,n}$'s are assumed to be *independent* and *identically distributed* (i.i.d) complex Gaussian, with zero mean and variance $1/n_T$ to normalize the overall transmission power. Consequently, the received signal vector is

$$\tilde{\mathbf{r}}_n = \mathbf{H}\tilde{\mathbf{x}}_n + \mathbf{n}_n,$$

where $\mathbf{n}_n$ is a complex *additive white Gaussian noise* (AWGN) vector with variance σ_n^2 for each element. Therefore, the average *signal-to-noise ratio* (SNR) per receive antenna is $\text{SNR} = \sigma_x^2/\sigma_n^2$.

The signal detection is iteratively performed by a forward matrix $\mathbf{A}^{(i)} \in \mathbb{C}^{n_T \times n_R}$, a feedback matrix $\mathbf{B}^{(i)} \in \mathbb{C}^{n_T \times n_T}$, and a diagonal matrix $\mathbf{D}^{(i)} \in \mathbb{C}^{n_T \times n_T}$. At the first iteration, *minimum mean-square-error* (MMSE) [35] criterion is used to determine the forward matrix, while the feedback matrix and the diagonal matrix are set to zero and identity, respectively:

$$\mathbf{A}^{(1)} = \left(\mathbf{G} + \frac{\sigma_n^2}{\sigma_x^2}\mathbf{I}_{n_T}\right)^{-1} \mathbf{H}^H, \tag{143}$$

$$\mathbf{B}^{(1)} = \mathbf{0}, \tag{144}$$

$$\mathbf{D}^{(1)} = \mathbf{I}_{n_T}, \tag{145}$$

where the superscript H denotes the Hermitian operator, $\mathbf{G} \triangleq \mathbf{H}^H\mathbf{H}$, $\mathbf{I}_{n_T}$ is a $n_T \times n_T$ identity matrix, and $\mathbf{0}$ is a $n_T \times n_T$ zero matrix.

From the second iteration ($i \geq 2$), the forward matrix is chosen as the *matched matrix*,

the feedback matrix and the diagonal matrix are chosen to cancel interference:

$$\mathbf{A}^{(i)} = \mathbf{H}^H, \tag{146}$$

$$\mathbf{B}^{(i)} = \bar{\mathcal{D}}\{\mathbf{G}\}, \tag{147}$$

$$\mathbf{D}^{(i)} = \mathcal{D}\{\mathbf{G}\}^{-1}, \tag{148}$$

where $\mathcal{D}\{\mathbf{W}\}$ denotes a diagonal matrix that removes all the off-diagonal elements of a square matrix $\mathbf{W}$ and $\bar{\mathcal{D}}\{\mathbf{W}\}$ is a matrix that removes all the diagonal elements of the matrix $\mathbf{W}$. It is obvious that

$$\bar{\mathcal{D}}\{\mathbf{W}\} = \mathbf{W} - \mathcal{D}\{\mathbf{W}\}.$$

Either hard or soft decisions can be fed back to the feedback matrix. Since the forward matrix $\mathbf{A}^{(i)}$ and its input are same after the second iteration, the same output vector will be used in subsequent iterations and only feedback matrix outputs need to be updated.

4.2 ST-EST and Its Impact

Similar to [32], an EST is an orthonormal transform that spreads the energy of each symbol x_n over the entire block. The EST in Figure 11 (a) is called a *space-time* (ST) EST since it spreads each symbol energy over space and time. Denote $\mathbf{E} \in \mathbb{C}^{N\times N}$ to be an EST matrix and $(\mathbf{E})_{m,n}$ to be the element of $\mathbf{E}$ at the m-th row and n-th column, respectively. The *ideal* ST-EST should satisfy

- $|(\mathbf{E})_{m,n}| = \frac{1}{\sqrt{N}}$
- $\sphericalangle(\mathbf{E})_{m,n}$ is pseudo-randomly and uniformly distributed over $[-\pi, \pi]$

Here $|x|$ and $\sphericalangle x$ denote the magnitude and the angle of a complex number x, respectively. Similar to [32], an ST-EST can be implemented by

$$\mathbf{E} = \mathbf{PU}, \tag{149}$$

where $\mathbf{P}$ is a pseudo-random permutation matrix and $\mathbf{U}$ is a unitary matrix. As indicated in [32], Fourier transform and Hadamard transform are good candidates for $\mathbf{U}$ since they can be implemented by existing fast algorithms. The pseudo-random permutation is necessary

to ensure random distribution of the phase $\sphericalangle(\mathbf{E})_{m,n}$, which is very important for the EST-based MIMO system to reach good performance.

Figure 12 can further illustrate the importance of the ST-EST in the proposed structure in Figure 11. Figure 12 (a) illustrates the effect of space-domain spreading. For a MIMO

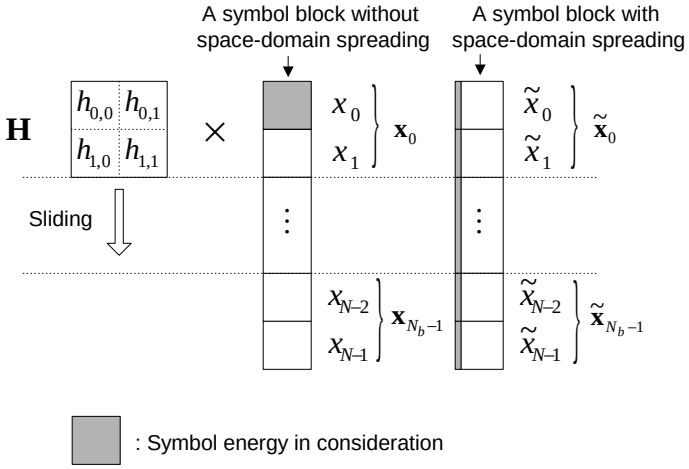

(a) Effect of space-domain spreading

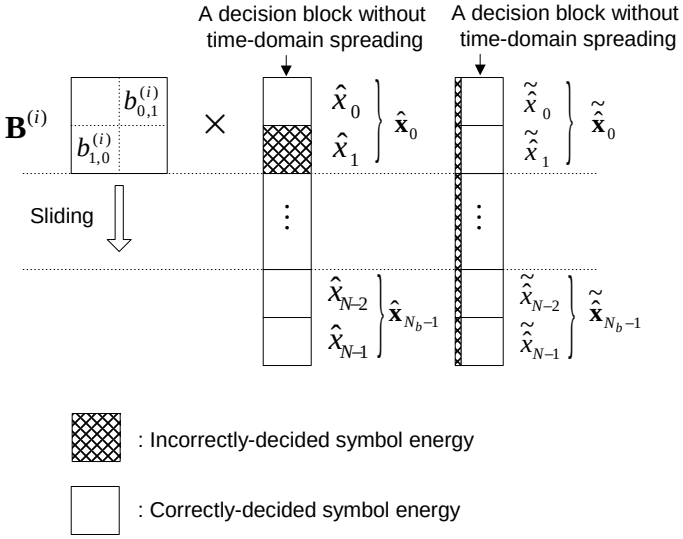

(b) Effect of time-domain spreading

Figure 12. Principle of ST-EST.

system with $n_T = n_R = 2$, consider the transmission of a specific symbol, x_0, in a block. Without space-domain spreading, it uses only the first column of the channel matrix, i.e., $h_{0,0}$ and $h_{0,1}$. If the magnitudes of $h_{0,0}$ and $h_{0,1}$ are small, the detection of x_0 will have a

large probability of error. The overall performance, averaged over the block, is dominated by the worst symbol detection. With space-domain spreading, however, x_0 uses all the elements in the channel matrix. Therefore, space-domain spreading effectively provides spatial diversity and enhances the performance. Figure 12 (b) illustrates the effect of time-domain spreading. Consider the input of the feedback matrix, which is from the decisions of the previous iteration. We assume that only one decision, $\hat{x}_1$, is incorrect in the previous iteration. Without time-domain spreading, the error will be captured by $b_{0,1}^{(i)}$. If $b_{0,1}^{(i)}$ has a significant magnitude, it will degrade the performance of the symbol detection for x_0. However, with time-domain spreading, the error energy is spread over the entire block. Even though it can be still captured by $b_{0,1}^{(i)}$ or $b_{1,0}^{(i)}$ and affects all symbol decision, its power has been reduced by a factor of N due to the spreading. Therefore, the time-domain spreading increases the reliability of the feedback signal. Moreover, the ST-EST enables iterative signal detection without employing error-correction coding as we have indicated before. As will be confirmed in our analysis and simulation, *symbol-error rate* (SER) of the signal detection decreases with the increase of the number of iterations if initial SER at the first iteration is below a threshold. Eventually, SER will be very close to that of the genie-aided receiver.

4.3 Complexity

Since there are N_b receive signal vectors per block, the block-wise complexity of the forward matrix, diagonal matrix, and the feedback matrix operation are $n_R n_T N_b$, $n_T N_b$, and $n_T^2 N_b$, respectively, when a hard decision is used in the proposed scheme. The complexity of EST or IEST is $N\log_2 N$ assuming the fast algorithms for Fourier or Hadamard transform used in constructing the EST. Therefore, we obtain the complexity as shown in the Table 3. The block-wise complexity of the conventional decision-feedback receiver (without ordering) is $(n_R n_T + n_T^2)N_b$. When $\log_2 N$ is comparable to n_T or n_R, the complexity of the proposed scheme for each iteration is similar to that of the conventional decision-feedback receiver.

Table 3. Computational Complexity. Y = required, N = not required.

Iteration (i)	$\mathbf{A}^{(i)}$	$\mathbf{D}^{(i)}$	IEST	EST	$\mathbf{B}^{(i)}$	Complexity
i = 1	Y	N	Y	N	N	$(n_T \log_2 N + n_R n_T) N_b$
i = 2	Y	Y	Y	Y	Y	$(2n_T \log_2 N + n_R n_T + n_T^2 + n_T) N_b$
i ≥ 3	N	Y	Y	Y	Y	$(2n_T \log_2 N + n_T^2 + n_T) N_b$

4.4 Performance Analysis

In this section, we analyze the performance of the ST-EST-based iterative scheme described in the previous section. For simplicity, we assume employing the ideal ST-EST.

Denote $\mathbf{W} \in \mathbb{C}^{N \times N}$ and $\mathbf{U} \in \mathbb{C}^{N \times N}$ to be a square matrix and a unitary matrix, respectively. The following matrix identities will be used in our analysis:

ID-1: If $|(\mathbf{U})_{m,n}| = 1/\sqrt{N}$, then

$$(\mathbf{U}^H \mathcal{D}\{\mathbf{W}\}\mathbf{U})_{n,n} = \frac{1}{N} \sum_{n=0}^{N-1} (\mathbf{W})_{n,n}.$$

ID-2: Denote $\mathrm{tr}\{\mathbf{W}\}$ to be the trace of $\mathbf{W}$, then

$$\mathrm{tr}\{\mathbf{U}^H \bar{\mathcal{D}}\{\mathbf{W}\}\mathbf{U}\} = 0.$$

ID-3: For the ideal ST-EST, $\mathbf{E}$, and a sufficiently large N, $(\mathbf{E}^H \bar{\mathcal{D}}\{\mathbf{W}\}\mathbf{E})_{n,m}$ can be treated as a Gaussian random variable with zero mean and variance

$$\frac{1}{N^2} \sum_{l_1=0}^{N-1} \sum_{l_2=0, l_2 \neq l_1}^{N-1} |(\mathbf{W})_{l_1,l_2}|^2.$$

The first two identities ID-1 and ID-2 can be easily checked and ID-3 is proved in Appendix E.

To facilitate our analysis, we redraw Figure 11 (a) into a mathematically equivalent model in Figure 11 (b). In the equivalent model, we have used the following definitions,

$$\underline{\mathbf{n}} \triangleq \begin{pmatrix} \mathbf{n}_0 \\ \vdots \\ \mathbf{n}_{N_b-1} \end{pmatrix}, \quad \underline{\mathbf{x}}^{(i)} \triangleq \begin{pmatrix} \mathbf{x}_0^{(i)} \\ \vdots \\ \mathbf{x}_{N_b-1}^{(i)} \end{pmatrix}, \quad \underline{\mathbf{z}}^{(i)} \triangleq \begin{pmatrix} \mathbf{z}_0^{(i)} \\ \vdots \\ \mathbf{z}_{N_b-1}^{(i)} \end{pmatrix},$$

$$\mathbf{H}_{BD} \triangleq \text{diag}\{\underbrace{\mathbf{H}, \cdots, \mathbf{H}}_{N_b \text{ matrices}}\} \in \mathbb{C}^{N_b n_R \times N},$$

$$\mathbf{A}_{BD}^{(i)} \triangleq \text{diag}\{\underbrace{\mathbf{A}^{(i)}, \cdots, \mathbf{A}^{(i)}}_{N_b \text{ matrices}}\} \in \mathbb{C}^{N \times N_b n_R},$$

$$\mathbf{B}_{BD}^{(i)} \triangleq \text{diag}\{\underbrace{\mathbf{B}^{(i)}, \cdots, \mathbf{B}^{(i)}}_{N_b \text{ matrices}}\} \in \mathbb{C}^{N \times N},$$

and

$$\mathbf{D}_{D}^{(i)} \triangleq \text{diag}\{\underbrace{\mathbf{D}^{(i)}, \cdots, \mathbf{D}^{(i)}}_{N_b \text{ matrices}}\} \in \mathbb{C}^{N \times N}.$$

The decision vector at the i-th iteration can be expressed as

$$\begin{aligned} \underline{\mathbf{z}}^{(i)} &= \mathbf{E}^H \mathbf{D}_D^{(i)} \mathbf{A}_{BD}^{(i)} \mathbf{H}_{BD} \mathbf{E} \underline{\mathbf{x}} - \mathbf{E}^H \mathbf{D}_D^{(i)} \mathbf{B}_{BD}^{(i)} \mathbf{E} \hat{\underline{\mathbf{x}}}^{(i-1)} \\ &\quad + \mathbf{E}^H \mathbf{D}_D^{(i)} \mathbf{A}_{BD}^{(i)} \underline{\mathbf{n}}, \end{aligned} \tag{150}$$

where $\hat{\underline{\mathbf{x}}}^{(i-1)}$ is the hard or soft decision for $\underline{\mathbf{x}}$ at the $(i-1)$-th iteration.

At each iteration, the n-th decision variable, $z_n^{(i)}$ consists of signal, interference, and noise with power $\mathrm{P}_{si,n}^{(i)}$, $\mathrm{P}_{in,n}^{(i)}$, and $\mathrm{P}_{no,n}^{(i)}$, respectively. The SER of the n-th symbol at the i-th iteration is

$$p_n^{(i)} = \Psi(\text{SINR}_n^{(i)}), \tag{151}$$

where

$$\text{SINR}_n^{(i)} = \frac{\mathrm{P}_{si,n}^{(i)}}{\mathrm{P}_{in,n}^{(i)} + \mathrm{P}_{no,n}^{(i)}}$$

is the *signal-to-interference-noise ratio* (SINR) of the n-th symbol at the i-th iteration and $\Psi(\cdot)$ is a function that maps SINR to SER. Consequently, the SER at the i-th iteration is the average of the SER's of each symbol in a symbol block:

$$p^{(i)} = \frac{1}{N} \sum_{n=0}^{N-1} p_n^{(i)}. \tag{152}$$

4.4.1 MMSE Receiver

From (143)-(145) and (150), the decision vector at the first iteration can be written as

$$\underline{\mathbf{z}}^{(1)} = \underbrace{\mathcal{D}\{\mathbf{E}^H \mathbf{M}_{BD} \mathbf{E}\} \underline{\mathbf{x}}}_{\text{signal}} + \underbrace{\bar{\mathcal{D}}\{\mathbf{E}^H \mathbf{M}_{BD} \mathbf{E}\} \underline{\mathbf{x}}}_{\text{interference}} + \underbrace{\mathbf{E}^H \mathbf{A}_{BD}^{(1)} \underline{\mathbf{n}}}_{\text{noise}}, \tag{153}$$

where $\mathbf{M} \triangleq \mathbf{A}^{(1)}\mathbf{H}$ and $\mathbf{M}_{BD}$ is the block diagonal matrix extended from $\mathbf{M}$ in the same way as $\mathbf{A}_{BD}$ is extended from $\mathbf{A}$. Signal, interference, and noise powers of the n-th decision variable are

$$\mathrm{P}_{si,n}^{(1)} = \sigma_x^2[(\mathbf{E}^H\mathbf{M}_{BD}\mathbf{E})_{n,n}]^2,$$
$$\mathrm{P}_{in,n}^{(1)} = \sigma_x^2[((\mathbf{E}^H|\mathbf{M}_{BD}|^2\mathbf{E})_{n,n} - \{(\mathbf{E}^H\mathbf{M}_{BD}\mathbf{E})_{n,n}\}^2],$$

and

$$\mathrm{P}_{no,n}^{(1)} \quad = \quad \sigma_n^2(\mathbf{E}^H|\mathbf{A}_{BD}^{(1)}|^2\mathbf{E})_{n,n},$$

respectively, where $|\mathbf{M}_{BD}|^2 \triangleq \mathbf{M}_{BD}\mathbf{M}_{BD}^H$ and $|\mathbf{A}_{BD}^{(1)}|^2 \triangleq \mathbf{A}_{BD}^{(1)}\left(\mathbf{A}_{BD}^{(1)}\right)^H$. With the ideal ST-EST, each component power can be decomposed into its average and perturbation:

$$\mathrm{P}_{si,n}^{(1)} = \sigma_x^2[m_{si} + \alpha_n]^2, \tag{154}$$
$$\mathrm{P}_{in,n}^{(1)} = \sigma_x^2[m_{in} + \beta_n - 2m_{si}\alpha_n - \alpha_n^2], \tag{155}$$

and

$$\mathrm{P}_{no,n}^{(1)} = \sigma_n^2[m_{no} + \gamma_n], \tag{156}$$

where

$$m_{si} = \frac{1}{n_T}\sum_{l=0}^{n_T-1}(\mathbf{M})_{l,l}, \tag{157}$$
$$m_{in} = \frac{1}{n_T}\sum_{l_1=0}^{n_T-1}\sum_{l_2=0}^{n_T-1}|(\mathbf{M})_{l_1,l_2}|^2 - \left[\frac{1}{n_T}\sum_{l=0}^{n_T-1}(\mathbf{M})_{l,l}\right]^2, \tag{158}$$

and

$$m_{no} = \frac{1}{n_T}\sum_{l=0}^{n_T-1}(|\mathbf{A}^{(1)}|^2)_{l,l}, \tag{159}$$

are the averages derived using ID-1 and

$$\alpha_n = (\mathbf{E}^H\bar{\mathcal{D}}\{\mathbf{M}_{BD}\}\mathbf{E})_{n,n},$$
$$\beta_n = (\mathbf{E}^H\bar{\mathcal{D}}\{|\mathbf{M}_{BD}|^2\}\mathbf{E})_{n,n},$$

and

$$\gamma_n = (\mathbf{E}^H\bar{\mathcal{D}}\{|\mathbf{A}_{BD}^{(1)}|^2\}\mathbf{E})_{n,n}.$$

are the perturbations.

From ID-2, the averages of α_n, β_n, and γ_n are zero, respectively:

$$\frac{1}{N}\sum_n \alpha_n = \frac{1}{N}\sum_n \beta_n = \frac{1}{N}\sum_n \gamma_n = 0.$$

From ID-3, for a sufficiently large N, we can treat the perturbations as zero-mean Gaussian random variables with variances

$$\mathcal{V}\{\alpha_n\} = \frac{1}{n_T N}\sum_{l_1=0}^{n_T-1}\sum_{l_2=0,l_2\neq l_1}^{n_T-1} |(\mathbf{M})_{l_1,l_2}|^2, \tag{160}$$

$$\mathcal{V}\{\beta_n\} = \frac{1}{n_T N}\sum_{l_1=0}^{n_T-1}\sum_{l_2=0,l_2\neq l_1}^{n_T-1} |(|\mathbf{M}|^2)_{l_1,l_2}|^2, \tag{161}$$

and

$$\mathcal{V}\{\gamma_n\} = \frac{1}{n_T N}\sum_{l_1=0}^{n_T-1}\sum_{l_2=0,l_2\neq l_1}^{n_T-1} ((|\mathbf{A}^{(1)}|^2)_{l_1,l_2})^2, \tag{162}$$

respectively, where $\mathcal{V}\{\cdot\}$ denotes variance. For a large N, the perturbations are negligible, and the SER can be well approximated by

$$p^{(1)} \simeq \Psi(\overline{\mathrm{SINR}}^{(1)}), \tag{163}$$

where $\overline{\mathrm{SINR}}^{(1)}$ is the average of $\mathrm{SINR}_n^{(1)}$ obtained by ignoring the perturbations.

4.4.2 Genie-Aided Receiver

From the second iteration ($i \geq 2$), the matched matrix and interference canceller are used for the forward and backward matrices, respectively with appropriate normalization by $\mathbf{D}_D^{(i)}$, that is, $\mathbf{A}_{BD}^{(i)} = \mathbf{H}_{BD}^H$, $\mathbf{B}_{BD} = \bar{\mathcal{D}}\{\mathbf{G}_{BD}\}$ and $\mathbf{D}_D^{(i)} = \mathcal{D}\{\mathbf{G}_{BD}\}^{-1}$, where $\mathbf{G}_{BD}$ is a block diagonal matrix extended from $\mathbf{G}$. The decision vector is

$$\begin{aligned}\underline{\mathbf{z}}^{(i)} &= \underbrace{\underline{\mathbf{x}}}_{\text{signal}} + \underbrace{\mathbf{E}^H\mathcal{D}\{\mathbf{G}_{BD}\}^{-1}\bar{\mathcal{D}}\{\mathbf{G}_{BD}\}\mathbf{E}(\underline{\mathbf{x}} - \mathrm{dec}\{\underline{\mathbf{x}}^{(i-1)}\})}_{\text{interference}} \\ &+ \underbrace{\mathbf{E}^H\mathcal{D}\{\mathbf{G}_{BD}\}^{-1}\mathbf{H}_{BD}^H\underline{\mathbf{n}}}_{\text{noise}}.\end{aligned} \tag{164}$$

For the genie-aided receiver, interference is assumed to be known and can be completely removed; therefore, signal and interference powers at the n-th decision variable, $z_n^{(g)}$, are $\mathrm{P}_{si,n}^{(g)} = \sigma_x^2$ and $\mathrm{P}_{in,n}^{(g)} = 0$, respectively. Noise power is

$$\mathrm{P}_{no,n}^{(g)} = \sigma_n^2(\mathbf{E}^H\mathbf{L}_{BD}\mathbf{E})_{n,n}, \tag{165}$$

where $\mathbf{L}_{BD} \triangleq \mathcal{D}\{\mathbf{G}_{BD}\}^{-1}\mathbf{G}_{BD}\mathcal{D}\{\mathbf{G}_{BD}\}^{-1}$. The noise power can be decomposed into

$$\mathrm{P}_{no,n}^{(g)} = \sigma_n^2(Q_H + \delta_n), \tag{166}$$

where

$$Q_H \triangleq (\mathbf{E}^H\mathcal{D}\{\mathbf{L}_{BD}\}\mathbf{E})_{n,n} = \frac{1}{n_T}\sum_{n=0}^{n_T-1}\frac{1}{(\mathbf{G})_{n,n}} \tag{167}$$

and

$$\delta_n = (\mathbf{E}^H\bar{\mathcal{D}}\{\mathbf{L}_{BD}\}\mathbf{E})_{n,n}. \tag{168}$$

Similar to the previous subsection, for a sufficiently large N, δ_n is negligible, and the SER can be approximated by

$$p^{(g)} \simeq \Psi(\overline{\mathrm{SINR}}^{(g)}), \tag{169}$$

where

$$\overline{\mathrm{SINR}}^{(g)} = \frac{\mathrm{SNR}}{Q_H} \tag{170}$$

is obtained by ignoring the perturbation.

4.4.3 Iterative Receiver with Hard Decision

We analyze the performance of the iterative receiver with a hard decision. In this subsection, $\underline{\hat{\mathbf{x}}}$ is used to denote the hard decision for $\underline{\mathbf{x}}$. From (164), the decision vector of the iterative receiver with a hard decision for $i \geq 2$ is

$$\underline{\mathbf{z}}^{(i)} = \underbrace{\underline{\mathbf{x}}}_{\text{signal}} + \underbrace{\mathbf{E}^H\mathbf{J}_{BD}\mathbf{E}\underline{\mathbf{d}}^{(i-1)}}_{\text{interference}} + \underbrace{\mathbf{E}^H\mathcal{D}\{\mathbf{G}_{BD}\}^{-1}\mathbf{H}_{BD}^H\underline{\mathbf{n}}}_{\text{noise}}, \tag{171}$$

where $\mathbf{J}_{BD} \triangleq \mathcal{D}\{\mathbf{G}_{BD}\}^{-1}\bar{\mathcal{D}}\{\mathbf{G}_{BD}\}$ and $\underline{\mathbf{d}}^{(i)} \triangleq \underline{\mathbf{x}} - \underline{\hat{\mathbf{x}}}^{(i)}$ is the post-decision error vector at the i-th iteration. Signal and noise powers are the same as those of the genie-aided system, that is, $\mathrm{P}_{si,n}^{(i)} = \mathrm{P}_{si,n}^{(g)}$, $\mathrm{P}_{no,n}^{(i)} = \mathrm{P}_{no,n}^{(g)}$.

We consider the interference power under the assumption that there are $N^{(i-1)}$-symbol errors in a symbol block at the $(i-1)$-th iteration. Let $D^{(i)}$ be the set of indices of incorrectly detected symbols in a block after the i-th iteration, whose cardinality is $N^{(i)}$. Define v_n as the interference component in the n-th decision variable of $\mathbf{z}^{(i)}$ given $D^{(i-1)}$:

$$v_n = \sum_{l\in D^{(i-1)}} c_{n,l}d_l^{(i-1)}, \tag{172}$$

where

$$c_{n,l} \triangleq (\mathbf{E}^H \mathbf{J}_{BD} \mathbf{E})_{n,l}. \tag{173}$$

From ID-3, for a sufficiently large N, $c_{n,l}$ can be treated as a zero-mean Gaussian random variable with variance

$$\mathcal{V}\{c_{n,l}\} = \frac{K_H}{N}, \tag{174}$$

where

$$K_H \triangleq \frac{1}{n_T} \sum_{l_1=0}^{n_T-1} \sum_{l_2=0, l_2 \neq l_1}^{n_T-1} \frac{|(\mathbf{G})_{l_1,l_2}|^2}{(\mathbf{G})^2_{l_1,l_1}} \tag{175}$$

depends on channel parameters. Moreover, c_{n,l_1} and c_{n,l_2} are independent for $l_1 \neq l_2$ since they are Gaussian and $\mathcal{E}\{c_{n,l_1} c^*_{n,l_2}\} = \mathcal{E}\{c_{n,l_1}\}\mathcal{E}\{c^*_{n,l_2}\} = 0$. Since $c_{n,l}$ is independent of $d_l^{(i-1)}$, v_n is a sum of $N^{(i-1)}$ independent complex Gaussian random variables with zero mean and variance

$$\mathcal{V}\{c_{n,l} d_l^{(i-1)}\} = \sigma_x^2 \kappa(\frac{N^{(i-1)}}{N}) \mathcal{V}\{c_{n,l}\}, \tag{176}$$

where $\kappa(p)$ is a function of SER, p, and depends on the modulation scheme. For QPSK, $\kappa(p) \simeq 4/(2 - \frac{1}{2}p)$ as shown in [32]. Consequently, $\mathrm{P}^{(i)}_{in,n}(D^{(i-1)}) = \mathcal{V}\{v_n\}$, the conditional interference power in the n-th decision variable at the i-th iteration given $D^{(i-1)}$, can be treated as a χ^2-distributed random variable with $2N^{(i-1)}$ degrees of freedom [1]. For a large N, $\mathrm{P}^{(i)}_{in,n}(D^{(i-1)})$ can be approximated by its mean:

$$\mathrm{P}^{(i)}_{in,n}(D^{(i-1)}) \simeq \frac{N^{(i-1)}}{N} \kappa(\frac{N^{(i-1)}}{N}) \sigma_x^2 K_H \tag{177}$$

for its variance shrinks to zero as N grows to infinity, as shown in [33]. Therefore, using the procedures in [33], we obtain the following recursive equations for a very large N:

$$\overline{\mathrm{SINR}}^{(i)} = \frac{1}{K_H p^{(i-1)} \kappa(p^{(i-1)}) + \frac{Q_H}{\mathrm{SNR}}} \tag{178}$$

and the corresponding SER:

$$p^{(i)} = \Psi(\overline{\mathrm{SINR}}^{(i)}). \tag{179}$$

4.4.4 Iterative Receiver with Soft Decision

Using a soft decision, the performance of the iterative receiver can be further improved. Here, we summarize the algorithm for the soft-decision receiver. For simplicity, we assume that QPSK and the ideal ST-EST are employed. Also, in this subsection, $\underline{\hat{\mathbf{x}}}$ is used to denote the soft decision for $\underline{\mathbf{x}}$.

The normalized decision vector at the i-th iteration can be written as

$$\underline{\mathbf{z}}^{(i)} = \underline{\mathbf{x}} + \underline{\mathbf{e}}^{(i)}, \tag{180}$$

where $\underline{\mathbf{e}}$ is the pre-decision error vector consisting of noise and interference. We assume the n-th element of $\underline{\mathbf{e}}^{(i)}$, $e_n^{(i)}$ to be independent (for different n) complex Gaussian with power $(\sigma_{e,n}^{(i)})^2$ for each $n = 0, 1, ..., N-1$. Since all the variables in (180) are complex, they can be decomposed into its real (in-phase) and imaginary (quadrature) components, that is, $z_n^{(i)} \triangleq z_{I,n}^{(i)} + z_{Q,n}^{(i)}$, $x_n^{(i)} \triangleq x_{I,n}^{(i)} + x_{Q,n}^{(i)}$, and $e_n^{(i)} \triangleq e_{I,n}^{(i)} + e_{Q,n}^{(i)}$. To avoid repetition, hereafter, we describe only the in-phase component of a complex variable. The quadrature component can be similarly defined. For a system with a large block size, $(\sigma_{e,n}^{(i)})^2$ is asymptotically independent of n. Therefore, in this case, we can ignore the dependency of $(\sigma_{e,n}^{(i)})^2$ on n and obtain a simple algorithm for the soft decision, as shown below.

Similar to Subsection 2.4.4 , the *a posteriori log-likelihood ratio* (LLR) of $x_{I,n}$ at the i-th iteration is

$$\lambda_{I,n}^{(i)} = \lambda_{I,n}^{E,(i)} + \lambda_{I,n}^{P,(i)}, \tag{181}$$

where

$$\lambda_{I,n}^{E,(i)} = \frac{2z_{I,n}^{(i)}}{(\sigma_{e,I,n}^{(i)})^2} \tag{182}$$

and

$$\lambda_{I,n}^{P,(i)} = \lambda_{I,n}^{E,(i-1)} \tag{183}$$

are the *extrinsic* LLR and the *a priori* LLR, respectively.

For the first iteration and a large N, from (154)-(156) and (180),

$$(\sigma_{e,n}^{(1)})^2 = (\sigma_e^{(1)})^2 = \frac{\sigma_x^2 m_{in} + \sigma_n^2 m_{no}}{m_{si}^2}, \tag{184}$$

where we omitted the subscript n for (184) is independent of n. Since each component of $e_n^{(1)}$ has the same power, $(\sigma_{e,I}^{(1)})^2 = (\sigma_{e,Q}^{(1)})^2 = (\sigma_e^{(1)})^2/2$. Note that $\lambda_{I,n}^{P,(1)} = 0$ for there is no available *a priori* LLR at the first iteration.

From the second iteration ($i \geq 2$), the soft-decision $\hat{x}_n^{(i-1)}$ is fed back, whose in-phase component is

$$\hat{x}_{I,n}^{(i-1)} = \tanh(\frac{\lambda_{I,n}^{(i-1)}}{2}). \tag{185}$$

The soft-decision error for the n-th symbol at the i-th iteration is

$$\bar{d}_n^{(i)} = x_n - \hat{x}_n^{(i)}, \tag{186}$$

whose in-phase component power is

$$\mathcal{E}\{(\bar{d}_{I,n}^{(i)})^2 | z_{I,n}^{(i)}\} = 1 - (\hat{x}_{I,n}^{(i)})^2. \tag{187}$$

The decision vector can be obtained by replacing $\underline{\mathbf{d}}^{(i-1)}$ with $\underline{\bar{\mathbf{d}}}^{(i-1)}$ in (171). For a large N, similar to the hard-decision case, the conditional interference power can be approximated by its average value, whose in-phase component power is

$$\mathrm{P}_{in,I}^{(i)}(\underline{\mathbf{z}}^{(i-1)}) \simeq \frac{K_H}{N} \sum_{n=0}^{N-1} \mathcal{E}\{(\bar{d}_{I,n}^{(i-1)})^2 | z_{I,n}^{(i-1)}\}. \tag{188}$$

The (in-phase) pre-decision error power at the i-th iteration ($i \geq 2$) is

$$(\sigma_{e,I}^{(i)})^2 = \mathrm{P}_{in,I}^{(i)}(\underline{\mathbf{z}}^{(i-1)}) + \frac{\sigma_n^2}{2} Q_H. \tag{189}$$

Finally, the SER at the i-th iteration ($i \geq 1$) is

$$p^{(i)} = \Psi(\frac{\sigma_x^2}{(\sigma_e^{(i)})^2}), \tag{190}$$

where $(\sigma_e^{(i)})^2 = (\sigma_{e,I}^{(i)})^2 + (\sigma_{e,Q}^{(i)})^2$.

4.5 Asymptotic Property of Rayleigh Fading Channels

In this section, we discuss the statistical characteristics of two important parameters, K_H and Q_H, which are directly related to performance.

From (170), Q_H is related to the performance of the genie-aided receiver. When Q_H is high, the SER of the genie-aided receiver will be high. K_H is related to the interference

power of the iterative receiver. From (178), for a fixed $p^{(1)}$ and Q_H, the threshold SNR will be shifted to a higher value as K_H is increased. Therefore, for those channel realizations with high K_H and/or high Q_H, the threshold might occur at a very high SNR above the range of our interest.

As in [2], [3], [15], and [16], for a MIMO system designed to achieve the maximal efficiency or multiplexing gain in a Rayleigh fading environment, the configuration of an equal number of transmit and receive antennas is of particular interest. Therefore, we focus on MIMO channels when $n_T = n_R$ even though the results can be easily extended to the case when $n_T \neq n_R$. It can be seen from the definitions of Q_H and K_H in (167) and (175) that they are functions of the elements of the random matrix $\mathbf{G}$. When $n_T = n_R$ is small, both K_H and Q_H vary within a large range. In this case, the probability of encountering the channel realizations with high K_H and/or high Q_H will be significant, and the performance averaged over many channel realizations will be dominated by those worst channels. However, we will show that as $n_T = n_R$ grows, the distributions of K_H and Q_H will converge to one in *mean square sense* (MSS) [23]. In this case, most of the channel realizations are favorable, and the proposed scheme shows a significant performance.

Since K_H and Q_H are functions of $(\mathbf{G})_{p,q}$, respectively, we first study the statistical properties of $(\mathbf{G})_{p,q}$. Hereafter, for simplicity, we denote $h_{p,q} = (\mathbf{H})_{p,q}$ and $g_{p,q} = (\mathbf{G})_{p,q}$. A diagonal element of $\mathbf{G}$ is

$$g_{q,q} = \sum_{l=0}^{n_R-1} |h_{l,q}|^2, \tag{191}$$

and an off-diagonal element of $\mathbf{G}$ is

$$g_{p,q} = \sum_{l=0}^{n_R-1} h_{l,p}^* h_{l,q} \tag{192}$$

for $p \neq q$. Clearly, their means are $\mathcal{E}\{g_{q,q}\} = n_R/n_T$ and $\mathcal{E}\{g_{p,q}\} = 0$, respectively. Also, their variances are shown in Appendix F to be

$$\mathcal{V}\{g_{q,q}\} = \mathcal{V}\{g_{p,q}\} = \frac{n_R}{n_T^2}. \tag{193}$$

Furthermore, $g_{p,q}$ has the following properties:

P-1: For a large n_R, $g_{p,p}$ and $g_{p,q}$ $(p \neq q)$ can be treated as Gaussian random variables, respectively.

P-2: $g_{p,p}$ and $g_{q,q}$ $(p \neq q)$ are independent.

P-3: $g_{r,q}$ and $g_{s,q}$ (or $g_{q,r}$ and $g_{q,s}$) are independent for $r \neq s, r \neq q, s \neq q$ and a large n_R.

P-4: $g_{q,q}$ and $g_{s,q}$ (or $g_{q,q}$ and $g_{q,s}$) $(s \neq q)$ are independent for a large n_R.

P-5: For any positive integer m,

$$\mathcal{E}\{\frac{1}{g_{p,p}^m}\} \longrightarrow \frac{1}{(\mathcal{E}\{g_{p,p}\})^m}$$

as $n_T = n_R \longrightarrow \infty$.

P-1 can be proved by applying the *central limit theorem* (CLT) to (191) and (192), respectively. P-2 can be easily checked from the definition of $g_{p,p}$. P-3 can be proved by noting the fact that for a large n_R, $g_{r,q}$ and $g_{s,q}$ $(r \neq s, r \neq q, s \neq q)$ are Gaussian from P-1 and uncorrelated from $\mathcal{E}\{g_{r,q}g_{s,q}^*\} = \mathcal{E}\{g_{r,q}\}\mathcal{E}\{g_{s,q}^*\} = 0$. P-4 can be similarly proved as P-3. For the proof of P-5, note that

$$\mathcal{E}\{\frac{1}{g_{p,p}^m}\} = \int \frac{1}{x^m} f_g(x)dx,$$

where f_g is the *probability density function* (PDF) of $g_{p,p}$. For a large n_R, $g_{p,p}$ can be treated as a Gaussian random variable invoking the CLT; therefore, if $\mathcal{V}\{g_{p,p}\} \longrightarrow 0$, $f_g(x) \longrightarrow \delta(x - \mathcal{E}\{g_{p,p}\})$ from the definition of the Dirac Delta function $\delta(x)$ [24]. But, $\mathcal{V}\{g_{p,p}\} \longrightarrow 0$ from (193) as $n_T = n_R \longrightarrow \infty$ and P-5 follows.

Since finding the exact distributions of K_H and Q_H is not an easy task, we study only the asymptotic property. From the above properties of $g_{p,q}$, we show in Appendix G that

$$K_H \xrightarrow{m.s.s.} 1 \tag{194}$$

as $n_T = n_R \longrightarrow \infty$, where $\xrightarrow{m.s.s.}$ denotes the convergence in MSS. Also, it is shown in Appendix H that

$$Q_H \xrightarrow{m.s.s.} 1 \tag{195}$$

as $n_T = n_R \longrightarrow \infty$. Since $K_H = 1$ and $Q_H = 1$ corresponds to a favorable channel condition, the proposed iterative receiver shows a significant performance when $n_T = n_R$ is large.

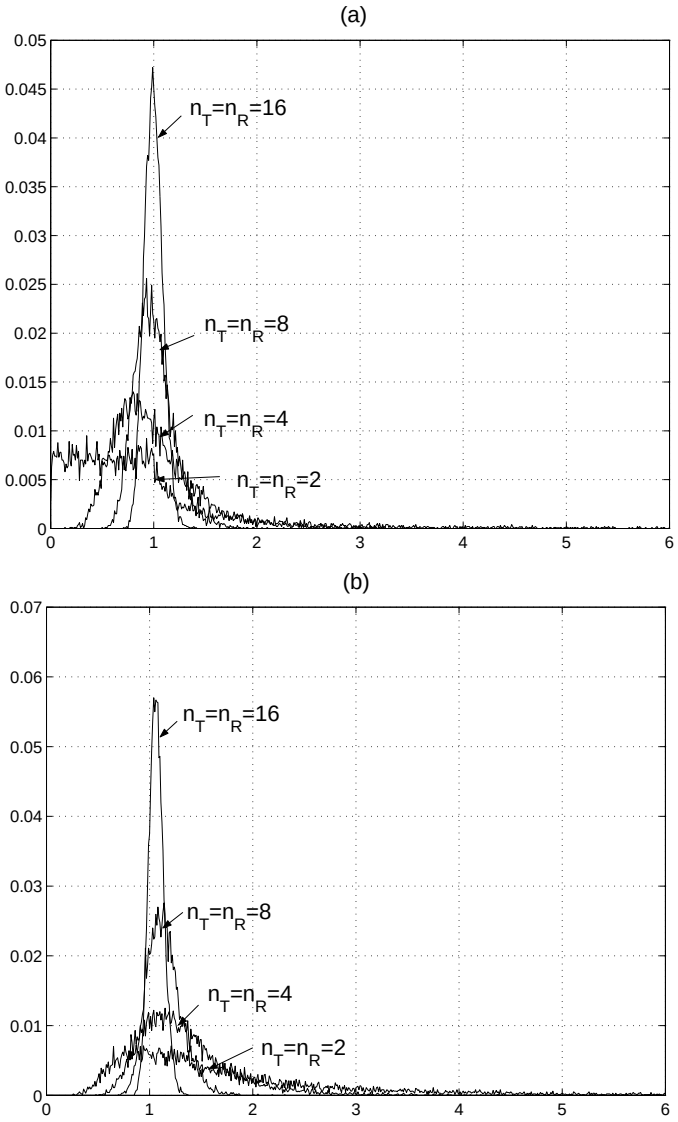

Figure 13. Distribution of (a) K_H and (b) Q_H for different numbers of $n_T = n_R$.

Figure 13 shows the distributions of K_H and Q_H obtained by computer simulation for different numbers of $n_T = n_R$. As shown in the figure, K_H and Q_H are getting concentrated near one, respectively, as $n_T = n_R$ increases.

4.6 Simulation results

In this section, we study the performance of the proposed iterative signal-detection approach by computer simulation. In our simulation, QPSK modulation is used with block size $N = 2048$. Fourier transform matrix is used for $\mathbf{U}$ to construct an ST-EST in (149). Hadamard transform matrix showed almost the same performance. In a Rayleigh fading environment, *bit-error-rate* (BER) performance versus average SNR per bit per receive antenna is provided.

Figure 14 shows the results when $n_T = n_R = 16$. Figure 14 (a) compares the genie-aided receiver with an ideal ST-EST (EST-genie), the analytical result with hard decision and an infinite block size, and simulation results of the hard-decision receiver with finite block size ($N = 2048$). From the figure, the SNR threshold is at about 9 dB. When SNR is below the threshold, the performance of the hard-decision receiver degrades with iteration because of error propagation. However, when SNR is above the threshold, the BER of the hard-decision receiver is improved as the iteration proceeds. After the fifth iteration, the hard-decision receiver performs only within 1 dB of the genie-aided receiver with an ideal ST-EST. Figure 14 (b) compares the performance of the proposed soft-decision receiver with that of the conventional receivers without an ST-EST, including conventional MMSE receiver (Conv-MMSE) [35], conventional ordered decision-feedback receiver (Conv-ODF) [16], [35], and conventional genie-aided receiver (Conv-genie) [35]. With a soft decision, the performance is significantly improved over the hard-decision receiver, especially at the low SNR region. After the second iteration, the soft-decision receiver outperforms Conv-ODF, and after the fifth iteration, it outperforms Conv-genie by about 0.5 dB. From the figure, it can be also seen that for both the MMSE receivers and genie-aided receivers, the corresponding systems with the ST-EST outperform those without an ST-EST.

Figure 15 shows similar results for $n_T = n_R = 4$. In this case, the performance improvement of the iterative signal detection with the hard decision is limited due high Q_H and K_H, as indicated in Section 4.5. However, as shown in Figure 15 (b), the soft-decision receiver can prevent severe error propagation of the hard-decision receiver and improves the SNR performance at BER $= 10^{-4}$ after the fifth iteration by 13 dB.

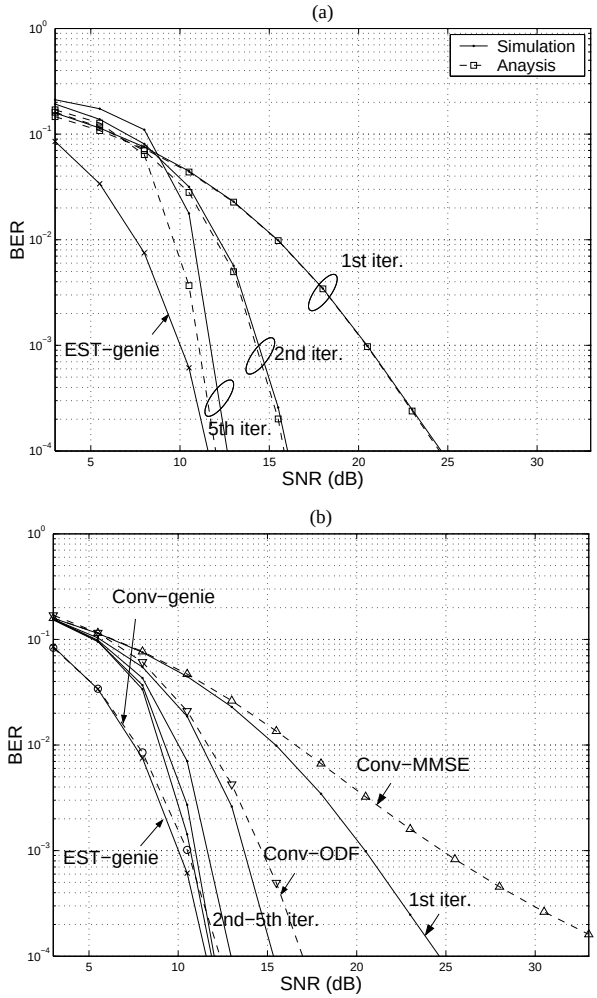

Figure 14. Performance of the proposed iterative signal-detection approach with (a) hard decision and (b) soft decision for MIMO flat fading channels when $n_T = n_R = 16$.

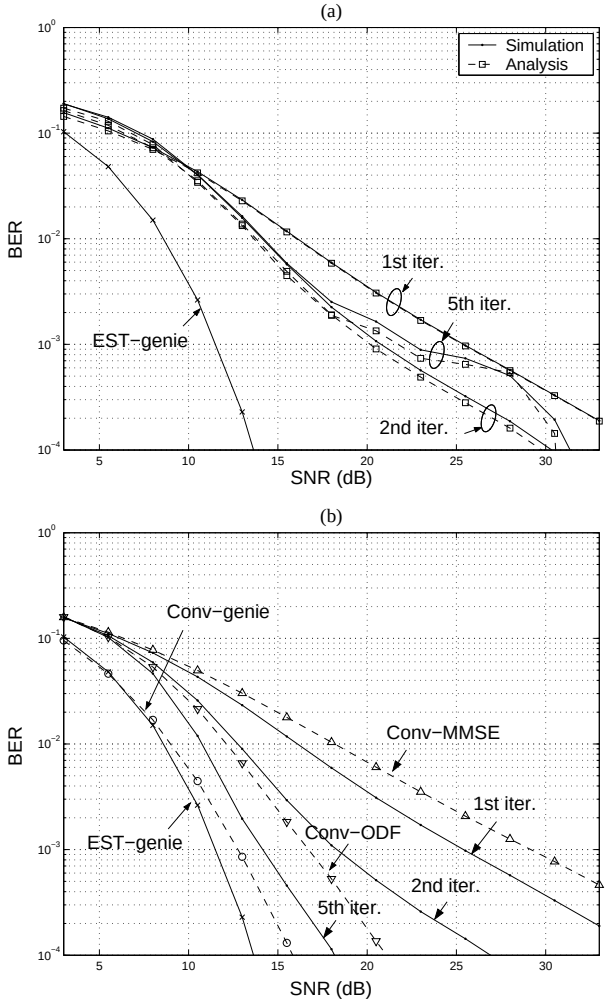

Figure 15. Performance of the proposed iterative signal-detection approach with (a) hard decision and (b) soft decision for MIMO flat fading channels when $n_T = n_R = 4$.

Figure 16 shows how the proposed scheme depends on the number of antennas. The

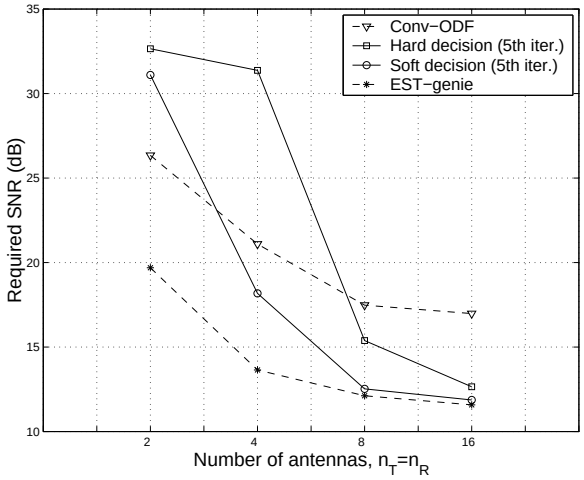

Figure 16. Required SNR to achieve BER = 10^{-4} for different number of antennas.

figure shows the required SNR to achieve a BER of 10^{-4} for the conventional ordered decision-feedback receiver (Conv-ODF), the hard-decision receiver after the fifth iteration, the soft-decision receiver after the fifth iteration, and the genie-aided receiver with an ideal ST-EST (EST-genie). From the figure, when $n_T = n_R \geq 4$, the soft-decision receiver outperforms Conv-ODF; when $n_T = n_R \geq 8$, both the hard- and soft-decision receivers show near genie-aided performance; and when $n_T = n_R \geq 16$, both the hard- and soft-decision receivers perform very close to EST-genie.

CHAPTER 5

ITERATIVE MIMO SIGNAL DETECTION BASED ON EST: FREQUENCY SELECTIVE FADING CHANNELS

The iterative approach for flat fading channels can be extended to frequency-selective fading channels as shown in Figure 17. The channel is modeled as a complex *finite impulse response* (FIR) matrix filter of length L whose n-th matrix tap is $\mathbf{H}_n \in \mathbb{C}^{n_R \times n_T}$ for $n = 0,\ 1, ..., L-1$. Each element of $\mathbf{H}_n$ is modeled as an i.i.d. complex Gaussian random variable with zero mean and variance $1/(n_T L)$ to normalize the transmission power. A cyclic prefix (CP) of length ν ($\nu \geq L-1$) is inserted at each transmit antenna to prevent interference from other symbol blocks.

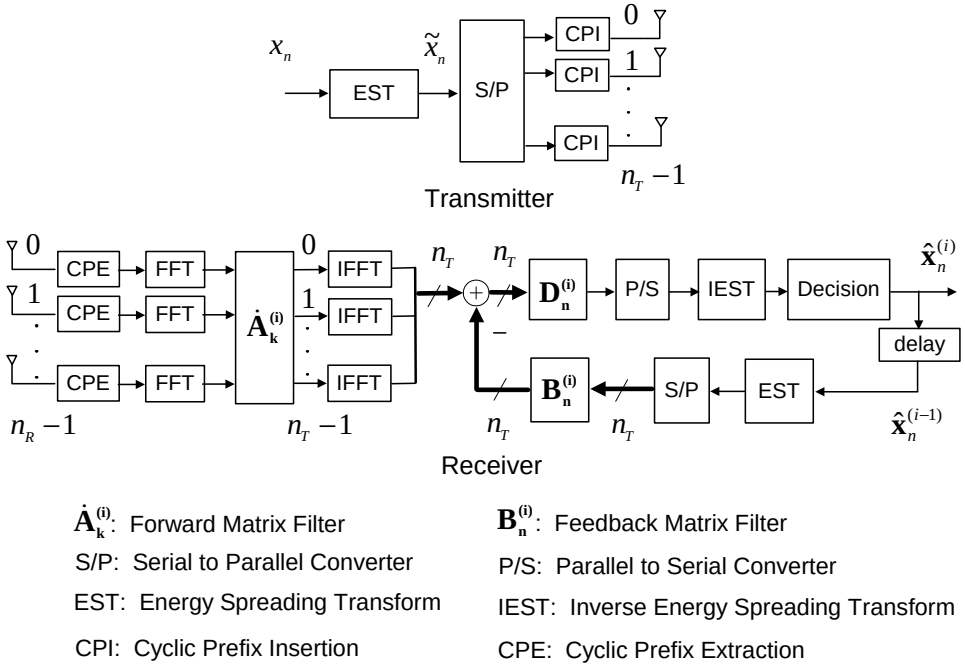

Figure 17. Iterative detection for MIMO frequency-selective fading channels.

The received signal vector after the CP extraction can be written as

$$\tilde{\mathbf{r}}_n = \sum_{l=0}^{L-1} \mathbf{H}_l \tilde{\mathbf{x}}_{(n-l)_{N_b}} + \mathbf{n}_n \tag{196}$$

for $n = 0,\ 1, ..., N_b - 1$, where $(k)_{N_b}$ is the residue of k modulo N_b. In frequency domain, (196) can be represented as

$$\dot{\tilde{\mathbf{r}}}_k = \dot{\mathbf{H}}_k \dot{\tilde{\mathbf{x}}}_k + \dot{\mathbf{n}}_k \tag{197}$$

for $k = 0,\ 1, ..., N_b - 1$, where the matrices or vectors with a dot represent the frequency-domain counterparts of their time-domain notations. For example,

$$\dot{\mathbf{H}}_k = \sum_{n=0}^{N_b-1} \mathbf{H}_n e^{-\frac{2\pi kn}{N_b}} \tag{198}$$

for $k = 0,\ 1, ..., N_b - 1$. $\dot{\tilde{\mathbf{r}}}_k$, $\dot{\tilde{\mathbf{x}}}_k$, and $\dot{\mathbf{n}}_k$ are similarly defined.

The detection is performed by a frequency-domain forward matrix-filter, $\dot{\mathbf{A}}_k^{(i)}$, a time-domain feedback matrix-filter $\mathbf{B}_n^{(i)}$, and a scaling matrix $\mathbf{D}^{(i)}$. At the first iteration, *minimum mean-square-error* (MMSE) scheme is used:

$$\dot{\mathbf{A}}_k^{(1)} = \left(\dot{\mathbf{G}}_k + \frac{\sigma_n^2}{\sigma_x^2}\mathbf{I}_{n_T}\right)^{-1} \dot{\mathbf{H}}_k^H, \tag{199}$$

$$\mathbf{B}_n^{(1)} = \mathbf{0}, \tag{200}$$

$$\mathbf{D}^{(1)} = \mathbf{I}_{n_T} \tag{201}$$

for $n, k = 0,\ 1, ..., N_b - 1$, where $\dot{\mathbf{G}}_k \triangleq \dot{\mathbf{H}}_k^H \dot{\mathbf{H}}_k$. From the second iteration ($i \geq 2$), the interference canceller is used:

$$\dot{\mathbf{A}}_k^{(i)} = \dot{\mathbf{H}}_k^H, \tag{202}$$

$$\mathbf{B}_n^{(i)} \triangleq \begin{cases} \bar{\mathcal{D}}\{\mathbf{G}_0\} & (n = 0) \\ \mathbf{G}_n & (n \neq 0), \end{cases} \tag{203}$$

$$\mathbf{D}^{(i)} = \mathcal{D}\{\mathbf{G}_0\}^{-1}, \tag{204}$$

where $\mathbf{G}_n \triangleq \sum_l \mathbf{H}_l^H \mathbf{H}_{l-n}$.

For the MIMO system in Figure 17, we need a *space-time-frequency* (STF)-EST that spreads the energy of a symbol in space, time, and frequency domain. Define $\mathbf{F}_{N_b} \in \mathbb{C}^{N_b \times N_b}$ to be a normalized Fourier transform matrix, that is, $(\mathbf{F}_{N_b})_{m,n} = \frac{1}{\sqrt{N_b}} e^{-j2\pi mn/N_b}$ and $\mathbf{F}_B = \mathbf{F}_{N_b} \otimes \mathbf{I}_{n_T}$, where $\otimes$ denotes the Kronecker product. The *ideal* STF-EST should satisfy

- The conditions required for the ideal ST-EST in Section 4.2

- $|(\mathbf{F}_B\mathbf{E})_{m,n}| = \frac{1}{\sqrt{N}}$
- $\sphericalangle(\mathbf{F}_B\mathbf{E})_{m,n}$ is pseudo-randomly and even-symmetrically distributed over $[-\pi, \pi]$

Employing the ideal STF-EST and following the similar procedures for the analysis in Section 2.4 and 4.4, we redrive the important parameters related to the performance. For the MMSE receiver, (157)-(159) are modified to

$$m_{si} = \frac{1}{N_b n_T} \sum_{k=0}^{N_b-1} \sum_{l=0}^{n_T-1} (\dot{\mathbf{M}}_k)_{l,l}, \tag{205}$$

$$\begin{aligned} m_{in} &= \frac{1}{N_b n_T} \sum_{k=0}^{N_b-1} \sum_{l_1=0}^{n_T-1} \sum_{l_2 \neq l_1}^{n_T-1} |(\dot{\mathbf{M}}_k)_{l_1,l_2}|^2 \\ &+ \frac{1}{N} \sum_{l=0}^{N-1} \left[(\dot{\mathbf{M}}_{BD})_{l,l}\right]^2 - \left[\frac{1}{N} \sum_{l=0}^{N-1} (\dot{\mathbf{M}}_{BD})_{l,l}\right]^2 \end{aligned} \tag{206}$$

and

$$m_{no} = \frac{1}{N_b n_T} \sum_{k=0}^{N_b-1} \sum_{l=0}^{n_T-1} (|\dot{\mathbf{A}}_k^{(1)}|^2)_{l,l}, \tag{207}$$

respectively, where $\dot{\mathbf{M}}_k \triangleq \dot{\mathbf{A}}_k^{(1)} \dot{\mathbf{H}}_k$ and $\dot{\mathbf{M}}_{BD}$ is a block diagonal matrix defined as

$$\dot{\mathbf{M}}_{BD} \triangleq \text{diag}\{\underbrace{\dot{\mathbf{M}}_0, \dot{\mathbf{M}}_1, \cdots, \dot{\mathbf{M}}_{N_b-1}}_{N_b \text{ matrices}}\} \in \mathbb{C}^{N_b n_R \times N}.$$

For the genie-aided receiver, (167) is changed to

$$Q_H \triangleq \frac{1}{n_T} \sum_{n=0}^{n_T-1} \frac{1}{(\mathbf{G}_0)_{n,n}}. \tag{208}$$

For the iterative detector, (175) becomes

$$K_H \triangleq \frac{1}{n_T} \sum_{l_1=0}^{n_T-1} \sum_{l_2=0, l_2 \neq l_1}^{n_T-1} \frac{|(\mathbf{G}_0)_{l_1,l_2}|^2}{(\mathbf{G}_0)_{l_1,l_1}^2} + \frac{1}{n_T} \sum_{n \neq 0} \sum_{l_1=0}^{n_T-1} \sum_{l_2=0}^{n_T-1} \frac{|(\mathbf{G}_n)_{l_1,l_2}|^2}{(\mathbf{G}_0)_{l_1,l_1}^2}. \tag{209}$$

Figure 18 shows the performance of the proposed scheme for a frequency-selective MIMO channel with $n_T = n_R = 4$ and $L = 4$. The elements of each matrix tap, $\mathbf{H}_n$ $(n = 0, ..., L-1)$, are i.i.d. Gaussian with zero mean and variance $0.0847 \cdot 0.8^n$, that is, a truncated exponential delay profile is used here. The STF-EST employed here is the same as the ST-EST used in Section V, that is, $\mathbf{E} = \mathbf{P}\mathbf{F}_N$. Figure 18 (a) compares the analytical and simulation results

for the hard-decision receiver. From the figure, when the SNR is above the threshold (8 dB), BER is improved with each iteration. Due to finite block length and imperfect energy spreading, there is a gap between the analysis and the simulation results. Figure 18 (b) shows the performance of the soft-decision receiver compared with that of the conventional receivers without an EST: conventional MMSE receiver (Conv-MMSE) and conventional genie-aided receiver (Conv-genie). As shown in the figure, the soft-decision receiver shows an improved performance over the hard-decision receiver. After the fifth iteration, the required SNR at BER = 10^{-4} is 1.7 dB better than that of the hard-decision receiver, which is very close to that of the conventional genie-aided receiver and only within 0.5 dB of the genie-aided receiver with an ideal STF-EST (EST-genie).

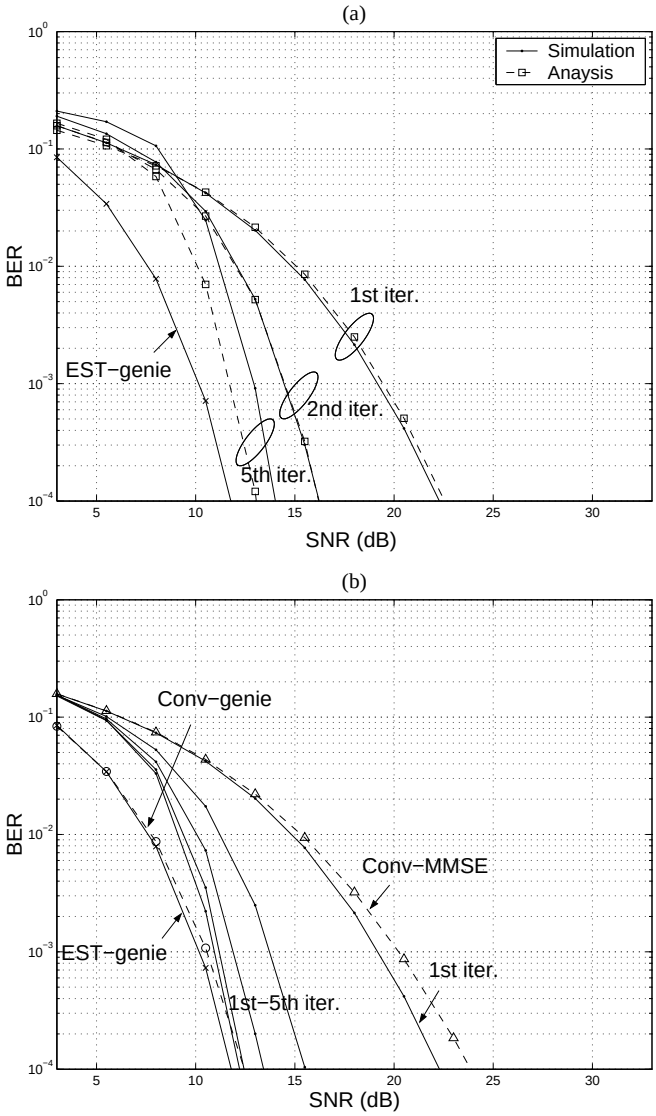

Figure 18. Performance of the proposed iterative signal-detection approach with (a) hard decision and (b) soft decision for MIMO frequency-selective fading channels when $n_T = n_R = L = 4$.

CHAPTER 6

CONCLUSION

This final chapter summarizes the major contributions of the thesis. In this thesis, we have proposed EST-based iterative signal-detection schemes for wireless communication. The specific application areas of our contributions are listed below:

- Channel equalization
- MIMO signal detection for flat fading channels
- MIMO signal detection for frequency-selective fading channels

In Chapter 2, we have proposed an iterative equalization technique based on EST. First, we have introduced EST, which spreads a symbol energy over the symbol block in time and frequency domain. Time-domain spreading increases the reliability of the feedback signal, while frequency-domain spreading obtains frequency diversity. Moreover, these properties of EST enable iterative equalization even without employing channel coding. As measures of spreading, time and frequency spreading factors have been defined. The ideal EST has perfect spreading both in time and frequency domain. In practice, an EST can be implemented by concatenating a random permutation matrix and a unitary matrix. Each element of the unitary matrix composing the EST should have the same magnitude. Normalized Fourier and Hadamard matrices are good candidates of this unitary matrix, because they can be implemented with low complexity using their fast algorithms.

Then, iterative equalization algorithms based on either hard or soft decision have been described. Above a certain SNR threshold, the performance of the hard-decision equalizer improves as the iteration proceeds until it approaches very close to the MFB. The frequency selectivity of a channel can be measured by the parameter K_h. For a larger K_h, the threshold occurs at a higher SNR. The soft-decision equalizer prevent the severe error propagation of

the hard-decision equalizer below the SNR threshold and improves the performance. Also, we have provided an analysis that predicts the performance of the proposed schemes.

In Chapter 3, we have proposed an improved scheme for the EST-based equalization. In the original scheme in Chapter 2, MMSE equalization is used for the first iteration and matched filter with interference canceller are used for the rest of the iteration. In the improved scheme, however, optimal forward and feedback equalization filters that maximize SINR at each iteration are employed. Another distinction of the improved scheme is that extrinsic LLR is used for the soft decision to be fed back to the feedback filter, while a posteriori LLR is used in the original scheme.

In Chapter 4, we have applied the EST-based iterative approach to the MIMO signal-detection problem for flat fading channels. In this case, a symbol energy is spread in space and time by EST. Therefore, we call the EST in this configuration as *space-time* (ST)-EST. Similar to the EST used in Chapter 2, ST-EST can be implemented by concatenating a random permutation matrix and a unitary matrix whose elements have the same magnitude. K_H and Q_H are two important parameters that characterize the channel and directly related to the performance. K_H and Q_H are related to the strength of interference power and the desired signal power, respectively. When k_H and/or Q_H is high, MIMO channel has very severe interference and/or low desired signal power.

For the simulation, we have focused on the MIMO system that has the same number of transmit and receive antennas, that is, $n_T = n_R$. For small $n_T = n_R$, the probability of encountering a severe channel with high K_H and/or Q_H can not be ignored, which dominates the average performance. However, as $n_T = n_R \longrightarrow \infty$, $K_H \longrightarrow 1$ and $Q_H \longrightarrow 1$ in MSS. In this case, the proposed scheme shows a significant average performance (near the genie-aided performance) because most of the MIMO channel realizations have moderate vlaues of K_H and Q_H close to 1.

In Chapter 5, we have extended the EST-based MIMO signal-detection scheme to frequency-selective fading channels. In this scheme, EST spreads a symbol energy over the block in space, time, and frequency domain.

The proposed iterative method based on EST is a powerful solution to the signal-detection problems in severe interference environments. It shows a significant performance close to that of an interference-free system only at the complexity of linear detectors.

APPENDIX A

DERIVATION OF (25)

Consider

$$(\mathbf{F}\mathbf{P}_1\mathbf{F}^H)_{m,n} = \frac{1}{N}\sum_{l_1}\sum_{l_2}(\mathbf{P}_1)_{l_1,l_2}e^{\frac{-j2\pi ml_1}{N}}e^{\frac{j2\pi nl_2}{N}} \quad (A.1)$$

$$= \frac{1}{N}\sum_{(l_1,l_2)\in O(\mathbf{P}_1)}e^{\frac{-j2\pi ml_1}{N}}e^{\frac{j2\pi nl_2}{N}}, \quad (A.2)$$

where $O(\mathbf{P}_1) \triangleq \{(l_1,l_2)|(\mathbf{P}_1)_{l_1,l_2}=1\}$ is the set of the positions in $\mathbf{P}_1$ where 1's are located. It is evident that $(\mathbf{F}\mathbf{P}_1\mathbf{F}^H)_{0,0}=1$. For $m=0$, $n\neq 0$,

$$(\mathbf{F}\mathbf{P}_1\mathbf{F}^H)_{m,n} = \frac{1}{N}\sum_{(l_1,l_2)\in O(\mathbf{P}_1)}e^{\frac{j2\pi nl_2}{N}} \quad (A.3)$$

$$= \frac{1}{N}\sum_{l_2=0}^{N-1}e^{\frac{j2\pi nl_2}{N}} \quad (A.4)$$

$$= 0. \quad (A.5)$$

Similarly, $(\mathbf{F}\mathbf{E}_2)_{m,n}=0$ for $m\neq 0$ and $n=0$. Consequently, $s_F(\mathbf{E}_2;0)=s_T(\mathbf{F}\mathbf{P}_1\mathbf{F}^H;0)=(N-1)/N$ for any permutation matrix $\mathbf{P}_1$. By similar argument, $s_F(\mathbf{E}_1;0)=s_T(\mathbf{E}_3;0)=(N-1)/N$.

APPENDIX B

DERIVATION OF (52)

From the second iteration ($i \geq 2$), the forward and feedback matrices are

$$\begin{aligned} \mathbf{A}_D^{(i)} &= \mathbf{H}_D^H, & \text{(B.1)} \\ \mathbf{C}(\mathbf{b}^{(i)}) &= \bar{\mathcal{D}}\{\mathbf{C}(\mathbf{g})\} \\ &= \bar{\mathcal{D}}\{\mathbf{F}^H|\mathbf{H}_D|^2\mathbf{F}\}, & \text{(B.2)} \end{aligned}$$

respectively. Since the matrix multiplied to $\mathbf{x}$ in (38) can be decomposed into

$$\begin{aligned} \mathbf{E}^H\mathbf{F}^H|\mathbf{H}_D|^2\mathbf{F}\mathbf{E} &= \mathbf{E}^H\mathcal{D}\{\mathbf{F}^H|\mathbf{H}_D|^2\mathbf{F}\}\mathbf{E} \\ &+ \mathbf{E}^H\bar{\mathcal{D}}\{\mathbf{F}^H|\mathbf{H}_D|^2\mathbf{F}\}\mathbf{E}, & \text{(B.3)} \end{aligned}$$

where

$$\mathbf{E}^H\mathcal{D}\{\mathbf{F}^H|\mathbf{H}_D|^2\mathbf{F}\}\mathbf{E} = g_o\mathbf{I} \quad \text{(B.4)}$$

from the identity (31). The decision vector for the iterative equalizer can be written as

$$\mathbf{z}^{(i)} = \underbrace{g_0\mathbf{x}}_{signal} + \underbrace{\mathbf{E}^H\mathbf{C}(\mathbf{b}^{(i)})\mathbf{E}\mathbf{d}^{(i-1)}}_{interference} + \underbrace{\mathbf{E}^H\mathbf{F}^H\mathbf{H}_D^H\mathbf{F}\mathbf{n}}_{noise}, \quad \text{(B.5)}$$

where

$$\mathbf{d}^{(i)} = \mathbf{x} - \hat{\mathbf{x}}^{(i)} \quad \text{(B.6)}$$

is the hard-decision-error vector at the i-th iteration. The decision vector for the genie-aided equalizer is

$$\mathbf{z}^{(i)} = \underbrace{g_0\mathbf{x}}_{signal} + \underbrace{\mathbf{E}^H\mathbf{F}^H\mathbf{H}_D^H\mathbf{F}\mathbf{n}}_{noise}, \quad \text{(B.7)}$$

with perfect cancellation of interference in (B.5).

APPENDIX C

DERIVATION OF (70) AND (100)

From (44), (45), and (46),

$$m_{si} = \frac{1}{N}\sum_k \frac{|H_k|^2}{|H_k|^2+\sigma_n^2/\sigma_x^2}, \tag{C.1}$$

$$m_{in} = \frac{1}{N}\sum_k \left(\frac{|H_k|^2}{|H_k|^2+\sigma_n^2/\sigma_x^2}\right)^2 - \left(\frac{1}{N}\sum_k \frac{|H_k|^2}{|H_k|^2+\sigma_n^2/\sigma_x^2}\right)^2, \tag{C.2}$$

$$m_{no} = \frac{1}{N}\sum_k \frac{|H_k|^2}{(|H_k|^2+\sigma_n^2/\sigma_x^2)^2}. \tag{C.3}$$

The mean SINR is

$$\overline{\mathrm{SINR}}^{(1)} = \frac{\sigma_x^2 m_{si}^2}{\sigma_x^2 m_{in}+\sigma_n^2 m_{no}} = \frac{1}{\frac{1}{N}\sum_k \frac{1}{\overline{\mathrm{SNR}}_{|H_k|^2+1}}} - 1, \tag{C.4}$$

where $\mathrm{SNR} = \sigma_x^2/\sigma_n^2$. The normalized pre-decision error power after MMSE equalization is

$$(\sigma_e^{(1)})^2 = \left(\overline{\mathrm{SINR}}^{(1)}\right)^{-1}\sigma_x^2, \tag{C.5}$$

where

$$\left(\overline{\mathrm{SINR}}^{(1)}\right)^{-1} = \frac{1}{\frac{1}{N}\sum_k \frac{|H_k|^2}{|H_k|^2+1/\overline{\mathrm{SNR}}}} - 1. \tag{C.6}$$

APPENDIX D

PROOF OF (92) FOR SUFFICIENTLY HIGH SNR

Assuming high SNR, we ignore -1 on the *left hand side* (LHS) of (92). After inverting and multiplying SNR > 1 on both sides of (92) (with -1 ignored), we get

$$\frac{1}{N}\sum_{k=0}^{N-1}\frac{1}{|H_k|^2+\frac{1}{\mathrm{SNR}}} > \mathrm{SNR}\alpha(p_s^{(1)})K_h p_s^{(1)} + \frac{1}{g_0}. \tag{D.1}$$

Since $p_s^{(1)} = \Psi(\mathrm{SINR}^{(1)})$ decays like $e^{-\beta\mathrm{SNR}}$ for sufficiently high SNR, where

$$\beta = \frac{1}{\frac{1}{N}\sum_{k=0}^{N-1}\frac{1}{|H_k|^2+\frac{1}{\mathrm{SNR}}}} \tag{D.2}$$

from (70), the *right hand side* (RHS) of (D.1) approaches

$$\mathrm{RHS} \longrightarrow \frac{1}{g_0} \tag{D.3}$$

as SNR $\longrightarrow \infty$. But, the LHS of (D.1) approaches

$$\mathrm{LHS} \longrightarrow \frac{1}{N}\sum_{k=0}^{N-1}\frac{1}{|H_k|^2} \tag{D.4}$$

as SNR $\longrightarrow \infty$ and using Jensen's inequality [25],

$$\frac{1}{N}\sum_{k=0}^{N-1}\frac{1}{|H_k|^2} \geq \frac{1}{\frac{1}{N}\sum_{k=0}^{N-1}|H_k|^2}\frac{1}{g_0}. \tag{D.5}$$

The equality in (D.5) holds when $|H_0|^2 = |H_1|^2 = ... = |H_{N-1}|^2$, but this corresponds to the frequency-flat channel for which equalization is not necessary.

APPENDIX E

PROOF OF ID-3

For the ideal ST-EST, $\mathbf{E}$, we can write $(\mathbf{E})_{l,n} = \frac{1}{\sqrt{N}} e^{\theta_{l,n}}$ and

$$(\mathbf{E}^H \bar{\mathcal{D}}(\mathbf{X})\mathbf{E})_{n,m} = \frac{1}{N} \sum_{l_1} \sum_{l_2 \neq l_1} (\mathbf{X})_{l_1,l_2} e^{j(\theta_{l_2,m} - \theta_{l_1,n})}. \tag{E.1}$$

Since $\theta_{l,n}$ is pseud-randomly and symmetrically distributed on $[-\pi, \pi]$, we treat $\theta_{l,n}$ as an independent random variable with zero-mean. Invoking the *central limit theorem* (CLT), (E.1) can be treated as a zero-mean Gaussian random variable with variance equal to the one in ID-3.

APPENDIX F

DERIVATION OF (193)

Since $h_{i,j} \sim \mathcal{N}(0, 1/n_T)$, the *moment generating function* (MGF) [34] of $|h_{i,j}|^2$ is

$$\phi_{|h_{i,j}|^2}(t) = \mathcal{E}\{e^{t|h_{i,j}|^2}\} = (1 - \frac{t}{n_T})^{-1} \tag{F.1}$$

and the MGF of $g_{j,j}$ is

$$\phi_{g_{j,j}}(t) = \prod_{i=0}^{n_R-1} \phi_{|h_{i,j}|^2}(t) = (1 - \frac{t}{n_T})^{-n_R}. \tag{F.2}$$

We can calculate the m-th moment of $|h_{i,j}|^2$ and $g_{j,j}$ from their MGFs, respectively. For $g_{j,j}$,

$$\mathcal{E}\{g_{j,j}^2\} = \phi_{g_{j,j}}^{(2)}(0) = \frac{n_R(n_R+1)}{n_T^2} \tag{F.3}$$

and the variance of $g_{j,j}$ is

$$\mathcal{V}\{g_{j,j}\} = \mathcal{E}\{g_{j,j}^2\} - (\mathcal{E}\{g_{j,j}\})^2 = \frac{n_R}{n_T^2}. \tag{F.4}$$

For $g_{i,j}$ $(i \neq j)$,

$$\mathcal{E}\{|g_{i,j}|^2\} = \sum_{p=0}^{n_R-1} \mathcal{E}\{|h_{p,i}|^2\}\mathcal{E}\{|h_{p,j}|^2\} = \frac{n_R}{n_T^2}, \tag{F.5}$$

and similarly for $i \neq j$,

$$\begin{aligned} \mathcal{E}\{|g_{i,j}|^4\} &= \sum_{p=0}^{n_R-1} \mathcal{E}\{|h_{p,i}|^4\}\mathcal{E}\{|h_{p,j}|^4\} \\ &+ 2 \sum_{p,r=0(p\neq r)}^{n_R-1} \mathcal{E}\{|h_{p,i}|^2\}\mathcal{E}\{|h_{p,j}|^2\}\mathcal{E}\{|h_{r,i}|^2\}\mathcal{E}\{|h_{r,j}|^2\} \\ &= \frac{2n_R(n_R+1)}{n_T^4}. \end{aligned} \tag{F.6}$$

The variance of $g_{i,j}$ $(i \neq j)$ is

$$\mathcal{V}\{g_{i,j}\} = \mathcal{E}\{|g_{i,j}|^2\} - |\mathcal{E}\{g_{i,j}\}|^2 = \frac{n_R}{n_T^2}. \tag{F.7}$$

APPENDIX G

DERIVATION OF (194)

From (175) and P-4 we get, for a large n_R,

$$\mathcal{E}\{K_H\} = \frac{1}{n_T} \sum_{l_1=0}^{n_T-1} \sum_{l_2=0, l_2 \neq l_1}^{n_T-1} \mathcal{E}\{|g_{l_1,l_2}|^2\} \mathcal{E}\{\frac{1}{g_{l_1,l_1}^2}\}. \tag{G.1}$$

From P-5 we have

$$\mathcal{E}\{\frac{1}{g_{l_1,l_1}^2}\} \longrightarrow \frac{1}{(\mathcal{E}\{g_{l_1,l_1}\})^2} = \left(\frac{n_T}{n_R}\right)^2 \tag{G.2}$$

as $n_T = n_R \longrightarrow \infty$. Substituting (F.5) and (G.2) into (G.1), we get

$$\mathcal{E}\{K_H\} \longrightarrow \frac{n_T - 1}{n_R} \longrightarrow 1. \tag{G.3}$$

as $n_T = n_R \to \infty$. Now, consider

$$\begin{aligned} \mathcal{E}\{K_H^2\} &= \frac{1}{n_T^2} \sum_p \sum_{q \neq p} \sum_r \sum_{s \neq r} \mathcal{E}\{\frac{|g_{p,q}|^2}{g_{p,p}^2} \frac{|g_{r,s}|^2}{g_{r,r}^2}\} \\ &= \sum_{i=1}^{4} \frac{N_i W_i}{n_T^2}, \end{aligned} \tag{G.4}$$

where N_i and W_i are the parameters corresponding to the i-th case ($1 \leq i \leq 4$) shown below:

- $i = 1$ ($p = r, q = s$):

$$N_1 = n_T(n_T - 1),\ W_1 = \mathcal{E}\{\frac{|g_{p,q}|^4}{g_{p,p}^4}\}$$

- $i = 2$ ($p = r, q \neq s$):

$$N_2 = n_T(n_T - 1)(n_T - 2),\ W_2 = \mathcal{E}\{\frac{|g_{p,q}|^2 |g_{p,s}|^2}{g_{p,p}^4}\}$$

- $i = 3$ ($p \neq r, q = s$):

$$N_3 = n_T(n_T - 1)(n_T - 2),\ W_3 = \mathcal{E}\{\frac{|g_{p,q}|^2}{g_{p,p}^2} \frac{|g_{r,q}|^2}{g_{r,r}^2}\}$$

- $i = 4$ $(p \neq r, q \neq s)$:

$$\begin{aligned} N_4 &= n_T(n_T-1)(n_T^2-3n_T+3) \\ W_4 &= \mathcal{E}\{\frac{|g_{p,q}|^2}{g_{p,p}^2}\frac{|g_{r,s}|^2}{g_{r,r}^2}\} \end{aligned}$$

From P-5 we have

$$\mathcal{E}\{\frac{1}{g_{l_1,l_1}^4}\} \longrightarrow \frac{1}{(\mathcal{E}\{g_{l_1,l_1}\})^4} = \left(\frac{n_T}{n_R}\right)^4 \tag{G.5}$$

as $n_T = n_R \longrightarrow \infty$. From (F.3)-(F.6), (G.5), and P-2-P-5 we get

$$\begin{aligned} \frac{N_1W_1}{n_T^2} &\longrightarrow \frac{2(n_T-1)(n_R+1)}{n_Tn_R^3} \longrightarrow 0, \\ \frac{N_2W_2}{n_T^2} &\longrightarrow \frac{(n_T-1)(n_T-2)}{n_Tn_R^2} \longrightarrow 0, \\ \frac{N_3W_3}{n_T^2} &\longrightarrow \frac{(n_T-1)(n_T-2)}{n_Tn_R^2} \longrightarrow 0, \end{aligned}$$

and

$$\frac{N_4W_4}{n_T^3} \longrightarrow \frac{(n_T-1)(n_T^2-3n_T+3)}{n_Tn_R^2} \longrightarrow 1$$

as $n_T = n_R \longrightarrow \infty$. Therefore, $\mathcal{E}\{K_H^2\} \longrightarrow 1$ and

$$\mathcal{V}\{K_H\} = \mathcal{E}\{K_H^2\} - (\mathcal{E}\{K_H\})^2 \longrightarrow 0 \tag{G.6}$$

as $n_T = n_R \longrightarrow \infty$. From (G.1) and (G.6) (194) follows.

APPENDIX H

DERIVATION OF (195)

From P-5,

$$\mathcal{E}\{Q_H\} = \mathcal{E}\{\frac{1}{g_{l,l}}\} \longrightarrow \frac{1}{\mathcal{E}\{g_{l,l}\}} = \frac{n_T}{n_R} = 1 \tag{H.1}$$

as $n_T = n_R \longrightarrow \infty$. Since $g_{p,p}$ and $g_{q,q}$ $(p \neq q)$ are independent from P-2,

$$\mathcal{V}\{Q_H\} = \frac{1}{n_T}\mathcal{V}\{\frac{1}{g_{l,l}}\} = \frac{1}{n_T}[\mathcal{E}\{\frac{1}{g_{l,l}^2}\} - (\mathcal{E}\{\frac{1}{g_{l,l}}\})^2].$$

From (G.2) and (H.1),

$$\mathcal{V}\{Q_H\} \longrightarrow \frac{1}{n_T}[\frac{n_T^2}{n_R^2} - \frac{n_T^2}{n_R^2}] = 0 \tag{H.2}$$

as $n_R = n_T \longrightarrow \infty$. From (H.1) and (H.2) (195) follows.

REFERENCES

[1] J. G. Proakis, *Digital Communications,* 2nd ed. New York: McGraw-Hill, 1989.

[2] G. J. Foschini and M. J. Gans, "On limits of wireless communications in a fading environment when using multiple antennas," *Wireless Pers. Commun.,* pp. 311-335, 1999.

[3] G. J. Foschini, "Layered space-time architecture for wireless communication in a fading environment when using multi-element antennas," *Bell Labs Technical Journal,* pp. 41-59, Autumn 1996.

[4] C. Berrou and A. Glavieux, and P. Thitimajshima, "Near Shannon limit error-correction coding and decoding: Turbo codes," in *Proc. IEEE Int. Conf. Commun.*, pp. 1064-1070, 1993.

[5] L. R. Bahl, J. Cocke, F. Jelinek, and J. Raviv, "Optimal decoding of linear codes for minimizing symbol error rates," *IEEE Trans. Inform. Theory*, vol. IT-20, pp. 284-287, Mar. 1974.

[6] J. Hagenauer and P. Hoeher, "A Viterbi algorithm with soft-decision outputs and its applications," in *Proc. IEEE Global Telecomm. Conf.*, pp. 1680-1686, 1989

[7] C. Douillard *et al.*, "Iterative correction of intersymbol interference: Turbo equalization," *Eur. Trans. Telecommun.*, vol. 6, pp. 507-511, Sep.-Oct. 1995.

[8] C. Laot, A. Glavieux, and J. Labat, "Turbo equalization: adaptive equalizatioin and channel decoding jointly optimized," *IEEE J. Select. Areas Commun*, vol. 19, pp. 1744-1752, Sep. 2001.

[9] M. Tüchler, R. Koetter, and A. Singer, "Turbo equalization: Principles and new results," *IEEE Trans. Commun.*, vol. 50, pp. 754-767, May 2002.

[10] S. M. Alamouti, "A simple transmit diversity technique for wireless communications," *IEEE J. Select. Areas Commun.*, vol. 16, pp. 1451-1458, Oct. 1998.

[11] J. H. Winters, "The diveristy gain of transmit diversity in wireless systems with Rayleigh fading," *IEEE Trans. Veh. Technol.*, vol. 47, pp. 119-123, Feb. 1998.

[12] V. Tarokh, N. Seshadri, and A. R. Calderbank, "Space-time codes for high data rate wireless communication: performance criterion and code construction," *IEEE Trans. Inform. Theory,* vol. 44, pp. 744-765, Mar. 1998.

[13] V. Tarokh, H. Jafarkhani, and A. R. Calderbank, "Space-time block codes from orthogonal designs," *IEEE Trans. Inform. Theory,* vol. 45, pp. 1456-1467, July 1999.

[14] P. Wolniansky, G. Foschini, G. Golden, R. Valenzuela, "V-BLAST: an architecture for realizing very high data rates over rich-scattering wireless channel," *Int. Symp. on Sig. Sys., and Elec.,* pp. 295-300, Oct. 1998.

[15] W. Zha and S. D. Blostein, "Modified decorrelating decision-feedback detection of BLAST space-time system," *International Conference on Communications,* vol. 1, pp. 335-339, May 2002.

[16] B. Hassibi, "An efficient square-root algorithm for BLAST," *IEEE International Conference on Acoustics, Speech, and Signal Preocessing,* vol. 2, pp. 737-740, June 2000.

[17] M. Sellathurai and S. Haykin, "Turbo-Blast for wireless communications: theory and experiments," *IEEE Trans. Signal Processing,* vol. 50, pp. 2538-2546, Oct. 2002.

[18] T. Hwang and Y. (G.) Li, "A bandwidth efficient block transmission with frequency-domain equalization," in *Proc. IEEE 6th CAS Symp. on Emerging Technologies*, pp. 433-436, 2004.

[19] A. V. Oppenheim and R. W. Schafer, *Discrete-Time Signal Processing*: Prentice Hall, 1989.

[20] D. Williamson, R. A. Kennedy, and G. W. Pulford, "Block decision feedback equalization," *IEEE Trans. Commun.*, vol. 40, pp. 255-264, Feb. 1992.

[21] D. Falconer, S. L. Ariyavisitakul, A. Benyamin-Seeyar, and B. Eidson, "Frequency-domain equalization for single-carrier broadband wireless systems," *IEEE Commun. Mag.*, vol. 40, pp. 58-66, Apr. 2002.

[22] G. Golub and C. Van Loan, *Matrix Computations,* 3rd ed. Baltimore: Johns-Hopkins, 1996.

[23] A. Papoulis, *Probability, Random Variables, and Stocastic Processes,* 3rd ed. McGraw-Hill, 1991.

[24] R. Bracewell, *The Fourier Transform and Its Applications,* 3rd ed. New York: McGraw-Hill, 1999.

[25] T. M. Cover and J. A. Thomas, *Elements of Information Theory,* Newyork: Wiley, 1991.

[26] B. Porat and B. Friedlander, "Blind equalization of digital communications channels using high-order moments," *IEEE Trans. Signal Processing*, vol. 39, pp. 522-526, Feb. 1991.

[27] A. M. Chan and G. W. Wornell, "A class of block-iterative equalizars for intersymbol interference channels: fixed channel results," *IEEE Trans. Commun.*, vol. 49, pp. 1966-1976, Nov. 2001.

[28] N. Benvenuto and S. Tomasin, "Block iterative DFE for single carrier modulation," *IEE Electronics Letters*, vol. 38, pp. 1144-1145, Sep. 2002.

[29] G. L. Stüber, *Principles of Mobile Communication,* 2nd ed. Kluwer, 2000.

[30] S. Baro, G. Bauch, A. Pavlic, and A. Semmler "Improving BLAST performance using space-time block codes and turbo decoding," *IEEE Global Telecomm. Conference,* vol. 2, pp. 1067-1071, Nov. 2000.

[31] T. Abe and T. Matsumoto, "Space-time turbo equalization in frequency-selective MIMO channels," *IEEE Trans. Veh. Technol.*, vol. 52, pp. 469-475, May 2003.

[32] T. Hwang and Y. (G.) Li, "Novel iterative equalization based on energy spreading transform," to appear in *IEEE Trans. Signal Processing*.

[33] T. Hwang, Y. (G.) Li, and H. Sari, "Energy spreading transform based iterative signal detection for MIMO fading channels," to appear in *IEEE Trans. Wireless Commun.*

[34] S. M. Ross, *Introduction to Probability Models,* 7th ed. San Diego: Academic Press, 2000.

[35] J. R. Barry, E. A. Lee, and D. G. Messerschmitt, *Digital Communication,* 3rd ed. Boston: Kluwer Academic Publishers, 2003.

[36] S. Verdú, *Multiuser Detection,* Cambridge, U.K.: Cambridge Univ. Press, 1988.

VITA

Taewon Hwang was born in Seoul, Korea. He received B.S. and M.S. degrees in Electronics Engineering from Yonsei University, Seoul, Korea in 1993 and in Electrical and Computer Engineering from Georgia Institute of Technology, Atlanta, Georgia in 1995, respectively. From 1995 to 2000, he was a Member of Technical Staff at Electronics and Telecommunications Research Institute (ETRI), Daejeon, Korea. From 2001 to 2005, he was a Graduate Research and Teaching Assistant in the Department of Electrical and Computer Engineering at the Georgia Institute of Technology. From May 2005 to August 2005, he worked as an intern with Qualcomm, Corporate R&D Group, San Diego, California on the CDMA 1xEvDO performance-enhancement project. His research interest interests are in wireless communications, with a current focus on channel equalization and MIMO signal detection.